Report

LOBBE TECHNOLOGIES LTD.

Lobbe Technologies Ltd.
P.O. Box 3570
Regina, Saskatchewan
S4P 3L7

MATHEMATICAL MODELLING OF COPROCESSING KINETICS

Prepared By

A. J. Szladow
R. K. Chan
J. Tscheng

35 SPP

MICROMEDIA

Work on this project was conducted under the auspices of the Canada Centre for Mineral and Energy Technology, under the support of PERD, Department of Energy, Mines and Resources, Canada.

D.S.S. File No.	06SQ. 23440-6-9140
D.S.S. Serial No.	23440-6-9140
CANMET Scientific Authority	Dr. S. Fouda/J.F. Kelly

September 9, 1987

NOTICE

This report was prepared by Lobbe Technologies Ltd. as an account of work sponsored by the Canada Centre for Mineral and Energy Technology, Department of Energy, Mines and Resources, Canada. Neither Lobbe Technologies Ltd., nor any person acting on their behalf:

(a) Makes any warranty or representation, express or implied, with respect to the accuracy, completeness, or usefulness of the information contained in this report, or that the use of any information, apparatus, method of process disclosed in this report may not infringe privately owned rights; or

(b) Assumes any liabilities with respect to the use of, or damages resulting from the use of, any information, apparatus, method or process disclosed in this report.

EXECUTIVE SUMMARY

Since 1979, CANMET has been conducting research and process development work on coprocessing of Canadian heavy oil/bitumen and coal for production of alternative transportation fuels. As a continuation of these studies, in 1986, CANMET undertook a program on Mathematical Modelling of Coprocessing Kinetics, with special emphasis on development of reaction engineering models for improved process performance and operation. This report describes the results and conclusions of that study including recommendations for future work in the coprocessing area.

The principle results and conclusions are:

1. The completed review of the-state-of-the-art of coal liquefaction and heavy oil upgrading kinetics pointed to many common features in both processes. The key variable in both processes is temperature. The degree and rate of coal and heavy oil conversion is determined predominantly by bond scission, hydrocracking and thermal cracking reactions.

2. The thirteen sets of data provided by CANMET were very good, as judged by the mass balances and standard deviations for individual product components. This permitted development of stringent statistical criteria for goodness of fit for the developed models.

3. The products of coprocessing were successfully classified (lumped) by their solubility and/or distillation points. The products' characteristics were also found, for the most part, to be independent of the severity of the process severity. This is essential for development of sound kinetic models.

4. Matching the relative yields and hydrogen consumption for the coprocessing products, CANMET data compared favorably with those of HRI and other process developers. The final conclusions called for a more

detailed evaluation of CANMET and other coprocessing data in order to provide a more scientific assessment of various processes. We also recommend that CANMET undertake an experimental program to evaluate gas hold-up in their stirred-tank reactors before a detailed comparison with data generated in tubular reactors is made.

5. Analysis of the effects of temperature and space velocity on product yield and selectivity showed the product yield structure to be determined primarily by the severity of the process, i.e., by temperature and the extent of thermal cracking. This explains why the effect of the quality of solvent, hydrogen consumption, or space velocity is negligible at the studied coprocessing conditions. It also explains why simple correlations can be obtained between the yield of coprocessing products and severity of the process as measured by pitch conversion, and why coal conversion is similar for coal liquefaction and coprocessing, in spite of different solvents.

6. The understanding of coprocessing reactions was greatly aided by the Multiple Classification analysis, which depicted the overall effects of temperature and space velocity on the yield structure of coprocessing products. Multiple Classifications analysis also explained the difficulties in modelling preasphaltenes, i.e., pointed to the change in sign of preasphaltene's apparent activations energy, possibly due to an adduct formation. It is felt that understanding the mechanism and kinetics of the preasphaltene adduct formation is important in development of an improved process design strategy for coprocessing. The adduct is most likely to be formed from pitch generating heavy oil fractions, which may influence pitch conversion kinetics. The adduct also "links" the heavy oil upgrading and coal conversion reaction paths.

7. Based on the Multiple Classification Analysis reaction paths, coprocessing models were formulated. The derived reaction equation and kinetic rate expression were those for a CSTR, with the rate equations written in terms of dimensionless yields of coprocessing products, on a moisture-and-ash-free slurry. The rate constants were regressed by using the Least Square method to minimize the residuals between the predicted and experimental rate data. The rate constant coefficients were later calculated from the regressed rate constants. This approach provided additional understanding of the physical meaning of the regressed rate constants, and how the rate constants are affected by the alternative reactions paths.

8. A number of reaction networks were evaluated for two types of models: a sequential model and a parallel reactions model. The principle criterion for evaluation was the percent of variance explained by the studied models. Another criterion was how accurately the model explains the yield structure of coprocessing products. The target variance explained was 92.5 percent for the eight-component model. The best model, a parallel type model which incorporated some sequential characteristics, explained 90.0 percent of total variance. This was considered satisfactory in view of the difficulties with modelling preasphaltenes.

9. Testing of the derived kinetics model for sensitivity to the assumptions made showed that models' predictive capabilities did not change with the selection of different gas hold-ups and fraction of feed flashed at the reactor T and P. This observation reveals that the choice of reaction network is determined, in principle, by the yield structure of the coprocessing products and not by the assumption made.

It was recommended that the future comprehensive experimental program address the effect of catalyst, heavy oil, coal concentration and hydrogen uptake on coprocessing yield and selectivity using developed statistical analysis methods and kinetic models. It was also suggested that the new factorial design for these experiments be carried out at a temperature range of 425 to 475°C.

TABLE OF CONTENTS

		Page
1.	INTRODUCTION	1
	1.1. Project Objectives	1
2.	BACKGROUND AND LITERATURE REVIEW	5
	2.1. Coal Liquefaction Kinetics	6
	2.1.1. Mechanisms	6
	2.1.2. Kinetics	11
	2.1.3. Rate Expressions	16
	2.1.4. Model Selection	19
	2.2. Hydrocracking of Residue and Heavy Oil	21
	2.2.1. Mechanisms	21
	2.2.2. Kinetics	27
	2.3 Approach to Coprocessing Kinetics	32
3.	REVIEW OF CANMET'S'S DATA	37
	3.1. Product Definition and Analysis	38
	3.2. Material Balance	42
	3.3. Source of Variance and Accuracy of the Results	43
	3.4. Comparison to Other Studies	50
	3.5. Reactor Hydrodynamics	56
	3.6. Statistical Significance of Various Treatments	59
	3.7. Product Yield and Selectivities	65
4.	DEVELOPMENT AND FORMULATION OF KINETIC MODELS	69
	4.1. Multiple Classification Analysis	69

TABLE OF CONTENTS (Continued)

		Page
4.2.	Definition of Lumps or Pseudo-Components	83
4.3.	Definition of Initial Components for Coal	89
4.4.	Lumped Kinetic Equations for CSTR	93
4.5.	Development of Computer Codes and Algorithms	95
5.	TESTING OF DEVELOPED MODELS	100
5.1.	Selection Criteria for Developed Models	102
5.2.	Six Component Models	103
5.3.	Special Difficulties in Modelling Coprocessing Kinetics	113
5.4.	Modelling the Yield and Distribution of Distillate Fractions	118
5.5.	Sensitivity of the Developed Models to Assumptions	137
6.	CONCLUSIONS AND RECOMMENDATIONS	140
7.	REFERENCES	149
	APPENDICES	153

LIST OF TABLES

Table		Page
1	LUMPED KINETIC MODELS FOR COAL LIQUEFACTION	13
2	CORRELATION OF CCR AND ASPHALTENE	25
3	ACTIVATION ENERGY FOR COKE FORMATION BY ASPHALTENE	31
4	TWO FACTOR ANOVA FOR REPLICATED DATA	46
5	SOURCE OF VARIANCE	49
6	COMPARISON OF CANMET AND HRI COPROCESSING DATA	55
7	SUMMARY OF ANOVA ANALYSIS	61
8	FACTOR MATRIX	84
9	ANALYSIS OF VARIANCE (H/C VS T AND SV)	86
10	ANALYSIS OF VARIANCE (C VS T AND SV)	87
11	ANALYSIS OF VARIANCE (H VS T AND SV)	88
12	SUMMARY OF SIX-COMPONENT MODELS	105
13	KINETIC CONSTANTS FOR MODELS 6, 8 AND 9	106
14	YIELD AND DISTRIBUTION OF C1-C4 HYDROCARBON GASES	117
15	RATE CONSTANT COEFFICIENTS FOR MODEL 52 AND 61	122
16	PERCENT OF VARIANCE EXPLAINED BY MODELS 52, 61 AND 53	136
17	EFFECT OF ASSUMPTIONS ON MODEL 52	139

LIST OF FIGURES

Figure		Page
1	SUMMARY OF PRODUCT ANALYSIS	41
2	MASS BALANCE HISTOGRAM	45
3	CORRELATION BETWEEN PITCH AND COAL CONVERSION	51
4	CORRELATION BETWEEN COAL CONVERSION AND ASPHALTENES AND PREASPHALTENES	52
5	CORRELATION BETWEEN PITCH AND COAL CONVERSION	53
6	DISTILLATE FRACTIONS YIELD (Missing Data Calculation)	62
7	COAL AND PITCH CONVERSION (Missing Data Calculation)	63
8	SELECTIVITY OF DISTILLATE FRACTIONS	67
9	SELECTIVITY OF COPROCESSING PRODUCTS	68
10ab	MULTIPLE CLASSIFICATION ANALYSIS	71
10cde	CONTINUED	73
10fgh	CONTINUED	75
10ijk	CONTINUED	77
10lmn	CONTINUED	79
10opr	CONTINUED	81
10st	CONTINUED	82
11	PLOT OF THFI CONVERSION vs. SPACE TIME	90
12	PLOT OF Ln (Time) vs. 1/T	92
13	COMPUTER PROGRAMS	99
14	SEQUENTIAL AND PARALLEL MODELS	101
15	THFI YIELD	107

LIST OF FIGURES (Continued)

Figure		Page
16	PREASPHALTENES YIELD	108
17	ASPHALTENES YIELD	109
18	OIL YIELD	110
19	DISTILLATES YIELD	111
20	C1-C4 YIELD	112
21	EFFECT OF TEMPERATURE ON PREASPHALTENES	114
22	MODEL 52	120
23	MODEL 61	121
24	THFI YIELD	124
25	PREASPHALTENES YIELD	125
26	ASPHALTENES YIELD	126
27	OIL YIELD	127
28	HEAVY GAS OIL 1 AND 2 YIELD	128
29	LIGHT GAS OIL YIELD	129
30	NAPHTHA YIELD	130
31	C1-C4 YIELD	131
32	MODEL 63	132
33	C1-C4 YIELD	133
34	MODEL 53	135

1. INTRODUCTION

Since 1979, CANMET has been conducting research and process development work on coprocessing of Canadian heavy oil/bitumen and coal for production of alternative transportation fuels. The work completed at CANMET included factorial design of coprocessing experiments aimed at ascertaining the coprocessing kinetics and mechanisms. As a continuation of these studies, in 1986, CANMET undertook a program on Mathematical Modelling of Coprocessing Kinetics, with special emphasis on development of reaction engineering models for improved process performance and operation. This report describes the results and conclusions of that study including recommendations for future work in the coprocessing area.

1.1. Project Objectives

The overall objectives of this project were: 1) to provide an analysis of bitumen/heavy oil and coal coprocessing kinetics in order to develop reaction engineering models for the future design and optimization of the process; and, 2) to generate ideas and methods useful in studying the simultaneous processing of coal and bitumen/heavy oil, which would be helpful in the development of CANMET's coprocessing technology.

The specific objectives of this project included the following:

- to review coprocessing data generated at the CANMET Energy Research Laboratory and perform an analysis of the data with a view of identifying and quantifying the effects of process variables on the rates of generation and selectivities of coal/heavy oil or bitumen coprocessing products.
- to formulate and test kinetic models for coprocessing reactions.
- to predict the yield structure and product distribution for coprocessing.

The proposed approach consisted of three tasks:

1. Review of CANMET's Data: The experimental data generated in CANMET's in-house program was to be reviewed. These data included evaluation of experimental conditions, product definitions and analytical procedures used, comparison of specific product yields and selectivities, and statistical significance of various treatments and effects. In addition, literature on coprocessing and kinetics of coal liquefaction and heavy oil upgrading were to be

reviewed, including comparison of CANMET's data to other reported data.

2. Development and Formulation of Kinetic Models: An analysis of reaction paths for coprocessing products and the effect of process variables was to provide input into the formulation of kinetic models of coprocessing. Special requirements for development of the models would include development of lumped kinetics for CSTR (continuous stirred-tank reactor), development of computer codes and algorithms for models, and performing reactor engineering analysis of the reaction paths for coprocessing products.

3. Evaluation of Kinetic Models: The formulated models were to be tested for simulating the dynamic behaviour of coprocessing reactions in terms of heavy oil and coal conversion, and the yield and selectivities of coprocessing products. This would include development of appropriate statistics and regressing data for the rate constants, development of model correlation criteria, analysis of reaction networks and lumping procedures, and testing of the final models for sensitivity to various assumptions.

The proposed approach was to facilitate a more fundamental understanding of the kinetics of coprocessing

and would provide practical models for design and optimization of the process.

The proposed scope of the project was limited to the CANMET data base, i.e., a 2^3 factorial design, with three levels of temperature and three levels of space velocity. The total experimental matrix included 9 runs with one cell missing.

2. BACKGROUND AND LITERATURE REVIEW

There is a broad acceptance of kinetic models in industry based on the evidence that kinetic models contribute strongly to the development, design and operation of commercial processes. It is quite common today for a process licensing agreement to include a kinetic model which permits studying technical and economic feasibility including optimization of a process. For example, kinetic models have been successfully applied to processes such as fluid catalytic cracking, hydrodesulphurization of crude oils, catalytic reforming, etc.

Modelling of bitumen/heavy oil and coal coprocessing is an example of modelling of complex reaction mixtures where the reacting species form a continuum described by a boiling point distribution, molecular weight or chemical functionality. Modelling such a system entails an understanding of the mechanism of coal liquefaction or heavy oil processing. The theoretical developments which underlie the modelling of the kinetics of coal liquefaction or heavy oil upgrading are discussed below.

2.1. Coal Liquefaction Kinetics

2.1.1. Mechanisms

It is generally agreed that mechanisms of coal liquefaction proceed through a series of steps involving a complex reaction mixture of coal, e.g., hydrocarbon solvent and products. The net result of the liquefaction reactions depends on the type of coal (its organic and inorganic structure), the type of solvent used (its ability to stabilize coal fragments), temperature, pressure of hydrogen or other reacting gas, and residence time and type of reactor.

Coal liquefaction reactions can be classified into several reaction types - bond scission, hydrocracking, thermal cracking, etc. - describing chemical and physical changes taking place during the process. The severity of each reaction depends on the temperature of processing, on coal properties and liquefaction environment (solvent, gas, reaction vessel). Depending on the stage of coal liquefaction, different reactions may become dominant in the process. A general discussion of the key stages in coal liquefaction is presented below.

Coal Dissolution

Scission of physical bonds and weak chemical bonds such as oxygen linkages leads to almost complete solubility of high molecular weight products in polar solvents like pyridine and tetrahydrofuran, and limited solubility in non-polar solvents like benzene and toluene. Reactions taking place during this stage do not, in general, change the basic units of coal organic matter, but rearrange the peripheral polar and non-polar groups such as -COOH, long aliphatic chains, etc. (Whitehurst, et al., 1977). Another reaction proceeding in the early stages, at higher temperatures, is cleavage of carbon-carbon bonds with formation of free radicals (Neavel, 1976). These radicals must be stabilized by hydrogen either from coal molecules (coal hydroaromatic moities) or from a donor solvent. The result of such hydrogen transfer and the accompanying change of structure is a net increase in the aromatic character of reactants and products during the first stage (Whitehurst, et al., 1977). The dissolution step is also relatively insensitive to the quality of solvent due to the ability of coal hydroaromatic moities to transfer hydrogen.

The products of the first stage are typically defined as preasphaltenes and asphaltenes. The chemical structures of these products are believed to include the essential characteristics of coal organic molecules except for the

side-chain functional groups and molecular size. Hydrogenation that may take place at this stage is not likely to be significant. Hydrogenation at this stage is also masked by the net effect of deoxygenation and structural rearrangement. There is very little net hydrogen uptake and few light or gaseous hydrocarbons are formed. An interesting feature during the early stages with non-hydrogenating solvent, at a low space time, is that yields of oil may be negative indicating an adduct formation between the solvent and primary liquefaction products (Sato, 1976, Cronauer, et al., 1979).

Under a hydrogen deficient environment (poor donor solvent), the first stage leads to formation of soluble products which are later converted via retrogressive reactions to insoluble products resembling original coal or coke. These retrogressive reactions are believed to involve condensation reactions of free radicals and oxygen functional groups, such as acidic-OH. They become predominant at temperatures above 743K and a long residence time, even in the presence of hydrogenated solvent (Cronauer, et al., 1978).

Hydrocracking and Hydrogenation

Primary liquefaction products (preasphaltenes and asphaltenes) can undergo significant molecular and chemical

changes at higher temperatures (625K) and longer residence times in the presence of hydrogen. The major reactions are believed to resemble hydrocarbon processing reactions with cleavage of carbon bonds, and saturation and hydrogenation of heterofunctional groups containing oxygen, sulphur and nitrogen. The products are similar to hydrocarbon processing products and can be classified into oils or distillates, pitch and hydrocarbon gases. The light distillate fractions can be further characterized by boiling point into naphtha, light gas oil and heavy gas oil. In order to use the products defined by solubility or distillation as pseudo-components in kinetic studies, it is important that the products derived from different runs and at different stages have the same characteristics. Aczel (1976) characterized the structure of oils, asphaltenes and preasphaltenes from several liquefaction runs and found that products produced in the preheater and the reactor were about the same, even though the amounts were different.

The second stage of coal liquefaction has characteristics of hydrocracking and hydrogenation processes. It is sensitive to the pressure of hydrogen, the presence and type of catalyst, catalytic effects of the feed, etc. Depending on the hydrogen pressure and on temperature, there may be a net hydrogen consumption or production, with the latter occurring when the rate of thermal cracking is larger than the rate of hydrogenation.

In practice, hydrogen pressures larger than 2000 psi at temperatures above 450°C, have been used to prevent dehydrogenation and formation of coke.

Both the dissolution stage and hydrogenation stage may occur at higher temperatures, and they may proceed consecutively or concurrently during the liquefaction run. Heavier organic molecules may be undergoing structural rearrangement while the lighter products can be undergoing hydrocracking and hydrogenation. One has to remember that the feed contains a mixture of molecules with a wide range of molecular weights and a varied distribution of heteroatoms and functional groups. The task of describing the kinetics of liquefaction reactions requires identification of the chemical and physical transitions which are dominant, and explanation of how they depend on the change in the environment (temperature, pressure, etc.) Modelling of such a complex reaction system would entail identifying significant reaction paths, defining lumping criteria for reactants and products, developing reaction networks (models), defining rate expressions for pseudo-components (lumps), clarifying how these rate expressions depend on the processing variables and finally, testing the derived models for their representation of the essential dynamic characteristics of the process. These modelling aspects of coal liquefaction are discussed in the next section.

2.1.2. Kinetics

A number of reaction networks have been proposed to describe coal liquefaction in general, and coal liquefaction kinetics and yield and selectivity of products in particular. Over the years, as better understanding of the mechanisms of coal liquefaction has emerged, more detailed networks encompassing essential features of the process have been proposed. These networks were summarized in a general model proposed by Squires (1978).

In most reported kinetic studies the networks have utilized a concept of grouped species (lumps). The products and reactants were grouped into lumps which were postulated to behave as pseudo-components. The lumping procedure has, for the most part, reflected the degree of the knowledge of the products and the desired complexities of the proposed kinetic models. A more detailed discussion of the issues and problems in using lumped kinetics was presented by Liu and Lapidus (1973).

In general, the approach followed in describing the reaction network included reactant/product lumps like preasphaltenes, asphaltenes, oils, unreacted coal (residue) and gas. A summary of the different reaction networks tested and reported in the literature is presented in Table 1. An obvious conclusion from these networks is that the

depicted models are derived from a general network in which one would recognize discrete lumps for reactants and products, similar to the model proposed by Squires (1978). Depending on the liquefaction conditions and feed composition, such a generalized network would be reduced to a simpler network which represents the essential paths for liquefaction reactions.

An argument presented in opposition to the interpretation that such postulated reaction paths represent coal liquefaction mechanisms is that the derived mathematical models and their mathematical forms often contain a large number of constants, and are general enough to provide a mathematical description of specific experimental data irrespective of whether they represent the global mechanisms or not. Such kinetic models would correlate a given set of kinetic data, but would provide little information on liquefaction behaviour of different coals, in different vessels. The networks, themselves, would only be specific for a given set of experimental data. A more detailed discussion of these issues is presented in the next section.

A somewhat different formulation of the reaction paths for coal liquefaction was proposed by Shah, et al. (1978) using a boiling range classification for pseudo-components.

Table 1. LUMPED KINETIC MODELS FOR COAL LIQUEFACTION

Kinetic Structure	Investigator
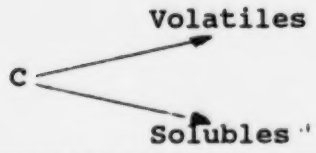	Falcum, et al., (1952)
C ⟶ A + O	Pelipetz, et al., (1955)
C ⟹ Solubles	Curran, et al., (1967)
	Leibenberd, et al., (1972)
	Yoshida, et al., (1976)
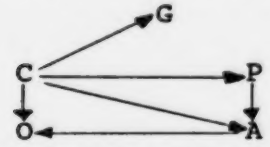	Cronauer, et al., (1978)
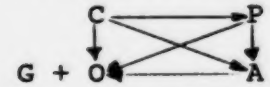	Shalabi, et al., (1979)
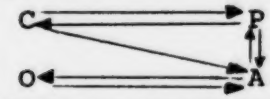	Gertenbach, et al., (1982)

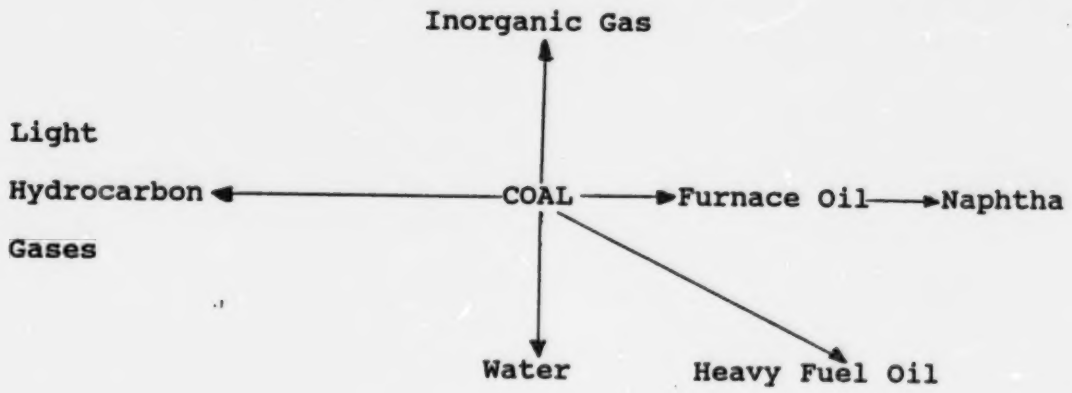

An important conclusion arising from the application of this network to a set of liquefaction data was that the rate of formation of gases and water can be described by only one reaction path for these products directly from coal.

A free radical chain mechanism for coal liquefaction reactions was proposed by Attar (1978). The reaction paths included three essential free radical steps, i.e., initiation, propagation and termination, and the derived model correlated the product yield and selectivity. The important conclusion drawn from this study was that the activation energies for the overall (lumped) liquefaction reactions have little theoretical significance. A similar conclusion was drawn using a different methodology by Szladow and Given (1981). Szladow and Given (1981) also have shown that if appropriate procedures are followed, the derived activation energies have specific properties which can be helpful in developing and evaluating different liquefaction models.

In yet another approach (Mohan, et al., 1981), liquefaction products were separated according to their chemical functionalities such as aromatics (A), ether compounds (E), nitrogen compounds (N), hydroxyl compounds (H), large multifunctional compounds (M), and unreacted coal (C). Several models were tested with this grouping and the best correlation was obtained for the model depicted below.

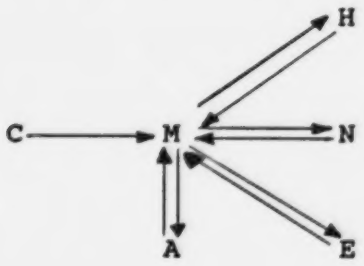

An interesting observation was also made suggesting that <u>multifunctional compounds follow different time/concentration profiles depending on temperature.</u>

Recently Prasad, et al., (1986a, 1986b) proposed a mathematical model based on the work of Aris and Gavalas (1966) utilizing the concept of reactions in a continuum. The reaction mixture was described in terms of the number of carbon atoms and the number of oxygen atoms per molecule. The products were grouped into pseudo-components based on molecular weight, and the product distribution was adjusted by a characteristic "molecular weight" of coal. The model was found to predict product distribution well for several

coals. The effect of a catalyst in the presence of a good donor solvent was shown to accelerate all reactions equally, without altering the selectivity. It was also concluded that the catalyst function in the presence of a poor solvent is primarily to promote hydrogen transfer reactions in the solvent.

An increased degree of sophistication in the proposed liquefaction models has been reflected by an increased understanding of the liquefaction mechanisms and increased computational capabilities for solving mathematical equations in the postulated models. It is generally believed that the proposed models describe the important chemical reactions taking place during liquefaction, and that they capture the reactant and product transformations. Still in doubt are the specifics of the networks and whether or not the models could yield meaningful results when applied to different coals and different reaction vessels. More on this subject is presented in the next section.

2.1.3. Rate Expressions

Most of the coal liquefaction kinetic models used pseudo-first order functions for rate expressions and an Arrhenius representation for rate constants.

$$\text{rate} = k(1-X)$$

where X = fractional coal conversion

k = A exp(-E/RT)

A = preexponential factor

E = Arrhenius activation energy

A slight modification to the above rate expression was proposed by several investigators (Curran, et al., 1967, Falcum, et al., 1952) in order to recognize that part of coal, i.e., mineral matter and inerts, is not reactive, and that at any temperature coal achieves an equilibrium fractional conversion, X_e, which is always less than 1.0.

The modified rate expression has been written in a form:

$$\text{rate} = k(X_e - X)$$

The value of X_e at long times depends on temperature, possibly pressure, and the nature of the donor solvent. It is not clear, however, whether at short contact times X_e is also a function of temperature. It may be postulated that at short contact times, X_e is characterized by the reactive part of coal (100% - percent mineral matter - percent inert organic part of coal) (Szladow and Given, 1982, Prasad, et al., 1986b).

It is not clear why the grouped species in the coal liquefaction models, which are characterized by diverse properties and molecular weights, would have pseudo-first order rate expressions for lumped kinetics. Perhaps it reflects the fact that not enough studies have been completed to clarify this issue. Earlier coal liquefaction models did postulate rate expressions with other than first-order kinetics (Wiser, 1968). For example, rate expressions included coal/solvent interactions:

$$\text{rate} = k(X_e - X)\ (S - X)$$

where S is the initial weight fraction of hydrogen donor solvent.

A similar development was recently proposed by Gallakota, et al., (1985). In the majority of cases, however, investigators used first order rate expressions which lead to a less complicated mathematical solution for rate constants.

A number of theoretical papers were published on the subject of complex reacting mixtures and on the order of global rate expressions for grouped species (Prater, et al., 1967, Wei, et al., 1969, Luss and Hutchinson, 1971). The order of rate expressions for the product lumps is not necessarily the same as the order of reactions that lead to that grouped species. The grouped species must conform to several criteria in order to be exactly lumpable, i.e., to

have kinetic dynamics that can be exactly described by first-order kinetics. With the use of lumps, such specific information is often lost (Bailey, 1972).

2.1.4. Model Selection

A criterion often applied for model selection is the extent to which the model correlates the experimental data. A least-square fit method would also be most likely used for optimization. Interestingly enough, not a single published investigation has reported proper statistics for the data and model analysis, which would indicate how much of the variance is due to the controlled variables and how much is due to errors. Our experience suggests that most of the reported coal liquefaction models do not justify the sought degree of least-square fit because of the presence of large experimental errors. In fact, it is doubtful that the least-square criterion is appropriate for discriminating between models with more than two or three constants unless appropriate statistical analysis is performed.

A different approach to the problem of discriminating between models which fit experimental data equally well was proposed by Szladow and Given, (1982). The proposed development showed how information about apparent activation energy and its dependence on conversion can be used to improve on kinetic models. It also showed how to remove

insensitivity problems associated with the model's kinetic parameters. The method was used successfully to reduce a large number of possible kinetic structures to a few structures that could be further tested.

Additional criteria concerning the number and the order of the formation and disappearance paths were proposed for coal liquefaction based on the work of Lee (1977). The development showed (Szladow and Given, 1982) how one can determine the number of necessary parallel reaction paths for the formation of coal liquefaction products, assuming pseudo-first order reactions for each step, and a pseudo-homogeneous, plug-flow model.

In summary, it should be stressed that reaction models obtained using simple criteria of pseudo-first order kinetics and Arrhenius expressions, without analysis of reaction paths and rate expressions, are not likely to describe dynamic behaviour of liquefaction reactions in different reactors at different conditions. The quoted newer developments permit some discrimination between models and allow the application of the principles of reaction engineering in design and optimization of coal liquefaction vessels.

2.2. Hydrocracking of Residue and Heavy Oil

2.2.1. Mechanisms

Hydrocracking generally consists of two primary reactions: cracking and hydrogenation. Other reactions, such as desulphurization, denitrogenation, demetallization, etc., are considered to be secondary reactions during hydrocracking of heavy oil and bitumen.

The severity of hydrocracking depends on the type of heavy oil/bitumen being processed, cut point of residue, residence time, temperature and pressure. The effect of pressure becomes insignificant when the system is operated at a pressure higher than the minimum level which is required to provide sufficient hydrogen concentration in the liquid phase to prevent the formation of coke.

Coking has been the major problem in upgrading heavy oil/bitumen with hydrogen. The mechanisms of coking and the method of preventing coke's formation, along with thermal cracking and hydrogenation, will be discussed in detail in the following section. The following section also discusses the influence of bitumen/heavy oil as solvent in coprocessing with coal and the effect of hydrocracking reactions on the overall coprocessing.

Thermal Cracking

Thermal cracking is one of the most important refining processes with or without the aid of catalysts. Fluid catalytic cracking, visbreaking, delayed coking and fluid coking are typical of thermal cracking used in refineries. Residue of bitumen or heavy oil cracks at temperatures above 660K and first produces smaller unstable free radicals (Belinko and Denis, 1976). The radicals, at different sizes, react with other radicals or hydrogen to form smaller stable products.

The cracking activity of the various hydrocarbons differs and decreases in the following order: normal paraffins, iso-paraffins, cycloparaffins, aromatics, aromatic naphthenes and polynuclear aromatics (Hus, 1981). Paraffins are primarily cracked to smaller paraffins and olefins. Practically no carbon and hydrogen are formed in the cracking of paraffins, so that little coke formation takes place in the cracking of paraffins. Olefins and diolefins, most of which exist in the naphtha fraction, usually have a short chain length and undergo little cracking.

Bitumen or heavy oil contains naphthenes and aromatics with long side chains, which are cracked in such a way that the side chains are shortened to methyl or ethyl groups.

Cracking of naphthene and aromatic rings occurs at temperatures higher than 763K without the presence of catalysts. This explains why the cracked products of bitumen or heavy oil have a high content of naphthene and aromatics. Under a hydrogen environment, such as the CANMET Hydrocracking process, distillate product contains a combined total of more than 50 wt% of naphthenes and aromatics.

Hydrogenation

The main function of non-catalytic hydrogenation, particularly at elevated pressure, is to stabilize free radicals produced during cracking. The removal of sulphur, nitrogen and oxygen are side reactions of the hydrocracking of bitumen and heavy oil.

Sulphur removal from hydrocarbons can be classified, although the definition is arbitrary, as destructive and non-destructive (Speight, 1981). The hydrotreating process is generally considered non-destructive. The kinetics of hydrotreating are well documented; however, the kinetics of hydrotreating can not be directly applied to destructive desulphurization, such as hydrocracking or coprocessing.

The difficulty of sulphur removal increases in the same order as cracking, i.e., aromatics> naphthenes> paraffins

(Speight, 1981). Therefore, one can conclude that sulphur removal in hydrocracking of bitumen occurs mainly on cracked light hydrocarbons in non-catalytic hydrocracking or coprocessing. This is evidenced by the fact that residual product pitch has the same sulphur content as feed in the CANMET Hydrocracking process. However, this has not been observed in coprocessing.

Coking

Carbon residue, expressed either as Conradson (CCR) or Ramsbottom, affects operation, but has received little attention in hydrocracking. The CCR has been used for predicting the amount of coke produced in the carbon rejection processes, such as fluid coking, flexicoking and delayed coking. The CCR is also used to predict the rate of catalytic deactivation in various catalytic processes (Sosnowski, et al., 1981). It seems that CCR may be correlated with maximum conversion in hydrocracking.

Asphaltenes are considered to be the principal component causing coke formation in hydrocracking and coprocessing. Table 2 shows a correlation between carbon residue and asphaltene content.

As seen from Table 2, asphaltene content is 2 - 6 wt% higher than CCR for all bitumen, heavy oil and its reduced

residue. It is not surprising that the asphaltene has much higher carbon content than other fractions.

Table 2. CORRELATION OF CCR AND ASPHALTENE

Feeds	CCR (wt%)	Asphaltene (wt%)	Reference
Athabasca pitch	27.5	30.6	deBruijn, et al., (1982)
Boscan 343 C+	16.7	22.3	deBruijn, et al., (1982)
Cold Lake bitumen	13.6	15.9	Speight (1981)
Cold Lake vac. bot.	17.1	23.5	Kelly, et al., (1984)
Lloydminster	9.1	12.9	Speight, (1981)
Lloydminster 343 C+	14.0	17.6	deBruijn, et al., (1982)

Asphaltenes are very soluble in aromatic hydrocarbons, but not in light paraffinic hydrocarbons. The mechanism of coke formation was illustrated by Hus (1981), who suggested that asphaltenes consist of a core micelle surrounded by high-molecular weight aromatic hydrocarbons from the malthene fraction. The micelle absorbs hydrocarbons with higher hydrogen content as satellites and is physically in equilibrium with the continuous phase through absorption forces.

This absorption equilibrium can be disturbed in several ways, for instance, by adding hydrocarbons rich in hydrogen and by increasing temperature. A portion of the absorbed

compounds then dissolves in the continuous phase, whereby the asphaltene cores precipitate and eventually degrade to form coke (Banerjee, et al., 1986). During thermal cracking, asphaltene can be formed by condensation, at higher conversion of aromatics and polynuclear aromatics.

The malthene in the micelle appears to be similar to resins. The physical and chemical properties are in transition between asphaltene and oils. Resins contain polar aromatics, which are soluble in pentane but insoluble in liquid propane. Under mild cracking conditions, the content of resins increases initially and then decreases with increasing temperature. However, the resins content appears to be insignificant at severe cracking conditions.

Bitumen and heavy oil have been considered good solvents for dissolving coal in coprocessing and have also been referred to as "hydrogen donor" agents. Bitumen and heavy oil contain less hydrogen than solvents used as hydrogen donor agents for coal liquefaction. Thus bitumen would not be considered a good hydrogen donor; however, in practice, bitumen and heavy oil have been found to be excellent solvents because of resins which contain polar aromatics. Among the three major components in bitumen, resins are likely to be the active component in dissolving coal. Asphaltenes are high in carbon content and do not have as strong a solubility as resin. There is 47 wt% of

resins and only 24 wt% asphaltenes in Athabasca vacuum bottoms.

In conclusion, asphaltene is the sole source for coke formation and is in good correlation with carbon residue content in bitumen or heavy oil. Resins appear to be an excellent solvent for coal in coprocessing. The high severity of cracking will cause the formation of asphaltene from the condensation of aromatic oil.

2.2.2. Kinetics

Many studies have been reported on the thermal cracking of heavy oil or other hydrocarbons. Most of the experiments were conducted at pressures less than 200 psig and in an inert gas environment. The operating conditions were generally different from those for coprocessing.

In a kinetic study on visbreaking (Hus, 1981), the cracking of short residue was represented by a monomolecular reaction, so that the fraction converted, X, of the feed can be expressed as:

$$\ln\left(\frac{1}{1-X}\right)=kt$$

where k was defined as velocity constant. In fact k is a parameter function of fluid velocity and rate constant. The k was then expressed by an Arrhenius equation:

$$\ln(k) = \frac{E}{RT} + b$$

The value of activation energy, E, as obtained for short residue was 40 Kcal/mol.

The single pseudo-component model was also applied to hydrocracking of a light hydrocarbon, n-decane (Beecher, et al., 1968). The products were later divided into three groups: nonbranched, branched and feed isomer (Flock, et al., 1976). Complex reaction schemes have been used for hydrocracking and hydroisomerization of n-decane, n-dodecane and n-octane (Steijns and Froment, 1981, Baltanas, et al., 1983). Seven reaction networks were proposed with only three lumped products. In a study of fluorene hydrocracking (Constant, et al., 1986), fourteen group components were identified ranging from alkane gas to methylfluorene. Without a detailed mechanism, twelve differential equations were developed for reactive components.

Stangeland (1974) proposed a kinetic model for the hydrocracking of the heavy gas oil fraction. In his model, the feed and product streams are assumed to contain a continuum of components that are characterized solely by boiling point. These components are then segregated into

fixed boiling ranges of 50°F each and treated as reactants. Each component undergoes a first order reaction to produce a spectrum of light products. This model results in a number of kinetic parameters equivalent to the number of components. Extensive mathematical computations would be required to obtain kinetic data for each component. Instead, Stangeland simplified the system by assuming kinetic rate, for each boiling range, as a function of boiling point, as below,

$$k(t) = k\,[T + A(T^3 - T)]$$

where T is the boiling point. The rate expression is a function only of a constant, A, which is to be determined. For the same approach, the product distribution consisting of only two parameters is shown below,

$$P(t) = [t^2 + B(t^3 - t^2)](1 - C)$$

where B and C are parameters to be determined by the shape of product TBP curve, and P(t) is the product distribution as a function of normalized product boiling point, t. This is an interesting concept and method.

For residue hydrocracking, two papers recently presented mathematical modelling of the respective reactors

for the CANMET Hydrocracking process (Liu, et al., 1985a, 1985b) and the H-Oil process (Li and Lin, 1981).

A single lumped variable, pitch, was used in modelling the CANMET reactor. Since pitch conversion is of main interest in the study, a simple process scheme, Pitch ---> Products was employed. However, this scheme is oversimplified so that important information is lost about the catalyst function, coke formation and yields of different products. An axial dispersion model was used in the CANMET Hydrocracking process in a macro approach to a tubular reactor system. The same model was also employed by the SRC coal liquefaction process (Parulekar and Shah, 1979).

A CSTR model was used (Li and Lin, 1981) to describe the thermal stability of the H-Oil ebullated reactor. Like CANMET, H-Oil assumed a single lumped variable in the model, and the kinetic constant as well as other variables, i.e., space velocity, were lumped into one parameter. No kinetic data were reported.

The formation of coke from asphaltene was the subject of a study by Banerjee, et al., (1986). A simple reaction was proposed for coke formation, asphaltene ----> coke, (Table 3).

Table 3. ACTIVATION ENERGY FOR COKE FORMATION BY ASPHALTENE

Feedstock	Reaction Coefficient (1/min)	Activation Energy (Kcal/g-mole)
Athabasca bitumen	448	10.5
Topped Athabasca	946	11.2
Cold Lake	273	9.8
Arabian vac. bot.	920	11.0

In a study by Khulbe, et al., 1984, the extent of asphaltene coking was determined during the pyrolysis of Cold Lake asphaltene. The experimental conditions were also identical to conditions reported by Banerjee, et al., (1986). The reaction rate expressed as a second order of reaction was found to fit well the data for decomposition of Cold Lake asphaltenes. The activation energy and the Arrhenius constant were calculated to be 56.6 Kcal/g-mole and 5.2×10^8 1/min. These values cannot be compared, however, to kinetic data derived using a different order of the rate expression.

In summary, it appears that no systematic studies have attempted to analyze the reaction mechanisms or the cracking of heavy oil/bitumen, with or without hydrogen, nor to investigate the comprehensive kinetics of the hydrocracking reaction. Without a comprehensive knowledge of the reaction

paths and kinetics, it is difficult to determine the exact contribution of hydrocracking to coprocessing of coal and heavy oil. However, a general approach can be formulated for important reactor paths in coprocessing, based on limited knowledge of hydrocracking and coal liquefaction kinetics and on general principles of chemical reactor engineering. This approach is presented in Section 2.3.

2.3. Approach To Coprocessing Kinetics

The above summary of coal liquefaction and heavy oil upgrading kinetics provides a state-of-the-art review of knowledge and methods used to describe the dynamic behaviour and chemical transformations taking place during these processes. A number of features common to these processes are listed below.

Similar chemical reaction types, such as bond scission, hydrocracking and thermal cracking occur in both processes but a different reaction type is dominant depending on the reaction environment and stage of the process. In both cases, cleavage of bonds results in formation of free radicals which must be stabilized by hydrogen either from donor molecules or from other hydrocracking molecules by internal rearrangement. The key operating variable is the temperature, with the degree and rate of bond cleavage determined predominantly by the processing temperature.

Preliminary products can undergo further chemical and molecular changes with a resultant product having a wide range of distribution of molecular weight, chemical functionalities and heteroatom content. These products can be classified based on solubility, boiling point, etc. The products' chemical character is determined by the feed properties, i.e., coal liquefaction products are more hydroaromatic; however, in both processes, the products can be classified into similar groups such as oils, distillates or hydrocarbon gases.

Under hydrogen-rich process conditions, both processes result in a net hydrogen uptake, and in lower molecular weight high hydrogen content products. In the case of hydrogen deficient conditions, both processes may yield significant quantities of coke and hydrogen gases as a result of thermal dehydrogenation processes. The balance between hydrogenation and dehydrogenation reaction is very complex, since even in the hydrogen-rich environment, the heavier molecules may undergo structural rearrangement and dehydrogenation, while the lighter products may undergo hydrocracking and hydrogenation. Consequently, modelling the hydrogen distribution and net uptake is the most difficult of the kinetic aspects of the coal liquefaction and heavy oil upgrading processes. Such a task would be beyond traditional kinetic work and would require study into structural changes of reactants and products.

From the point of view of kinetic models, modelling of these complex reacting mixtures entails identifying dominant reaction paths, defining lumping criteria for reactants and products, defining reaction networks and rate expressions, and testing the desired kinetic models for their representation of the essential dynamic characteristics of these processes. As long as the defined product characteristics are the same for different runs and different stages, both processes should, in principle, be amenable to modelling using the concepts of lumps and pseudo-first order kinetics.

Although most of the modelling principles and techniques applied to coal liquefaction apply to heavy oil upgrading and vice versa, the actual emphasis and preferred methodologies differ slightly. In coal liquefaction, most of the attention has been focused on lumped kinetics using solubility as a criterion for lump definition and characterization. In heavy oil upgrading, lump kinetics employ functional groups or boiling point range more often as a lumping criterion. This may reflect the fact that products of heavy oil upgrading are generally lighter and more amenable to the latter characterization. Indeed, in the case of coke formation from heavy oil, most studies used solubility determination as the criterion defining the lumping of the coking products.

In summary, modelling of coal liquefaction and heavy oil kinetics entails a number of common features, with each relying heavily on experiences in the other field. The choice of specific methodology, in general, reflects specific product characteristics or process stages, rather than fundamental differences in process chemistry or dynamics. It is felt, therefore, that the modelling of coprocessing may relate to a number of methods successfully applied to coal liquefaction or heavy oil upgrading. The actual choice of lump criteria or definition will depend more on experimentation than on kinetics.

We recommend the following approach to modelling coprocessing kinetics:

- analyze CANMET coprocessing data for completeness and accuracy.
- review the effects of reactor type, dimensions, gas holdup, etc., on the data.
- confirm the independence of the lump definition on the severity of the process.
- determine the major effects of process-independent variables, i.e., temperature and space velocity, using analysis of variance (ANOVA) procedures.
- determine the overall effects of temperature and space velocity using Multiple Classification Analysis. Present the results in graphic form, depicting the effects of temperature and space

velocity levels on the yield and selectivity of coprocessing products.

- determine probable kinetic structures and models as suggested by the statistical analysis.
- analyze the reaction paths and required number of initial lumps for coal.
- determine rate constants and apparent activation energies for coprocessing.
- determine the utility of the models by analysis of the percent of variance explained by the models, for all coprocessing data and for each product.
- review the reaction paths and models as required to simulate the CANMET coprocessing data.

3. REVIEW OF CANMET'S DATA

Thirteen sets of experimental data were received from CANMET for analysis and development of kinetic models. The data were generated during the March, 1983 to March, 1985 experimental programs at the Energy Research Laboratories at Bell's Corners. The experiments were conducted in a continuous coprocessing hydroliquefaction unit, a detailed description of which was given elsewhere (Fouda, et al., 1982). The unit is equipped with instrumentation to measure and record feed, reactor and receiving vessel temperatures, line pressures, and flow rates (mass) with sufficiently high accuracy for modelling the kinetics of coprocessing.

The process conditions for the thirteen runs were within the ranges:

Temperature: 400 to 455°C
Nominal Slurry Space Velocity: 0.50 to 1.54 kg/L/hr
Reactor Pressure: 2000 psig (one run at 2500 psig)
Hydrogen Flow: 3.99 to 8.10 L/min
Run Duration: 80 to 180 min
Total Feed Processed: 402 to 600g
Coal Concentration: 29.71 to 33.88 maf wt% feed

A summary of the detailed yield structure is provided in Appendix 1.

3.1. Product Definition and Analysis

The collected product streams were combined and the whole product was analyzed for the following product fractions:

Naphtha: weight percent of IBP -205°C liquid product, including C_5 and C_6 hydrocarbons, based on moisture-and-ash-free (maf) slurry feed.

Light Gas Oil: weight percent of 205 - 315°C liquid product based on maf slurry feed.

Heavy Gas Oil 1: weight percent of 315-435°C liquid product based on maf slurry feed.

Heavy Gas Oil 2: weight percent of 435-525°C liquid product based on maf slurry feed.

Oils: weight percent of pentane solubles in the residue (+525°C) based on maf and slurry feed.

Asphaltenes: weight percent of toluene soluble, pentane insolubles in the residue (+525°C) based on maf slurry feed.

Preasphaltenes: weight percent of tetrahydrofuran solubles, toluene and pentane insolubles in the residue (+525°C) based on maf slurry feed.

Tetrahydrofuran Insolubles (THFI): weight percent of ash-free tetrahydrofuran insolubles in the residue (+525°C) based on maf slurry feed.

Hydrogen Sulphide: weight percent of hydrogen sulphide gas based on maf slurry feed, determined by gas chromatographic analysis.

Water: weight percent of water based on maf slurry feed, determined by distillation.

Carbon Oxides: weight percent of carbon monoxide and dioxide (combined) based on maf slurry, determined by gas chromatographic analysis.

C1-C4: weight percent of combined methane, ethane, ethylene, propane, propylene, butane and butylene based on maf slurry feed, determined by gas chromatographic analysis.

Hydrogen Consumption: weight percent hydrogen consumed based on maf slurry feed.

Coal Conversion: 100 minus weight percent ash-free THF insolubles in the residue (+525°C) based on the feed coal.

Pitch Conversion: 100 minus weight ash-free residue (+525°C) based on maf pitch in the feed (heavy oil and coal).

A summary of the product workup and resulting product definitions are depicted in Figure 1.

The distillate products were also analyzed to obtain information on:

- specific gravity
- elemental composition C,H,N,S, and O
- H'NMR data and aromaticity
- GC-MS PONA analysis
- simulated distillation data
- molecular weight by vapour pressure osmometry

The residue (+525°C) was analyzed for:

- elemental composition C,H,N,S and O
- metal content Fe, Ni and V
- ash content

The solubility of residue in pentane, toluene and THF was determined using a sequential soxhlet extraction.

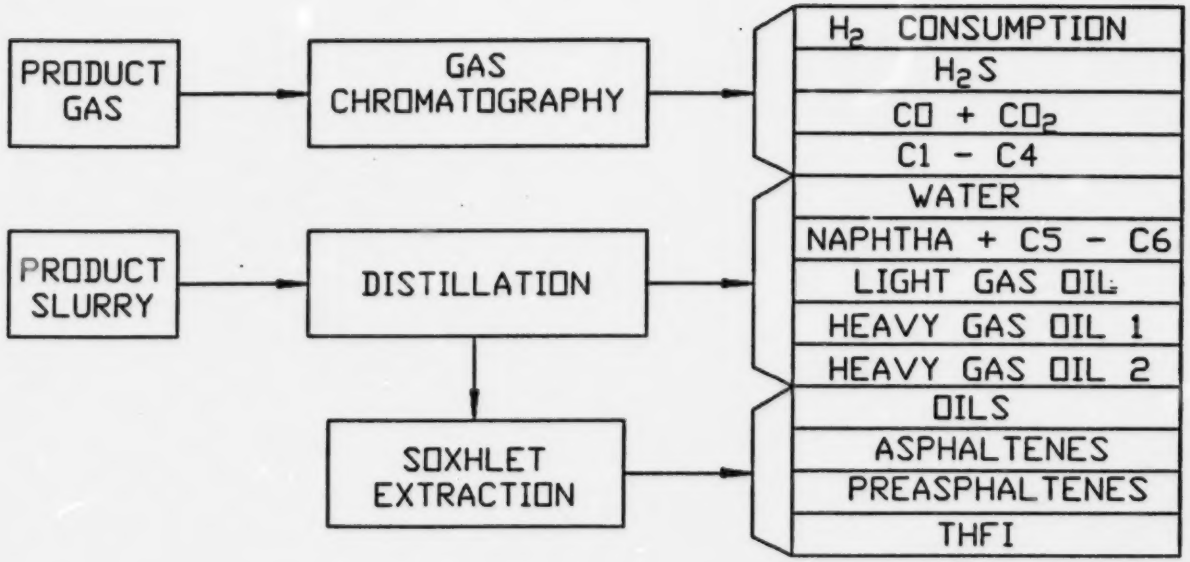

Figure 1. SUMMARY OF PRODUCT ANALYSIS

The above analytical information is provided in this report only where required.

3.2. Material Balance

The percent recovery of the input feed was between 96.40 and 105.02 percent for the thirteen runs, with standard deviation equal to 2.84 percent and a mean of 100.78.

These were calculated from:

INPUT:

1. Hydrogen introduced during the run period, calculated from the hydrogen flow rate and the duration of the test.

2. Slurry fed during the run period determined from the initial and final weights of the feed tank.

OUTPUT:

1. Liquid products collected in the receiver vessel during the test period, determined by the total weight.

2. Light ends discharged from the light ends condenser and weighed directly.

3. Effluent gases determined from the measurement of the exit gas volume and composition. The effluent gas volume was corrected for volume of slurry in the receivers.

The material balance (Figure 2) was very good for the range of experimental conditions and the bench-scale equipment. It facilitated good reproducibility for the product yield structure and a high correlation of the product yield and selectivity by the developed models.

3.3. Source of Variance and Accuracy of the Results

In order to determine how much of the variance in the coprocessing data is due to process variables and how much is due to errors in measurement, we had to relate the experimental variance to the standard deviation for each component group (lump).

Since the CANMET data set had only one experiment in each cell of the Latin Square Design, it was necessary to use additional data in sufficient number of replicates to calculate the standard deviation for coprocessing products. For this purpose, six replicate data sets at T = 450°C and sv = 1.0 were selected for statistical analysis. It was then assumed that the relative standard deviations for

coprocessing products are independent of the factor levels for temperature and space velocity.

Table 4 presents results of the two-factor ANOVA for the six selected replicate runs. The basic equation for the column and row means and standard deviations are given in Appendix 2. The R(i) to RSR(i) columns and C(j) to CSC(j) rows are defined as follows:

R(i) = mean value for row i
TVR(i) = total variance for row i
SR(i) = standard deviation for row i
RSR(i) = relative standard deviation for row i
t-statistics for 80% confidence interval
C(j) = mean value for column j
TVC(j) = total variance for column j
SC(j) = standard deviation for column j
RSC(j) = relative standard deviation for column j
t-statistics for 80% confidence interval.

It should be noted that the total variance of the six replicates (VT) is equal to the sum of variance due to dependent variables (VR), due to replicates (VC) and due to the residual error (VE)

$$VT = VR+VC+VE$$

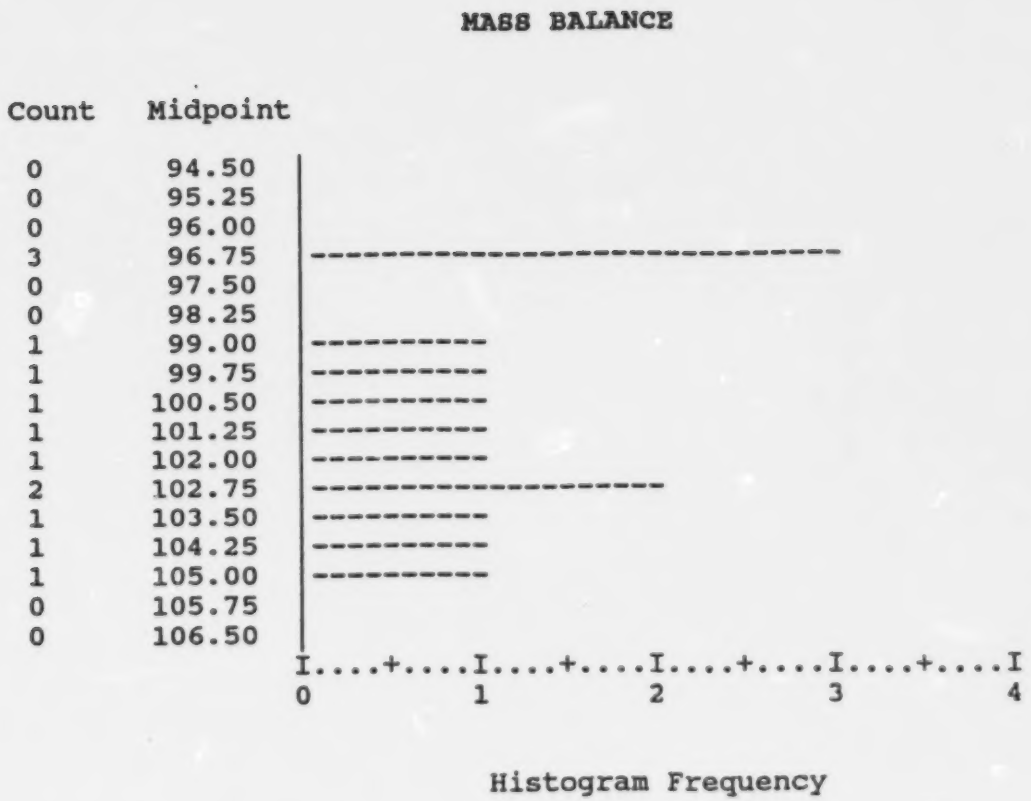

Figure 2. MASS BALANCE HISTOGRAM

Table 4. TWO FACTOR ANOVA FOR REPLICATED DATA

	1	2	3	4	5	6	R(i)	TVR(i)	SR(i)	RSR(i)
THFI	4.30	6.10	5.50	4.10	5.20	4.60	4.96	2.95	0.76	0.15
PA	3.50	1.60	2.50	7.90	6.20	6.50	4.70	31.26	2.51	0.53
A	7.40	5.70	8.20	12.60	11.40	12.70	9.66	43.83	2.96	0.30
OIL	15.50	11.10	12.10	6.50	7.90	5.80	9.81	69.96	3.74	0.38
HGO	27.60	31.90	27.00	25.30	23.00	23.90	26.45	51.05	3.19	0.12
LGO	21.80	19.30	21.40	21.60	20.10	19.00	20.53	7.55	1.22	0.05
NAPH	13.30	13.20	13.40	14.20	14.70	15.30	14.01	3.70	0.86	0.06
C1-C4	4.96	6.57	5.68	5.01	5.54	6.06	5.63	1.91	0.61	0.10
C(j)	12.29	11.93	11.97	12.15	11.75	11.73				
TVC(j)	554.9	663.6	502.2	432.4	332.2	360.1				
SC(j)	8.90	9.73	8.47	7.85	6.88	7.17				
RSC(j)	0.72	0.81	0.70	0.64	0.58	0.61				

It follows from these definitions, that (VR/VT)x100 indicates the percent of variance that is due to the process variables and which should be explained by the developed mathematical models. Substituting the values for VR and VT

$VR = 2.635 \times 10^3$ and $VT = 2.848 \times 10^3$

gives $(VR/VT) \times 100 = 92.5\%$

We should, therefore, expect that for an eight component grouping (HGO1 and HGO2 were grouped together), 92.5 percent of the total variance in the coprocessing data should be explained by the postulated mathematical models. Appendix 2 also provides two-factor ANOVA for the grouping of six components with the calculated percent of total variance due to process variables equal to 98.7 percent.

We have asked a similar question with respect to the individual components as to how much of component variance is due to the process variables. We have defined this variance by the equation:

$$F(i) = 100 - (V(S(i))/VT) \times 100$$

where V(S(i)) = variance due to error equal to the component standard deviation S(i)

$$V(S(i)) = S(i) \sum_{j=1}^{9} (X(i))$$

$$VT = \sum_{j=1}^{9} (X(i) - GMEAN)^2$$

and

GMEAN = the grand mean for all coprocessing data.

Table 5 presents the calculated percent of variance due to the process variables for each grouped component of the coprocessing products. It should be noted that the relatively low value for asphaltenes and oil is due to the use of the grand mean in the definition of the total variance, and the specific combination of the mean values for those dependent variables.

The component variance due to process variables is dependent on the product type. One would expect ,therefore, that material balances would be seriously affected by the variability of feed, complex characterization methods and variability of the equipment performance. However, the overall product balance and variance due to process variables were excellent, enabling us to proceed with the development of kinetic models.

Table 5. SOURCE OF VARIANCE

Variable	S(i), %	F(i), %
THFI	15.5	92.1
PA	53.5	91.7
A	30.6	52.4
OILS	38.1	66.0
HGO 1+2	12.1	94.1
LGO	5.9	98.8
NAPHT	6.1	99.4
C1-C4	10.9	99.7
TOTAL	-	92.5

3.4. Comparison to Other Studies

Figure 3 shows a general relationship between coal and pitch conversion. The data depict two quite distinct coprocessing regions:

- the lower severity region which is characterized by a rapid coal dissolution up to 50 percent and relatively little hydrocracking of heavy oil.
- the high severity region which is characterized by extensive pitch conversion paralleled by a gradual decrease of the asphaltene and oil content (Figures 4 and 5).

The concentration of preasphaltenes achieves its maximum at about 70 to 80 percent of coal conversion as could be expected for an intermediate product.

Investigations which were reviewed and compared to CANMET data are listed in the references. Data reported by Yoshida, et al., 1983, Ignasiak, et al., 1984, Audehn, 1984, Moschopedis, 1982, 1984, and Moschopedis and Ozum, 1984 could be compared to CANMET data only in a qualitative sense since those data were derived in a batch reactor. For the same reason, the data reported by Gates, 1982 and Curtis, et al., 1984 were excluded from a direct comparison.

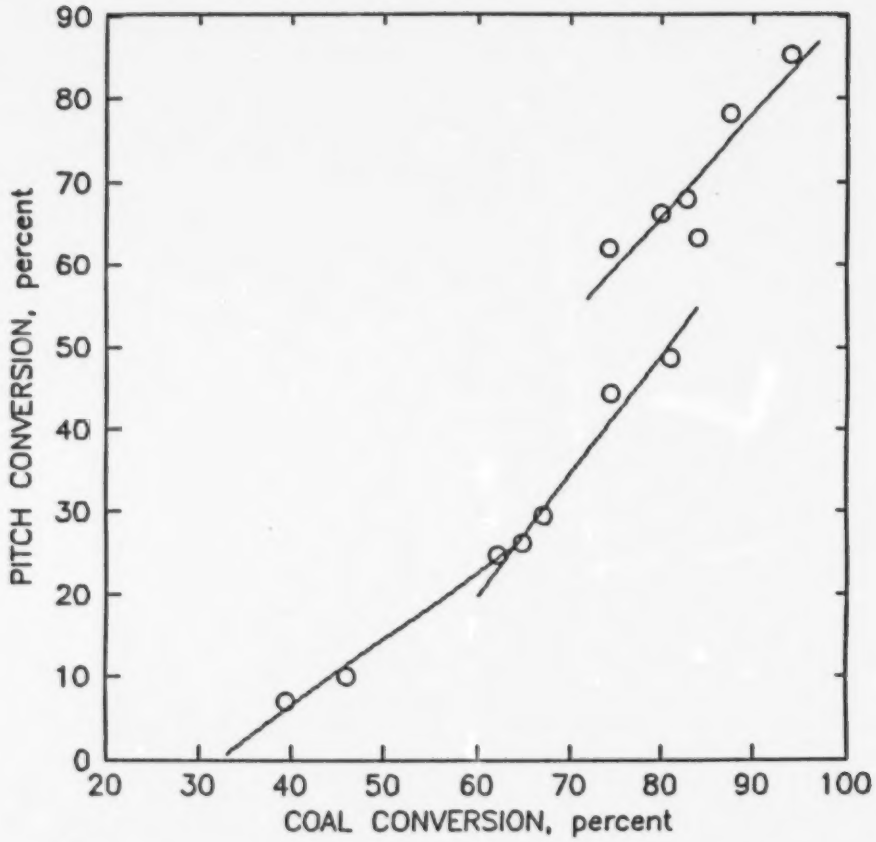

Figure 3. CORRELATION BETWEEN PITCH AND COAL CONVERSION

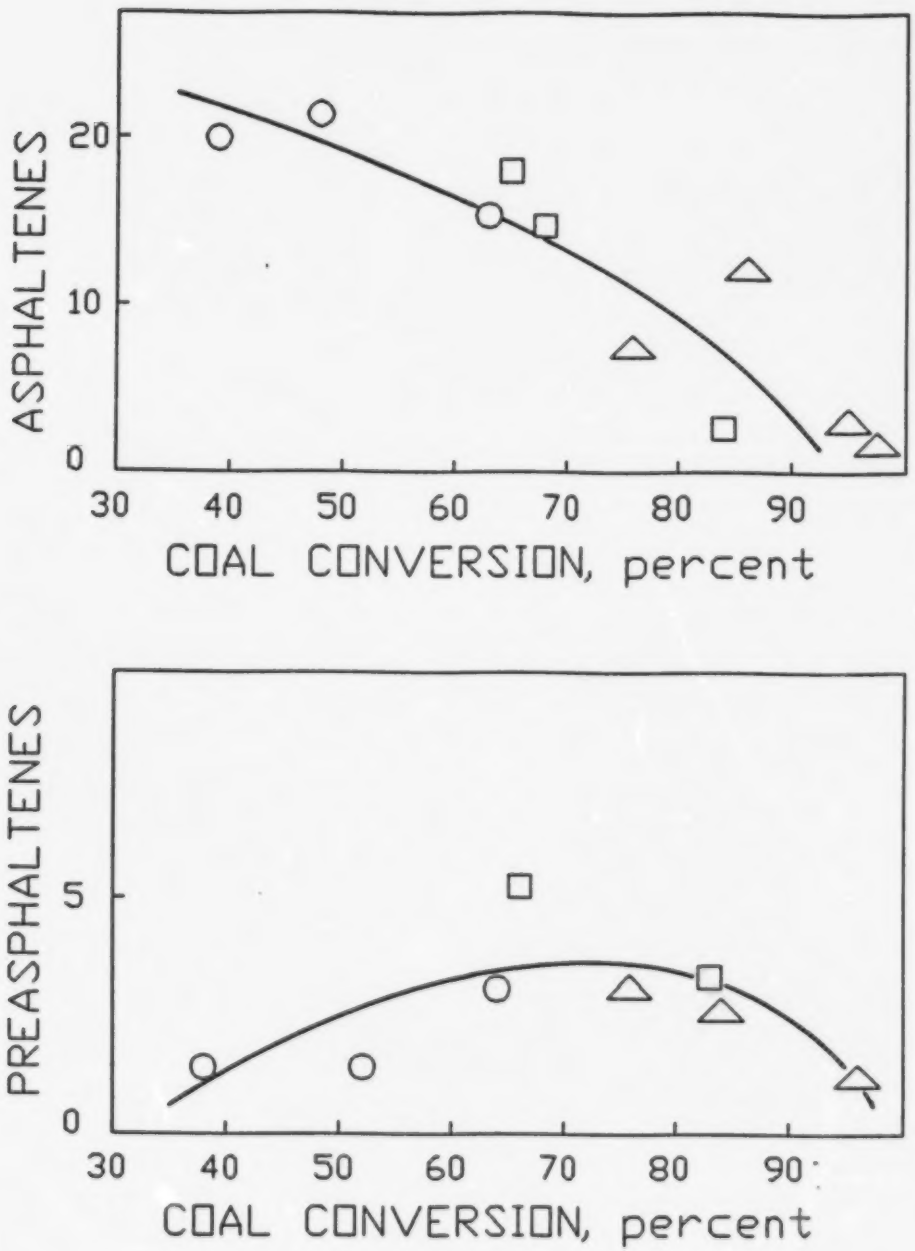

Figure 4. CORRELATION BETWEEN COAL CONVERSION AND ASPHALTENES AND PREASPHALTENES
○ 400°C; □ 425°C; △ 450°C

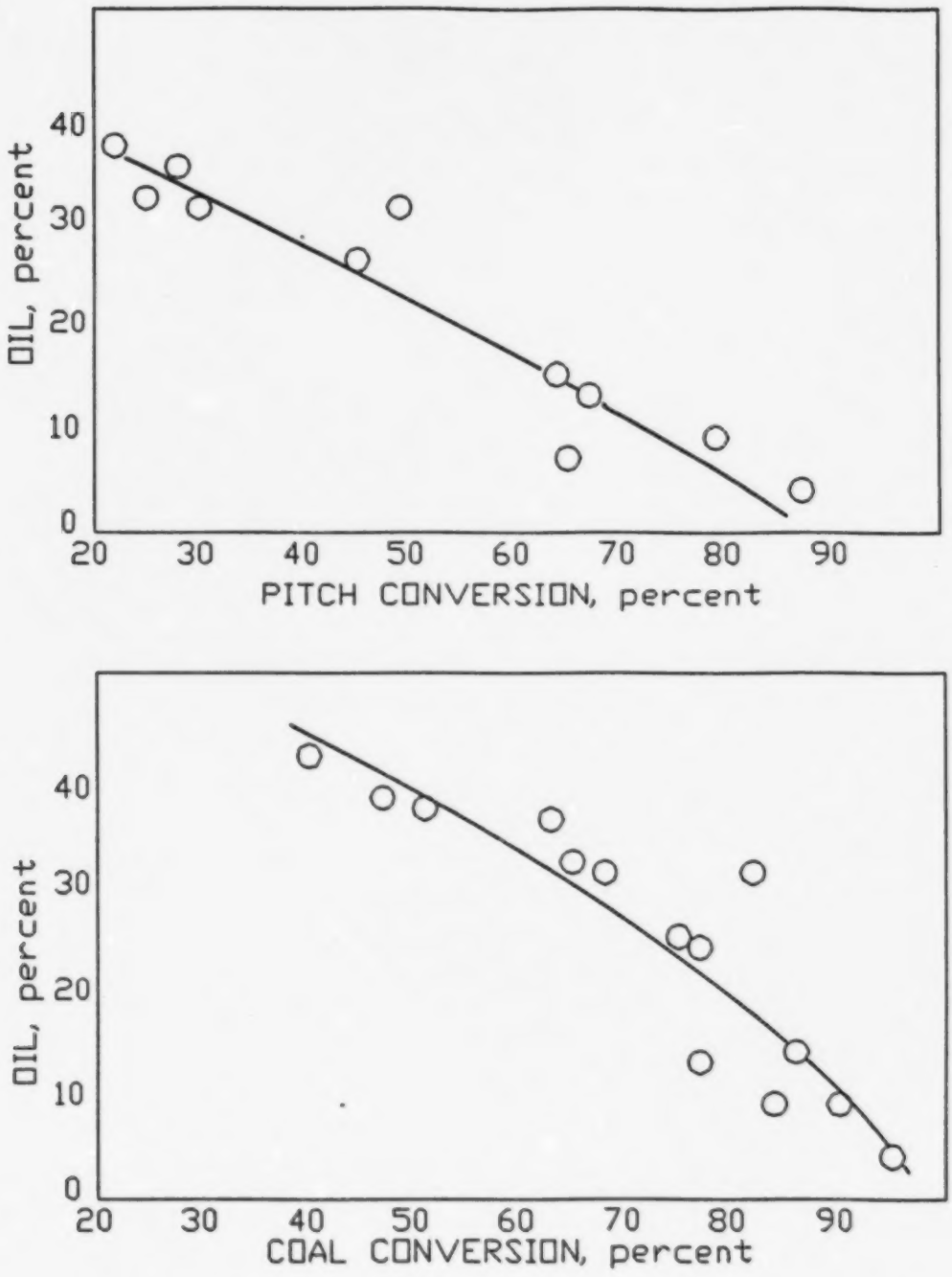

Figure 5. CORRELATION BETWEEN PITCH AND COAL CONVERSION AND OIL

The most suitable data for direct comparison were those from the experiments reported by MacAurthur, et al., 1985. The experiments were carried out in a continuous reactor using Cold Lake vacuum bottoms.

Table 6 depicts product yields, coal and pitch conversion and hydrogen consumption for CANMET run no. SF090683-1 and a selected MacAurthur (HRI) run. Because HRI researchers did not report the reactor temperature and space velocity, the depicted run was selected based on matching relative yields and hydrogen consumption for the products as indicated in Table 6.

There is very good agreement between yields and selectivities of CANMET and HRI experimental data. The discrepancy in the light and heavy gas oil yields may be attributed to the different cut points for these fractions used by CANMET and HRI. Another factor could be the difference in heavy oil feed, i.e., Cold Lake atmospheric bottoms (HRI) versus vacuum bottoms used by CANMET.

In conclusion, CANMET coprocessing data are in agreement with other published data, and specifically those reported by HRI for continuous coal/Cold Lake vacuum bottoms coprocessing.

Table 6. COMPARISON OF CANMET AND HRI COPROCESSING DATA

	HRI[1]	CANMET[2]
Coal Type	Alberta sub-bituminous	Forrestburg subbituminous
Heavy Oil	Cold Lake atm. bottoms	Cold Lake vac. bottoms
Oil/Coal Ratio	1.7:1	2:1
Reactor Temp.°C	?	455
Space Vel. Kg/L/hr	?	0.91
Coal Conv., wt%	92	89.7
Pitch Conv., wt%	80	79.8
Yields		
C1-C4	2.9	2.7
C4 - (198°C) 204°C	17.8	16.2
(198 - 343°C) 204 - 315°C	29.6	24.8
(343 - 524°C) 315 - 524°C	31.0	29.5
524°C+, excluding coal	14.2	14.6
Coal	3.4	3.3
H_2	3.7	3.5

[1]MacAurthur et al.,1985. The data have been adjusted to ash-free basis.

[2]CANMET run no. SF090683-1.

3.5. Reactor Hydrodynamics

One of the key questions in modelling kinetics is the assumption of reactor fluiddynamics and specifically, assumptions concerning reactor backmixing and gas holdup.

The coprocessing data provided by CANMET were obtained in a stirred-tank reactor with 3 inches internal diameter and 9 inches length. The reactor has one adjustable and one fixed impeller, one thermowell, and a dip tube mounted in the bottom closure for removal of coprocessing products. The total reactor volume is 1079.58 mL with gas phase volume of 786.62 mL and liquid phase of 292.96 mL (see Appendix 3).

CANMET reported that exploratory runs evaluating the effect of impeller speed on coprocessing results suggested that speed above 500 rpm provided backmixing equivalent to a perfectly stirred-tank reactor. Based on this information, we developed an equation for a continuous stirred-tank reactor (CSTR) for coprocessing reactions. The incorporated rate equations stipulated a number of consecutive and parallel paths for coprocessing reactions. Detailed equations and their derivations are given in Appendix 6.

The second assumption reviewed for coprocessing runs concerned the gas holdup in the reactor. A literature search on this topic showed no information on gas holdup for

processing of heavy oil in stirred-tanks. And, although it is recognized that gas holdup should be very small in a CSTR due to the agitation action of the impeller, we felt that some estimation of the gas holdup was essential even if the developed correlations do not directly apply to the CSTR.

The correlations chosen were those for gas holdup in light hydrocarbons in tubular reactors proposed by Bottom, et al., (1978) and Hikita, et al. (1974).

The proposed equations were as follows:

$\epsilon_g = 0.88\ U_g^{0.6}$ Bottom, et al., (1978) for d=2-10cm

and

$\epsilon_g = 0.8\ U_g^{0.47}\ (72/\sigma)^{2/3}(1/\mu_g)^{0.05}$ Hikita, et al., (1974)

The physical properties used in the calculations were those for hydrocracking reactor liquids: σ =100 dyne/cm, μ_l= 10cp and U_g is calculated at T and P of the reactor.

Detailed calculations are shown in Appendix 3. The gas holdup was found to be in the range of 0.9 to 2.4 percent of reactor volume, i.e., as expected it was low enough not to affect the calculated space velocities for the CANMET coprocessing runs.

The above theoretical conclusions are in conflict with the experimental results reported by Kang, et al., (1983). In their study of hydrodynamics of stirred-tank reactors for coal liquefaction, Kang, et al., (1983) observed that a large gas holdup was caused by a vortex formed around the agitator shaft and blade. The gas volume fraction increased from 0.04 to 0.20 as the stirrer speed increased from 700 to 1500 rpm. The vortex depth ranged from 1 to 6.5 inches for the tested agitator rotational speed. One could, therefore, conclude that, although theoretical correlations for gas holdup accurately predict gas holdup caused by the dispersed bubbles, at higher agitation speed, the major contribution to gas holdup is due to vortex formation which may constitute up to 20 percent of the reactor volume.

We recommend, therefore, that CANMET undertakes an experimental program to evaluate the gas holdup in reactors used in the process development. This information is important since it may mean that CANMET coprocessing yield may be up to 20 percent higher when compared to other coprocessing technologies, specifically, when the coprocessing data are compared to data derived from tubular reactors with space velocities corrected for the gas holdup.

3.6. Statistical Significance of Various Treatments

The experimental design provided by CANMET was based on a Latin Square factorial design with three temperature and space velocity factor levels. However, we had one missing observation for T= 400°C and SV= 1.0 which, in order to perform 2^3 factorial design analysis, had to be generated either experimentally or through appropriate statistical methods.

There are two basic methods for calculating missing observations in a factorial design: a regression method which is preferred where two or more observations are missing; and the Yates method which is preferred for ANOVA tables. We have chosen the Yates methods for the following reasons:

1. The missing observation is required for ANOVA tables.

2. The Yates method gives the same estimated treatment effects as the regression method.

3. The residuals for the calculated observations are equal to zero for the Yates method.

The last condition means that the calculated observations will not affect the variance or the statistical criteria used in the development of the kinetic models.

The basic equations for calculating missing observations using the Yates method is:

$$X_{ij} = \frac{n \sum_{j}^{r} X_{ij} + r \sum_{i}^{n} X_{ij} - \sum_{i}^{n} \sum_{j}^{r} X_{ij}}{(n-1)\ (r-1)}$$

where n = number of blocks (temperature factor levels)

r = number of treatments (space velocity factor levels)

Appendix 4 depicts the calculated missing observations for T = 400°C and SV = 1.0. Figures 6 & 7 show examples of the calculated observations for coal and pitch conversion and distillate yield.

Table 7 presents a summary of ANOVA for CANMET coprocessing data. ANOVA calculations were performed on a matrix of experimental data including one pseudo-observation for the missing data point for 400°C and space velocity of 1.0, generated using the Yates method. Also, to use a Latin Square design, space velocity data had to be truncated to factor levels of 0.5, 1.0 and 1.5. Detailed ANOVA tables are presented in Appendix 5.

Table 7. SUMMARY OF ANOVA ANALYSIS

	Percent of Variance Explained by		
Variable Name	Temp	SV	2-Way
Pitch	86	13	1
Coal	66	29	5
Oils	97	2	1
Asphaltenes	64	26	10
Preasphaltenes	33	39	28
THFI	75	25	--
Hydrogen Consumption	2	96	2
Hydrogen Sulphide	69	19	12
Carbon Oxides	13	81	6
Water	86	4	10
Total Distillates	85	14	1
Heavy Gas Oil 1	6	33	61
Heavy Gas Oil 2	82	15	3
Light Gas Oil	94	5	1
Naphtha	85	12	3
Total C1-C4	78	16	6
Methane	82	14	4
Ethane	60	33	7
Propane	80	10	10
Butane	93	3	4

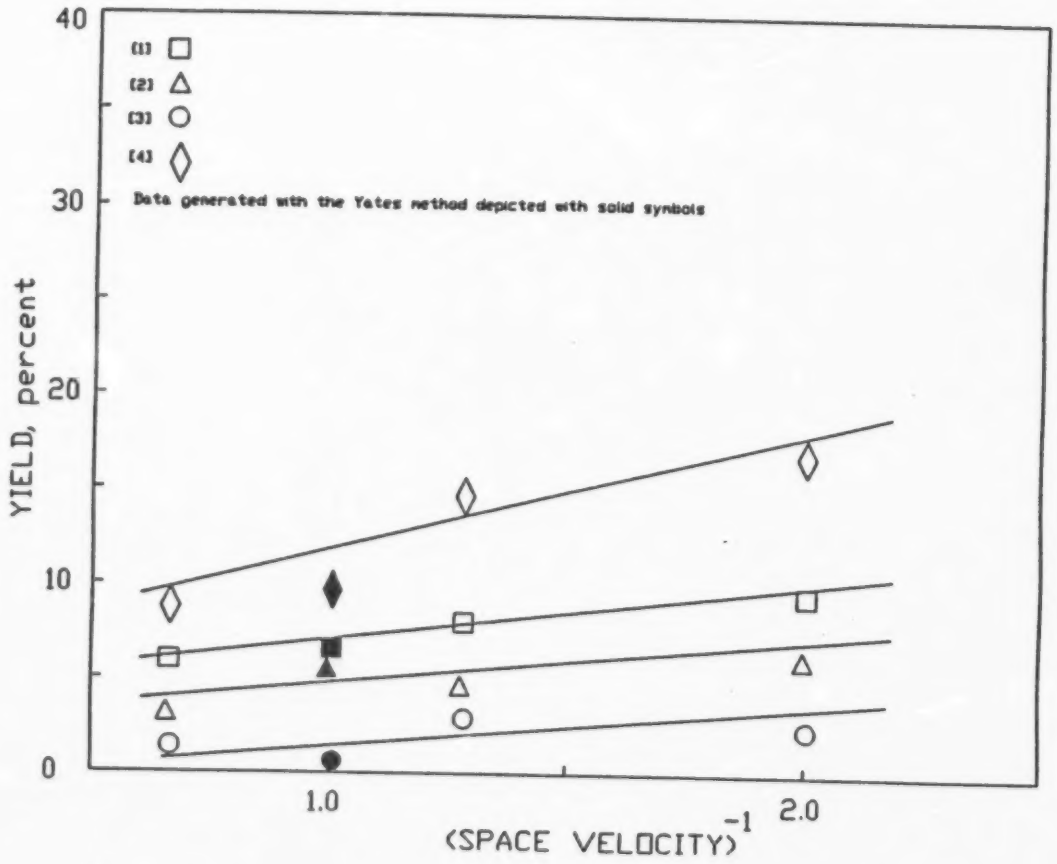

Figure 6. DISTILLATE FRACTIONS YIELD (Missing Data Calculation for fractions [1] to [4]

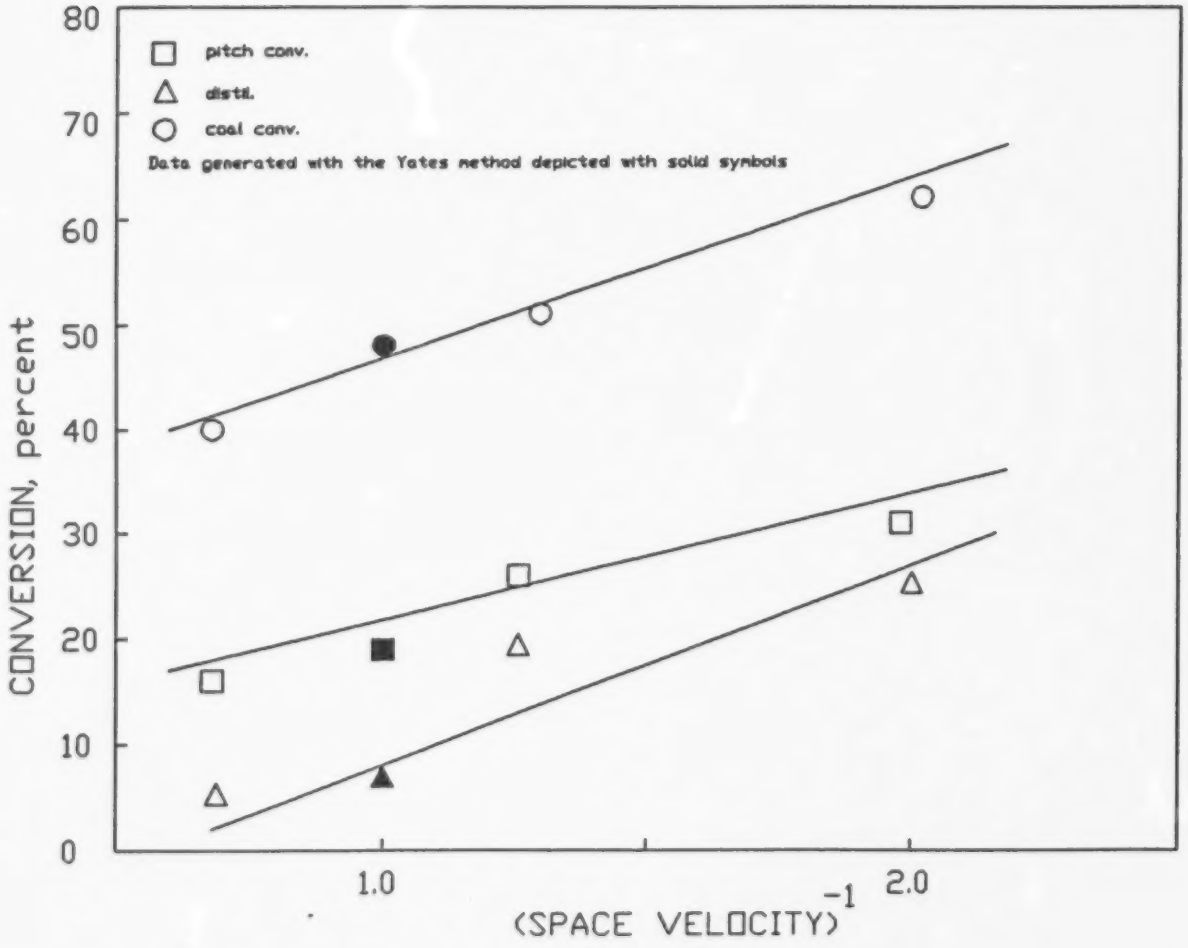

Figure 7. COAL AND PITCH CONVERSION (Missing Data Calculation)

For the most part, the yields of coprocessing products are a strong function of temperature, which is consistent with general mechanisms, such as scission of chemical bonds, discussed in the coal liquefaction and heavy oil processing review. Exceptions are generation of carbon oxides and hydrogen consumption, where the variance is explained primarily by the effect of space velocity. It could be construed that generation of carbon oxides and hydrogen consumptions involve reactions with low activation energies, e.g., cleavage of carboxyl groups and catalytic hydrogenation.

The yields of C1, C3 and C4 are also strong functions of the temperature with 80 to 93 percent of variance explained by the temperature effects. The ANOVA table indicates that thermal cracking and hydrocracking reactions are responsible for the formation of the C1, C3 and C4 products. The formation of ethane is somewhat less dependent on temperature with 60 percent of the variance explained by the temperature effects. The ethane formation follows a pattern (the presence of cross-effects) that could be expected for hydrocracking reactions of heavy oil and distillates. It seems, therefore, that the C1-C4 group may be formed directly via hydrocracking reactions of heavy oil as well as occurring as a byproduct of the hydrocracking of the distillate fractions.

An interesting effect is also shown by the 2-way interactions which are significant for preasphaltenes, asphaltenes, hydrogen sulphide and water production. A possible cause of these cross-effects are two generation sources for these products or different mechanisms at the temperature and space velocity levels. For example, asphaltenes could be formed directly from coal as well as from preasphaltenes. Preasphaltenes could be formed from coal and an adduct between heavy oil and intermediate products. Hydrogen sulphide and water could be formed from heavy oil, coal and the intermediate products.

In summary, ANOVA tables suggest that coprocessing products are formed by temperature sensitive reactions, and that hydrogen consumption may influence the characteristics of the products more than the product yield and selectivity.

3.7. Product Yield and Selectivities

The calculated ANOVA tables strongly underscore the effect of temperature on the yield and selectivity of the coprocessing products. The effect was very strong for pitch conversion where about 86 percent of variance is explained by the temperature levels. We would, therefore, expect pitch conversion to be a good measure of the severity of the process.

Figure 8 depicts the yield and selectivity of distillate fractions as a function of pitch conversion. Similarly, Figure 9 shows the yield of THFI + PA and A + O as a function of pitch conversion. Indeed, in both cases we obtained a simple correlation of coprocessing products vs. severity of the process, i.e., pitch conversion.

We should note, however, that in contrast to the variance of distillates, asphaltenes, THFI and other liquid group components, the variance of hydrogen consumption is explained mainly by the space velocity factor levels. We also could not demonstrate a simple correlation between the yield of coprocessing products and hydrogen consumption. (Note: There is an improved correlation between hydrogen consumption and distillate product yield for the 425 to 450°C temperature range as discussed in Section 4.2). Figures 6 and 7 clearly demonstrate, in conjunction with the ANOVA tables, that the yield of coprocessing products is determined primarily by thermal cracking reactions. This also explains why the quality of solvent, within a certain range of coprocessing conditions, does not affect the extent of coal liquefaction. This is because the principal driving force <u>is not</u> the availability and/or consumption of hydrogen, but cracking reactions for which rates are determined by temperature. Again, it should be emphasized that such mechanistic interpretation is correct only under certain coprocessing or coal liquefaction conditions.

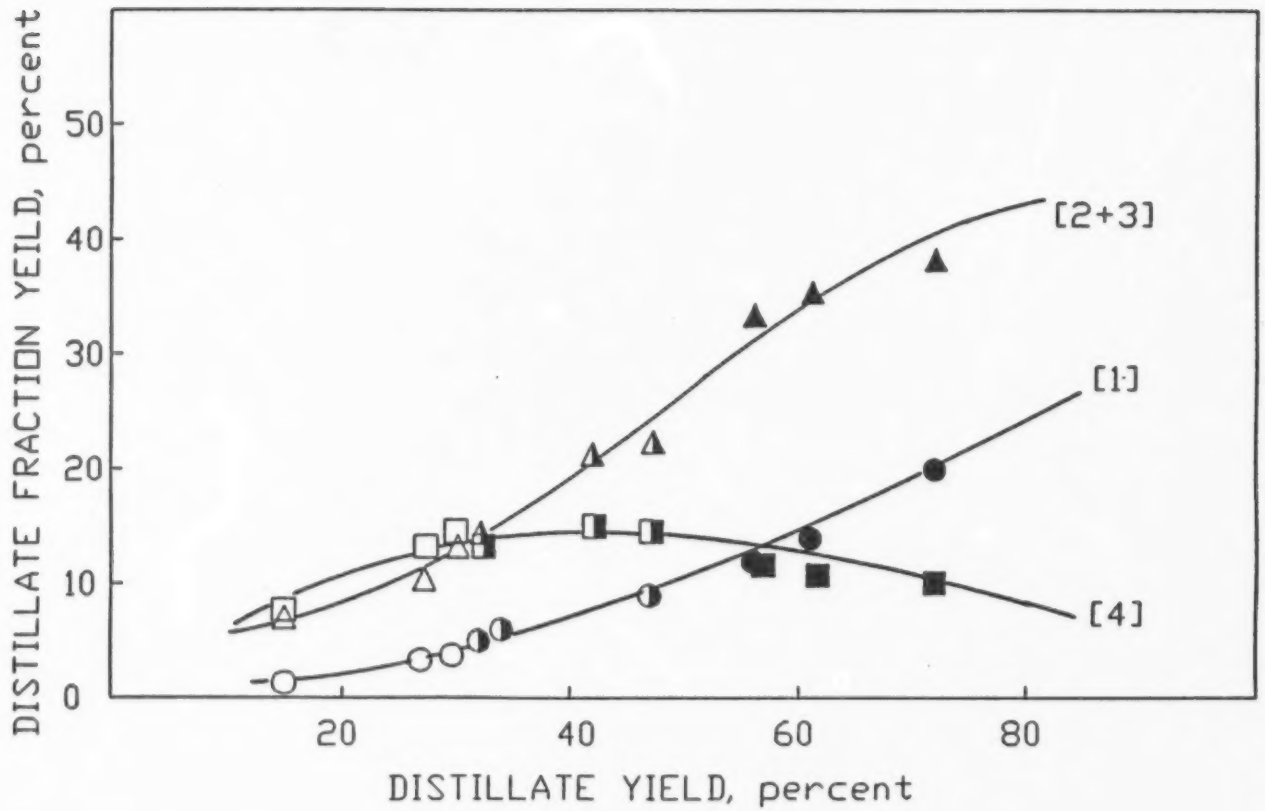

Figure 8. SELECTIVITY OF DISTILLATE FRACTIONS [1] to [4]
○ , □, △ 400°C; ◑ , ◨, ◭ 425°C; ● , ■, ▲ 450°C

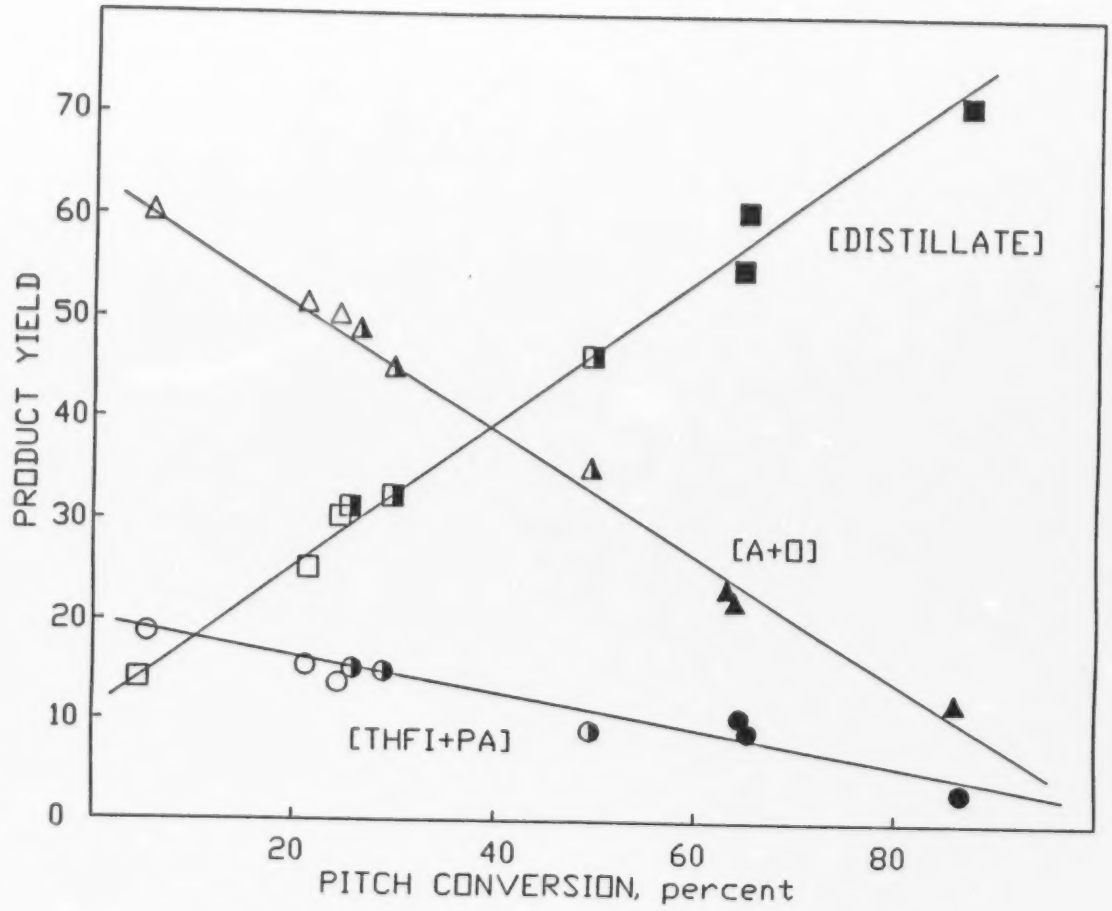

Figure 9. SELECTIVITY OF COPROCESSING PRODUCTS (See symbols in Figure 8.)

4. DEVELOPMENT AND FORMULATION OF KINETIC MODELS

4.1. Multiple Classification Analysis

It was felt that traditional ways of depicting the effects of process variables on product yield, such as plots of yield vs. space time for fixed temperatures, are difficult to interpret for a complex reacting mixture, such as coprocessing products. We concluded, therefore, that Multiple Classification Analysis may be more helpful in the development of understanding of the overall effects of temperature and space velocity on the yield and selectivity of coprocessing products.

Multiple Classification Analysis indicates the deviation of the dependent variables from their grand means, for each factor level. In other words, the depicted deviations (Figures 10a-t) indicate the effect of temperature and space velocity for all nine experimental runs together. As explained above, this technique is somewhat different from traditional graphic methods as it considers all experimental data together.

Multiple Classification Analysis does not indicate a cause-effect relationship; however, it may explain how temperature and space velocity affect the coprocessing

products. A more detailed discussion of each dependent variable is given below.

THFI- Figure 10a

Both the temperature and space velocity effects are strong, showing a decrease in THFI yield as temperature and time increase. The suggested network is:

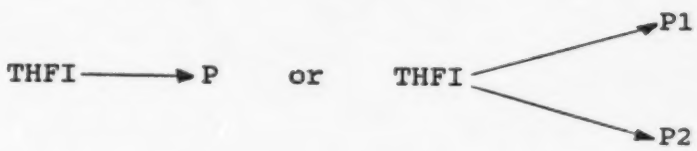

P = products

Oils - Figure 10b

As the temperature increases from 400°C to 450°C , the yield of oil decreases rapidly from +50 to -70 percent of the grand mean. The effect of temperature levels is strong, suggesting a large overall temperature rate coefficient or high apparent activation energies for oil conversion reactions. The effect of space time levels is weak, suggesting that the relative rates of formation and disappearance reactions are such that there is little net change in oil yield with time. A plausible reaction path reflecting those observations could be:

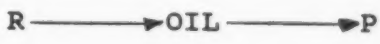

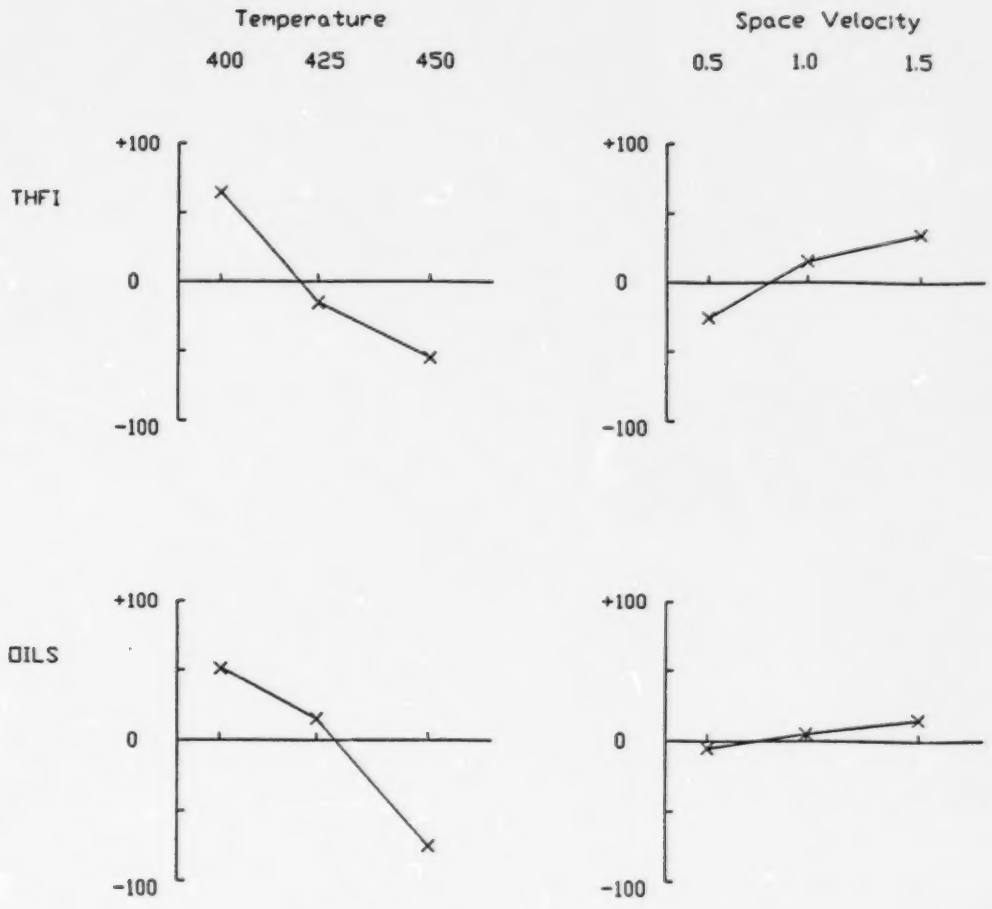

Figure 10ab. MULTIPLE CLASSIFICATION ANALYSIS

Distillates - Figure 10c

There is a strong effect of temperature and space time levels over the tested temperature/time range. The effect of space velocity is more pronounced at longer times suggesting a delay time in the formation of distillates, or that a second source of distillates becomes significant at longer space times. Suggested paths:

R = reactants

Asphaltenes - Figure 10d

The temperature effect is strong suggesting high activation energies and probable cracking of preasphaltenes. The effect of space velocity has a delay or a maximum, which would be characteristic of an intermediate product. Suggested reaction paths:

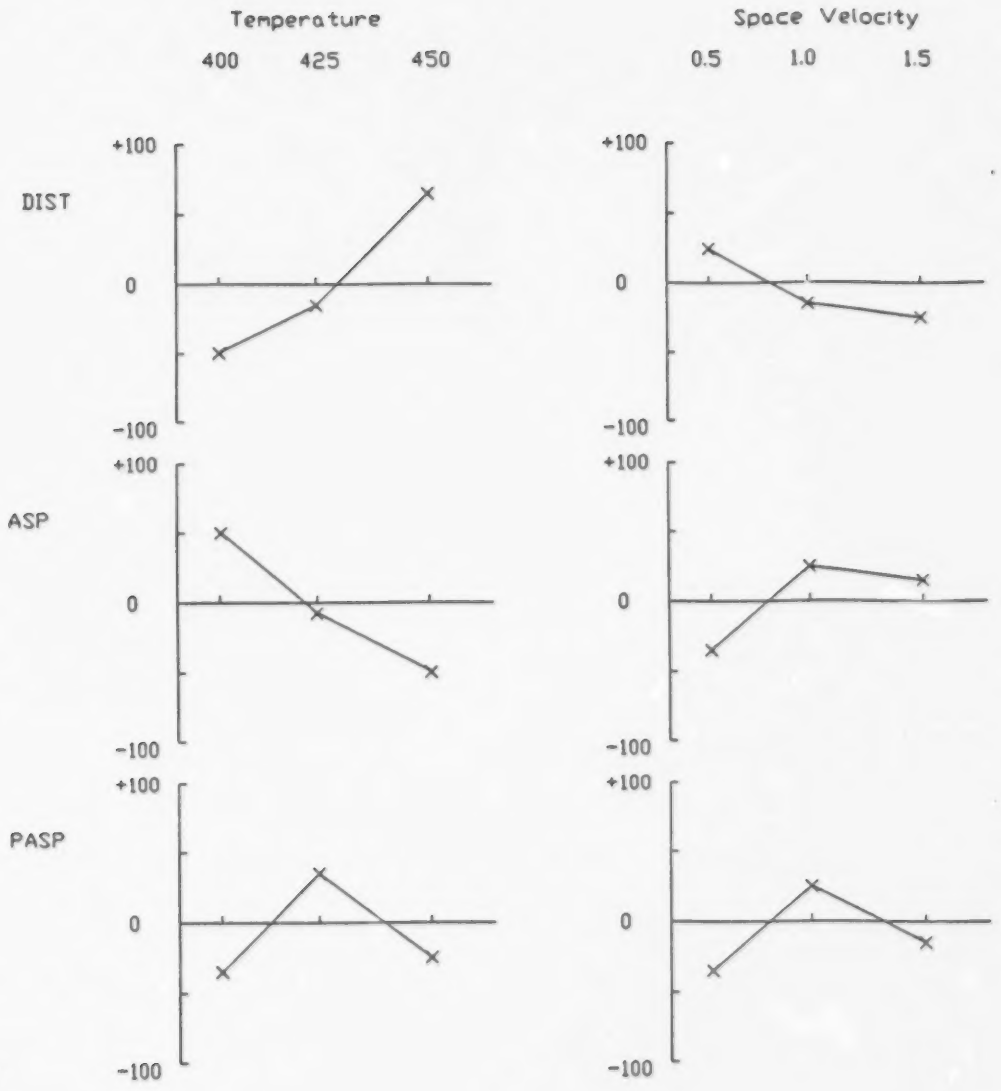

Figure 10cde. Continued

Preasphaltenes - Figure 10e

Both the temperature and space velocity effects show maxima over the studied factor levels. The maximum in the temperature effect may indicate different dominant mechanisms at lower and higher temperatures, e.g., formation of adducts, etc.

H_2O,H_2S,C1-C4 - Figure 10,f,g,h

The temperature effect is strong for all three compounds. The space velocity effect is strong for H_2S, strong (with a delay) for C1-C4, and weak for H_2O. Suggested reaction networks are:

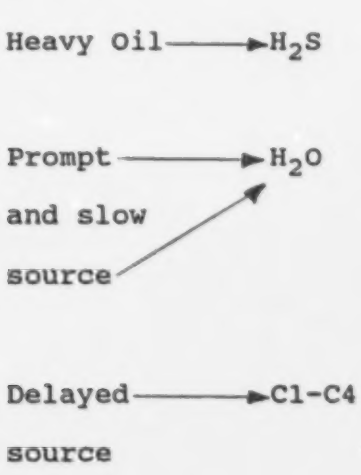

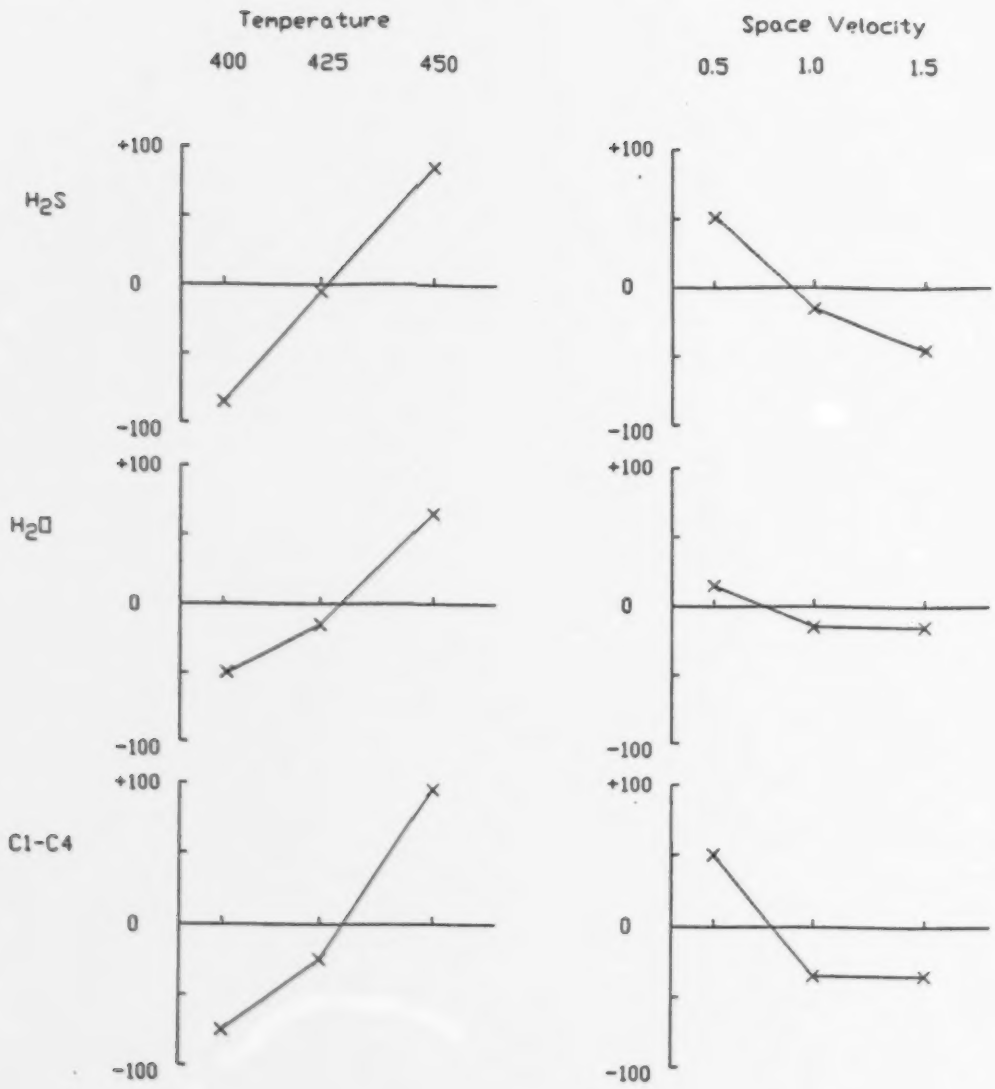

Figure 10fgh. Continued

Hydrogen Consumption and CO_x Figure 10i,j

Neither variable is sensitive to the temperature levels, possibly due to low apparent energies, e.g., catalysis for hydrogen consumption and decarboxylation for carbon oxides formation. The effect of the space velocity is not clear, possibly resulting from errors in measurements. The space velocity effects will have to be further evaluated pending the analysis of additional CANMET data.

Heavy Gas Oil 2 - Figure 10k

There is some variation of the yield with temperature and space velocity. It is not clear whether the slight maximum shown for temperature reflects errors, or whether similar to preasphaltenes, it indicates a change in the mechanism. The effect of space velocity is delayed, or perhaps shows some decrease in the early stages until sufficient yield is generated from heavy oil. Suggested paths:

$$R \longrightarrow HGO2 \text{ OR } R1 \xrightarrow[R2]{} HGO2$$

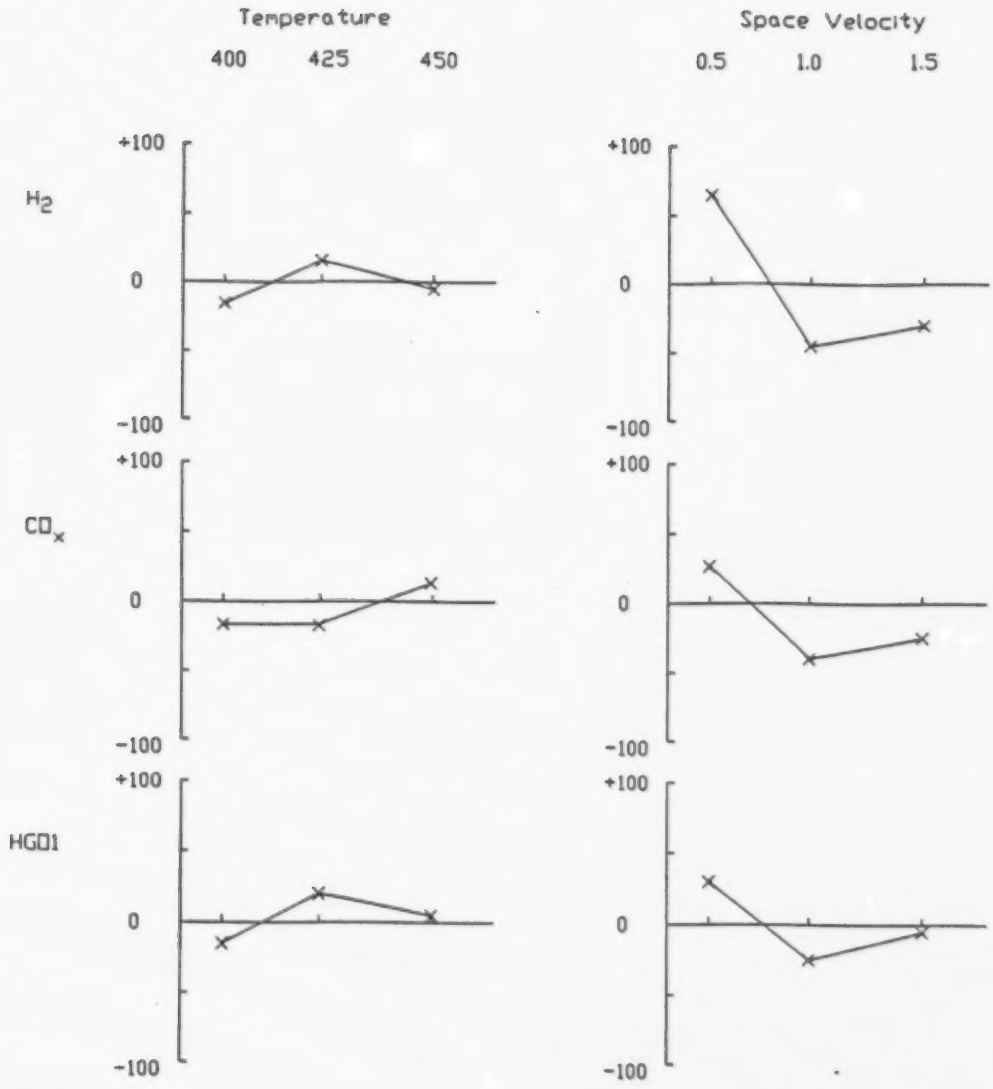

Figure 10ijk. Continued

Heavy Gas Oil 1 - Figure 10l

There is a strong effect of temperature and a delayed effect of space velocity. Suggested paths:

Heavy Gas Oil 1 + 2 - Figure 10m

The temperature effect is uniform over the 400 - 450°C range. The space velocity effect is delayed in the early stages allowing for a buildup of the products. A most plausible mechanism may be:

Light Gas Oil - Figure 10n

There is a strong increase in LGO yield at early stages suggesting that it may be formed directly from heavy oil. The temperature effect is strong at higher temperatures, again suggesting cracking reactions, perhaps from HGO. Possible reaction paths:

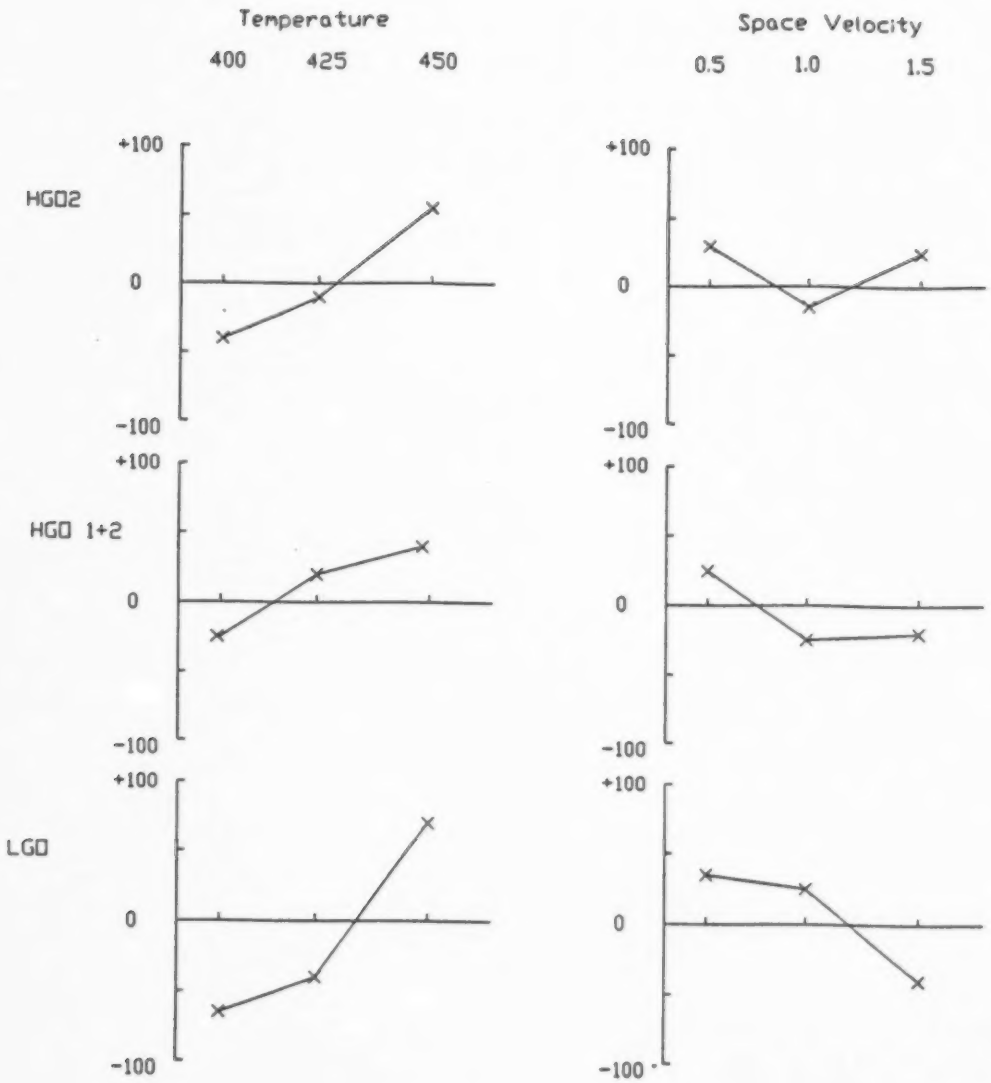

Figure 101mn. Continued

Naphtha - Figure 10o

A delay in the effect of space velocity and a strong effect of temperature suggest cracking reactions to be dominant in naphtha formation paths. Suggested reaction network:

C1-C4 Figures10 p-t

There is a strong effect of temperature and space time at higher levels, possibly a result of cracking reactions at higher temperatures and hydrogenation reactions at longer contact times. Suggested paths:

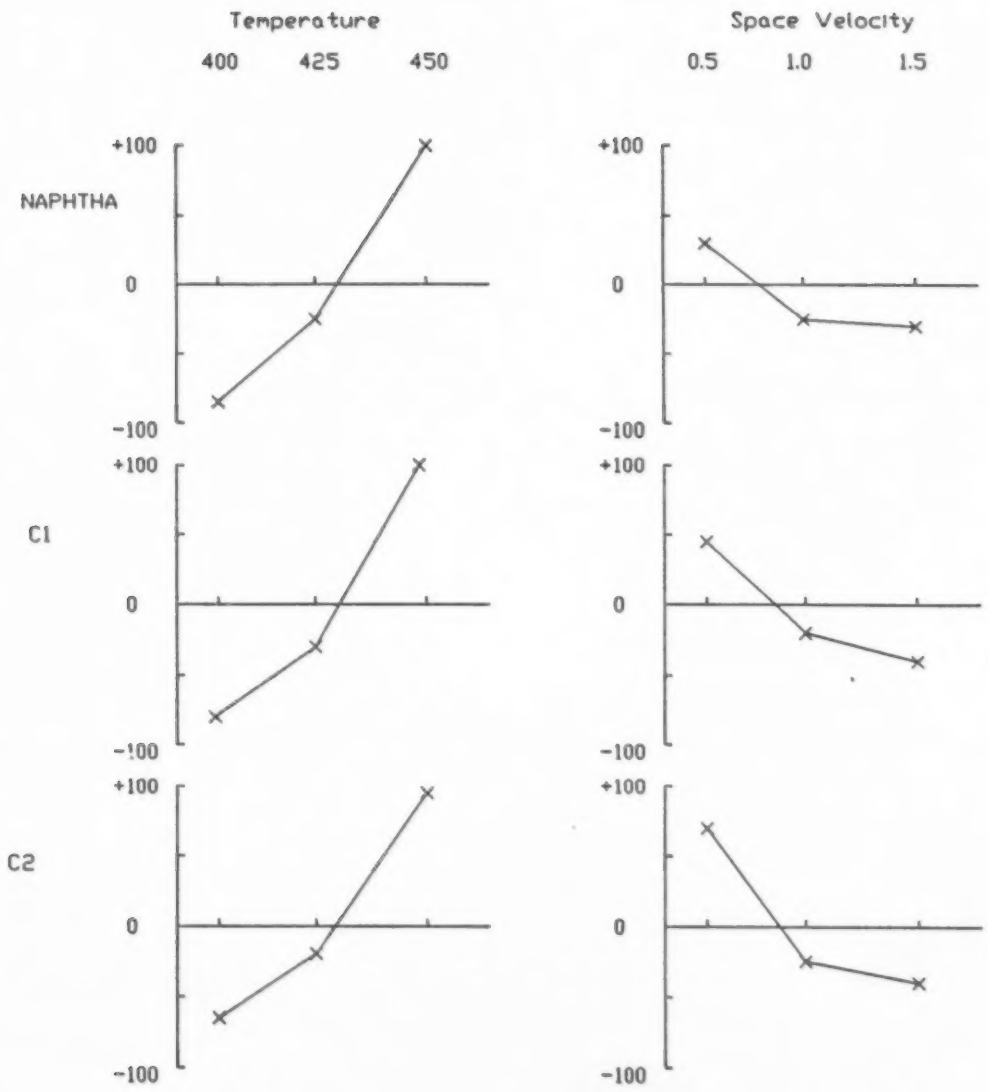

Figure 10opr. Continued

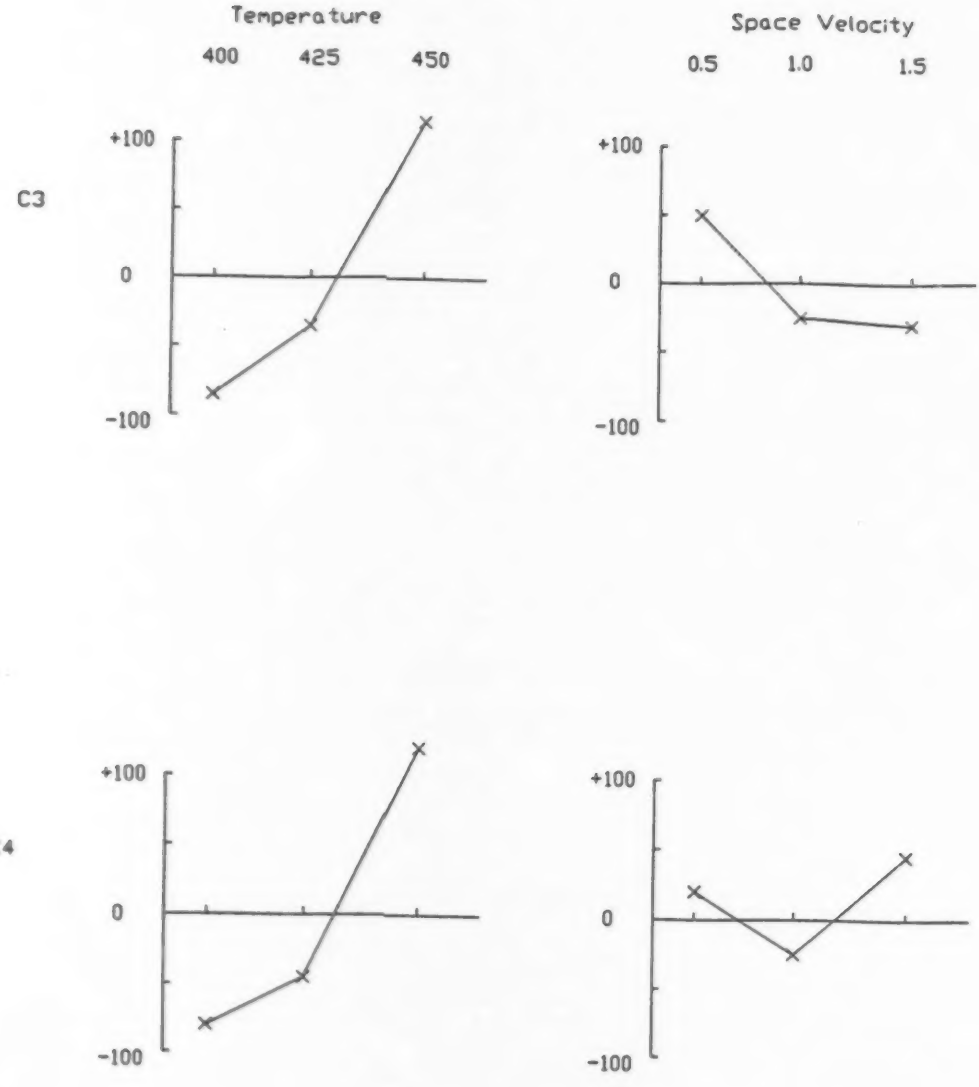

Figure 10st. Continued

4.2. Definition of Lumps or Pseudo-Components

CANMET's definition of the grouped product species follows the lumping criteria based on boiling point and solubility of the products (Figure 1). These criteria are useful, despite the limitations of lumped models discussed in Section 2, providing that the products defined are independent and do not change with the severity of the coprocessing.

In order to establish the independence of the product definition, a factor analysis was performed on two groupings of products (liquid & gases). The results showed (Table 8) the products to be independent, and correlation paths between products not to be explained by other dependent variables. The Kaiser-Meyer-Olkin measure was 0.37 for liquid grouping and 0.55 for gaseous grouping indicating a poor match between the products. A value of 0.8 is usually recommended in order to establish dependent variable factors.

More detail statistics for the performed factor analysis are shown in Appendix 5. An interesting effect was shown by the 1-tailed significance matrix for gaseous products, depicting a weak effect of hydrogen consumption on generation of H_2O and H_2S.

Table 8. FACTOR MATRIX

	Factor 1	Factor 2
DIST	0.99441	
THFI	0.96000	
ASP	0.93760	
OILS	0.93453	
PASP		0.99285
Kaiser-Meyer-Olkin Measure of Sampling Adequacy = 0.37207		
HGAS	0.96057	
H_2S	0.91404	
H_2O	0.87501	
LOGAS	0.75535	0.59750
HYGEN	0.63373	0.73817
Kaiser-Meyer-Olkin Measure of Sampling Adequacy = 0.55939		

It was surprising to see a rather poor correlation of hydrogen consumption with other dependent variables (Appendix 5). The calculated correlation matrix for all major coprocessing products showed weak correlations of hydrogen consumption with C1-C4 and distillate yields (0.4062 and 0.398). The correlation coefficients became larger, but still were not very strong, in the temperature range of 425 - 450°C (0.6900 and 0.7448, respectively). This is consistent with the interpretation of the Multiple Classification Analysis, showing two possible reaction paths for C1-C4, i.e., cracking and hydrogenation of intermediate products.

Another key question in reviewing the CANMET lumping criteria was the independence of coprocessing product characteristics on the severity of the process. To establish this independence we calculated ANOVA tables for carbon and hydrogen content and hydrogen to carbon ratio for distillates as a function of temperature and space velocity. Tables 9, 10 and 11 present results of the analysis of variance. The F-values for test statistics are less than the significance value $F(3,4)= 3.637$ for the studied data set. Our hypothesis tests were based on the ratios of the main effects mean square to the total mean square, indicating the independence of the product definition on the severity of coprocessing.

Table 9. ANALYSIS OF VARIANCE (H/C VS T AND SV)

Source of Variation	Sum of Squares	DF	Mean Square	F	Signif of F
Main Effects	0.007	4	0.002	2.000	3.637
Temp.	0.007	2	0.004		
SV	0.000	2	0.000		
2-Way Interactions	0.000	4	0.000		
Temp. SV	0.000	4	0.000		
Explained	0.008	8	0.001		
Residual	0.000	0	0.000		
Total	0.008	8	0.001		

Table 10. ANALYSIS OF VARIANCE (C VS T AND SV)

Source of Variation	Sum of Squares	DF	Mean Square	F	Signif of F
Main Effects	1.631	4	0.408	1.925	3.637
Temp	1.620	2	0.810		
SV	0.010	2	0.005		
2-Way Interactions	0.063	4	0.016		
Temp. SV	0.063	4	0.016		
Explained	1.694	8	0.212		
Residual	0.000	0	0.000		
Total	1.694	8	0.212		

Table 11. ANALYSIS OF VARIANCE (H VS T AND SV)

Source of Variation	Sum of Squares	DF	Mean Square	F	Signif of F
Main Effects	0.478	4	0.120	1.904	3.637
Temp.	0.476	2	0.238		
SV	0.002	2	0.001		
2-Way Interactions	0.023	4	0.006		
Temp. SV	0.023	4	0.006		
Explained	0.501	8	0.630		
Residual	0.000	0	0.000		
Total	0.501	8	0.063		

4.3. Definition of Initial Components for Coal

Reaction paths for conversion of THFI were evaluated using methods described by Szladow and Given (1982). In this approach, apparent activation energy is derived from conversion-time-temperature relationships directly without any assumptions for the rate equations or kinetic structure. The derived apparent activation energy E′ is the weighted average of activation energies of individual species E_i with the weighting coefficient equivalent to rates r_i of individual species.

$$E' = \Sigma r_i \, E_i / \Sigma r_i \qquad (1)$$

Apparent activation energy E′ can be derived from a general equation.

$$\frac{\partial \mathrm{Lnta}}{\partial {}^{1}/_{T}} = \frac{E'}{R} \qquad (2)$$

where t_a = time required to achieve conversion x = a.

CANMET coprocessing data were plotted using space time data corrected for the gas holdup ϵ (Figure 11).

space time = (space velocity) / $(1-\epsilon)$

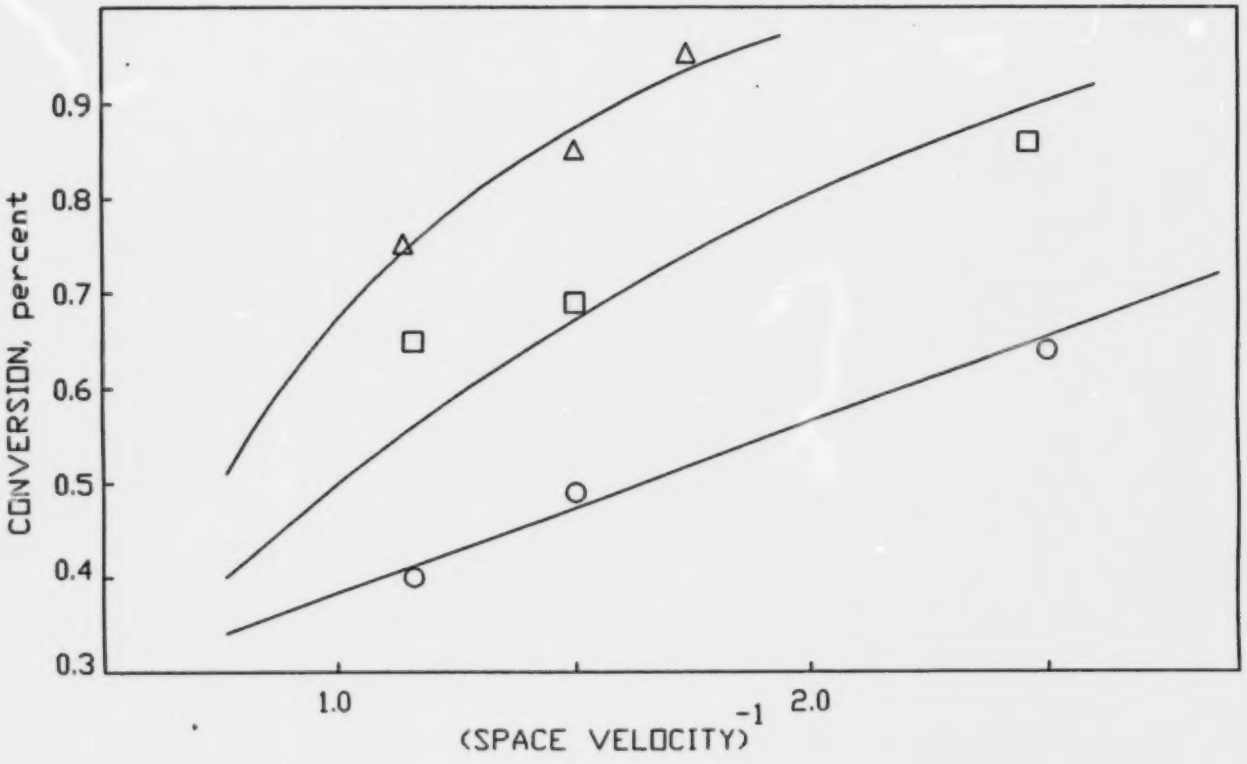

Figure 11. PLOT OF THFI CONVERSION vs. SPACE TIME

Logarithms of the conversion time were plotted vs. 1/RT for conversion X = 0.5 and X = 0.7 (Figure 12). The apparent activation energy is, in both cases, about 30 kcal and does not change with conversion over the 0.5 - 0.7 conversion range. This indicates that both kinetic structures:

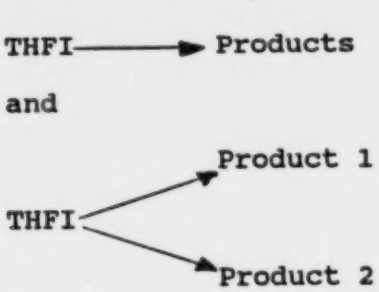

will describe correctly the dynamic behaviour of the reaction taking place during conversion of THFI to soluble materials. It also means that one initial lump is sufficient to describe THFI reactions in the studied conversion range.

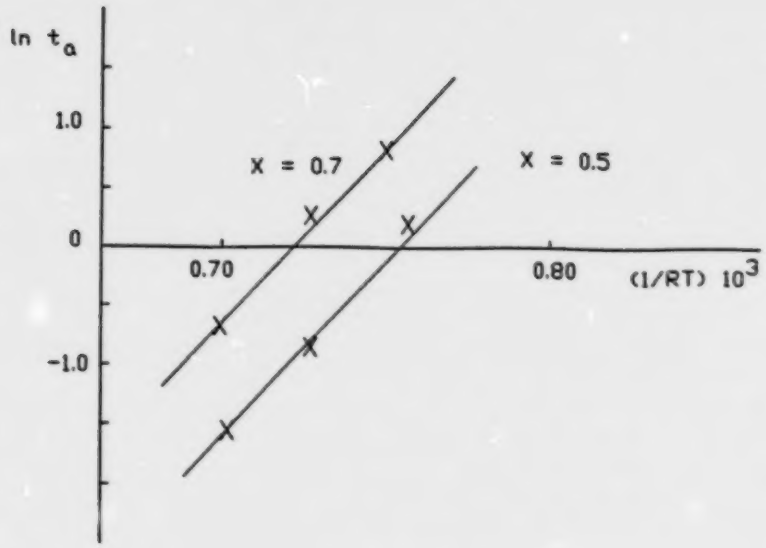

Figure 12. PLOT OF LN (Time) vs. 1/T

4.4. Lumped Kinetic Equations for CSTR

Lumped kinetic equations were derived for an n-component reacting mixture for a stirred-tank reactor. The basic equations were derived from a mass balance equation for component i in a stirred-tank.

$$F_i^{in}\,\Delta t - F_i^{out}\,\Delta t = r_i V'_R \Delta t \qquad (3)$$

where F_i = rate of mass flow of component i, kg/hr (in and out)

Δt = time interval for the test duration, hr

r_i = rate of formation/disappearance of component i, kg/hr L

V_R' = volume of reaction mixture, L

The rate r_i was related to other components via l reaction paths and rate constants k_{ij}, assuming first-order rate expressions with respect to mass concentration $m_{i,}$, in the reactor volume.

$$r_i = \sum_{i=1}^{n} \sum_{j=1}^{l} k_{ij}\,(m_i/V'_R) \qquad (4)$$

where n = number of i components

l = number of reaction paths

Appendix 6. shows a detailed derivation of kinetic rate equations. The final form of the equations was:

$$\frac{F^{in}(1-\phi)}{(1-\epsilon)\rho p\ V_R}(X_{i,o}-X_i) = r^{j\prime} \qquad (5)$$

where F^{in} = rate of total feed input, kg/hr

ϕ = mass fraction of feed/product flashed at reactor T,P

ρp = average density of products, kg/L

V_R = reactor volume (to the dip tube), L

ϵ = gas holdup

$X_{i,o}$ = Fi^{in}/F^{in}

X_i = Fi^{out}/F^{in}

r_i' = rate for component i hr^{-1}

For example, for the reaction network depicted in Figure 1, Appendix 9, we obtain the following set of equations:

$$(1)\quad Z(X_{THFI,o}-X_{THFI}) = -(k_1+k_3)X_{THFI} \qquad (6)$$

$$(2)\quad Z(X_{PA,o}-X_{PA}) = k_1X_{THFI}-k_2X_{PA} \qquad (7)$$

$$(3)\quad Z(X_{A,o}-X_A) = k_3X_{THFI}+k_2X_{PA}=(k_4+k_6)X_A \qquad (8)$$

$$(4)\quad Z(X_{oil,o}-X_{oil6}) = k_4\ X_A-k_5X_{oil} \qquad (9)$$

$$(5)\quad Z(X_{DIST,o}-X_{DIST}) = k_6X_A+k_5X_{oil}-k_7X_{DIST} \qquad (10)$$

$$(6)\quad Z(X_{C1-C4,o}-X_{C1-C4}) = k_7X_{DIST} \qquad (11)$$

$$Z = \frac{F^{in}\ (1-\phi)}{(1-\epsilon)\rho_p V_R}$$

The remaining task to determine values for A_i and E_i in the Arrhenius equations is to evaluate the k_i's for the above set of six equations, using the Least Squares method.

4.5. Development of Computer Codes and Algorithms

In Section 4.4 we derived the governing equations for an n-component mixture reacting via L coprocessing steps in a stirred-tank reactor. The equations were:

$$[F^{in}(1-\phi)/(1-\epsilon)\rho_p V_R]\ (X_{i,o}-X_i) = r_i' \qquad (12)$$

where r_i' represents a dimensionless rate for the formation and disappearance paths for component i. For example, application of equation (12) to a six-component model results in a set of six linear equations describing the concentration of component i (equations (6) - (11)).

In our approach to regress for the model rate constants, we applied the Least Squares method to minimize the residual errors between the model predicted and experimental rate data. For the n governing equations, we, therefore, define:

$$r'_1 = f_1\ (k_j, X_i) \qquad (13)$$

$$r'_n = f_n\ (k_j,\ X_i) \qquad (14)$$

where $f_1, f_2 \ldots f_n$ are linear functions of k_j's and x_i's

We also define the residual errors, i.e.,

$$e_i = f_i(k_j, X_j) - r'_i \qquad (15)$$

such that

$$E = \sum_{i=1}^{n} e^2_i = \text{minimum}$$

The objective is, therefore, to find the best k_i coefficients that minimize the E value. The necessary and sufficient conditions to meet this requirement are so-called normal equations:

$$\frac{\partial E}{\partial k_1} = \frac{\partial E}{\partial k_2} = \cdots = \frac{\partial E}{\partial k_n} = 0 \qquad (16)$$

which lead to a set of n equations with n unknowns. A detailed derivation of the normal equations for Model 1, for example, is presented in Appendix 7.

In the mathematical development leading to the evaluation of rate constant coefficients, the difference in our approach is that the rate constants were regressed based on coprocessing rates and the rate constant coefficients

were calculated from the derived rates, rather than directly by applying the Least Squares method to the difference between the predicted and experimental data. This approach leads to obtaining additional information on coprocessing kinetics such as how the calculated rate constants are affected by the alternative reaction paths, which are the main reactions for specific reaction networks, etc. The approach also allows a better understanding of the physical meaning behind the regressed rate constants and predicted yield structures for coprocessing products.

Figure 13 presents a diagram for computer algorithms developed to solve for the kinetic parameters for coprocessing. The main program (ZPROG. BAS) accepts two data files named ZINP.DAT and ZMOD.DAT, and outputs the result to a file named ZOUT.DAT.

The ZINP.DAT file includes the experimental values for all X_i and $X_{i,o}$. ZMOD.DAT stores the characteristics of the model including the matrix describing the reaction paths in the model. The steps that the computer program takes are as follows:

1. Read data from ZINP.DAT and ZMOD.DAT.
2. Set up the normal equations.
3. Solve the normal equations using Lobbe's subroutines ROOTS and ADDROW.

4. Call the subroutine SEARCH to calculate A_i and E_i values from the calculated k_i values.
5. Calculate the X_i values from the model equations and regressed constants k_i's.
6. Evaluate the goodness of fit by using statistical criteria defined in Sections 3.3 and 5.1.
7. Write the results in the output file ZOUT.DAT.

Appendix 8 presents a listing of the program ZPROG.BAS including notes on the development of the normal equations. The program takes about 2 minutes to execute on an IBM PC/XT with an 8087 math coprocessor chip.

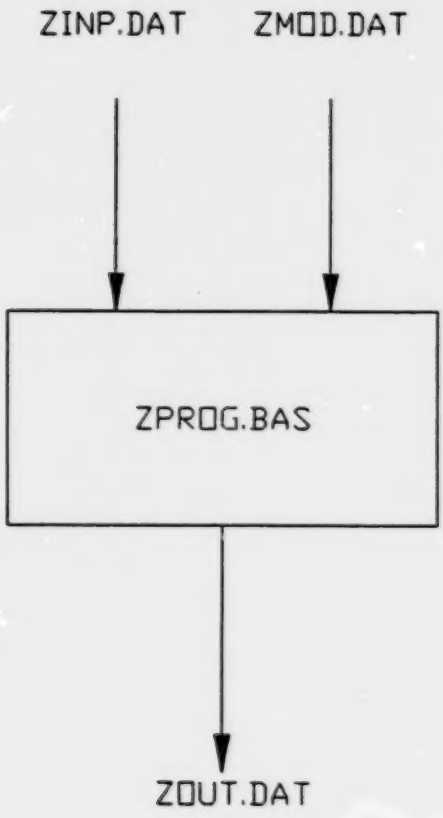

Figure 13. COMPUTER PROGRAMS

5. TESTING OF DEVELOPED MODELS

Two different types of kinetic models were examined for prediction of the yield structure of coprocessing products, i.e., 1) models that have essentially sequential characteristics; and 2) models with parallel reaction paths for coprocessing products (Figure 14). In sequential models, coal reacts to preasphaltenes and asphaltenes which are upgraded further to oil and distillates. The heavy oil reacts in a similar fashion, first by being converted to heavy gas oil then to lighter distillate fractions and finally to hydrocarbon gases. In parallel models, the feed (coal and heavy oil) is upgraded to lighter components via parallel reaction paths.

There is a fundamental difference between the two models in terms of process optimization. For a sequential model, the implication is that all products reach a maximum beyond which addition of hydrogen results in generation of C1-C4 hydrocarbon gases. Also, the rate of generation of desirable products decreases with time after their precursors reach their maximum concentration. For example, the rates of naphtha and light gas oil formation decrease after heavy oil fractions reach their maxima.

SEQUENTIAL MODEL

PARALLEL MODEL

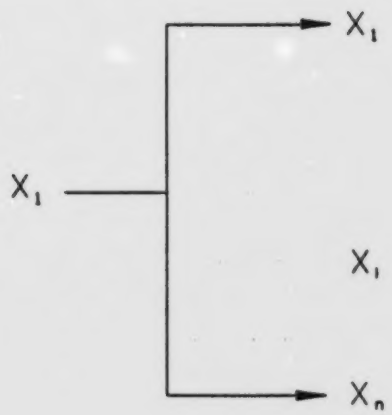

Figure 14. SEQUENTIAL AND PARALLEL MODELS

In a parallel model, the yield of products continuously increases, within a defined range of coprocessing conditions, with the selectivity of products determined by their relative rate of formation and disappearance. Development of a process optimization strategy is less complex for a parallel model, but it depends more on the relative economic value of the coprocessing products.

5.1. Selection Criteria for Developed Models

Three statistical criteria were used in discrimination and selection of the models:

1. The extent to which the total variance could be explained by the model. The definition and calculations of the total variance were given in Section 3.3.

2. The extent to which the individual component variance was explained by the model. This criterion recognizes that, in formulating our objectives, we may be more interested in how well the model predicts naphtha yield rather than the overall structure of coprocesing products. The definition of i component variance is also given in Section 3.3.

3. How well the model predicts the yield structure for coprocessing products, in other words, how accurate is the model. The predictions were based on the rate constants regressed from CANMET experimental data.

In our approach to evaluating new models or kinetic structures, we would use criterion 1, i.e., the extent to which total variance is explained, as the first and main criterion. Later, as specific difficulties in the model were addressed, we would review criteria 2 and 3. This approach allows a step-wise evaluation of the models with a proper interpretation of rate constants and reaction paths.

5.2. Six Component Models

In our initial approach we started by modelling six major components of coprocessing, i.e., with distillate fractions lumped into one group. Appendix 9 presents the nine reaction networks studied, which were based on reaction paths postulated in Section 4. Among the nine networks, Models 6, 8 and 9 predicted the yield structure well enough to warrant further consideration. (The percent of variance explained was 84, 82 and 83 percent.)

Models 6, 8 and 9 were of a sequential type, with the exception of the C1-C4 formation paths, and explained

between 82 and 84 percent of the total variance (Table 12) vs. the 98.7 percent that could be expected from a model which would account for all effects of the process variables (see Section 3.3). The accuracy with which Models 6, 8 and 9 predict the yields of coprocessing products was very good except for the yield of preasphaltenes and C1-C4 gases (Figures 15-20).

Table 13 summarizes the models' kinetic rate constants including Arrhenius coefficients. There are some difficulties with rate coefficients for Models 8 and 9 (E_5 and E_6 = 0), and one would choose model 6 as better representing the six-component yield structure for coprocessing products.

Table 12. SUMMARY OF SIX-COMPONENT MODELS

Model	Percent of Variance Explained	Number of Rate Constants
ZM1	69	7
ZM2	61	6
ZM3	64	8
ZM4	0	8
ZM5	0	7
ZM6	84	5
ZM7	0	7
ZM8	82	6
ZM9	83	5
"Best"	98.7	N/A

Table 13. KINETIC CONSTANTS FOR MODELS 6, 8 AND 9

Rate Constant	MODEL 6		MODEL 8		MODEL 9	
	A_i	E_i	A_i	E_i	A_i	E_i
k_1	3.66E13	43,710	3.66E13	43,710	3.08E13	43,450
k_2	1.39E06	19,420	1.39E06	19,420	0.90E06	18,840
k_3	7.45E10	35,090	7.45E10	35,090	7.19E10	35,090
k_4	1.06E19	60,910	1.58E21	67,910	8.73E18	60,620
k_5	5.37E11	42,260	1.12E-1	0.0000	3.22E-3	0.0000
k_6	-------	------	1.67E-2	0.0000	------	------

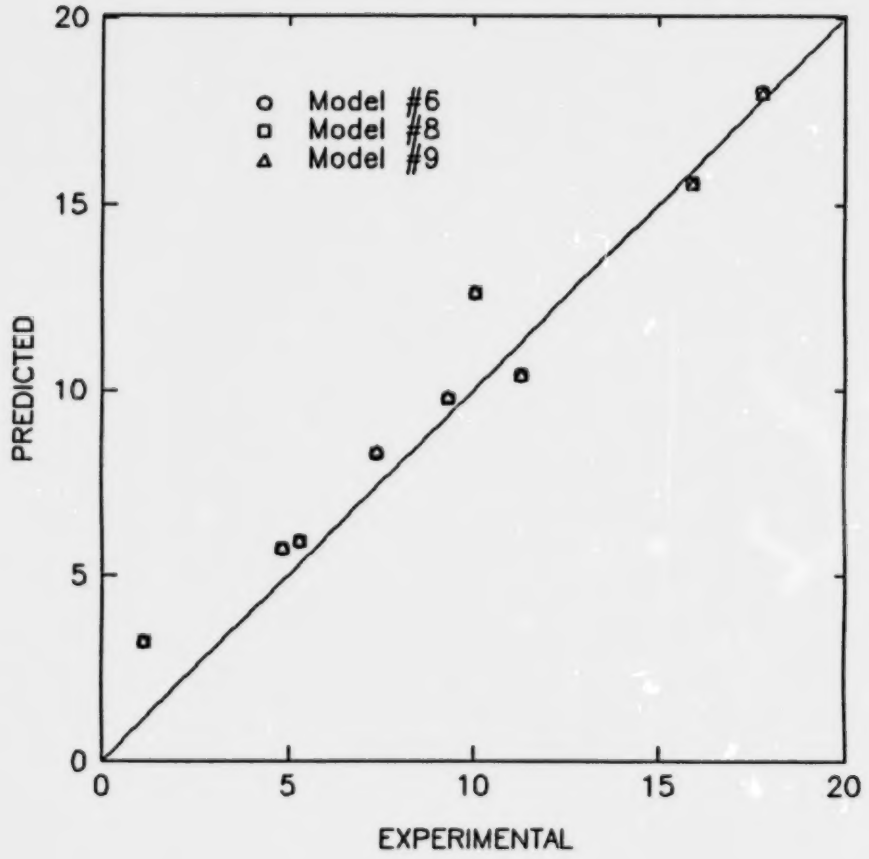

Figure 15. THFI YIELD

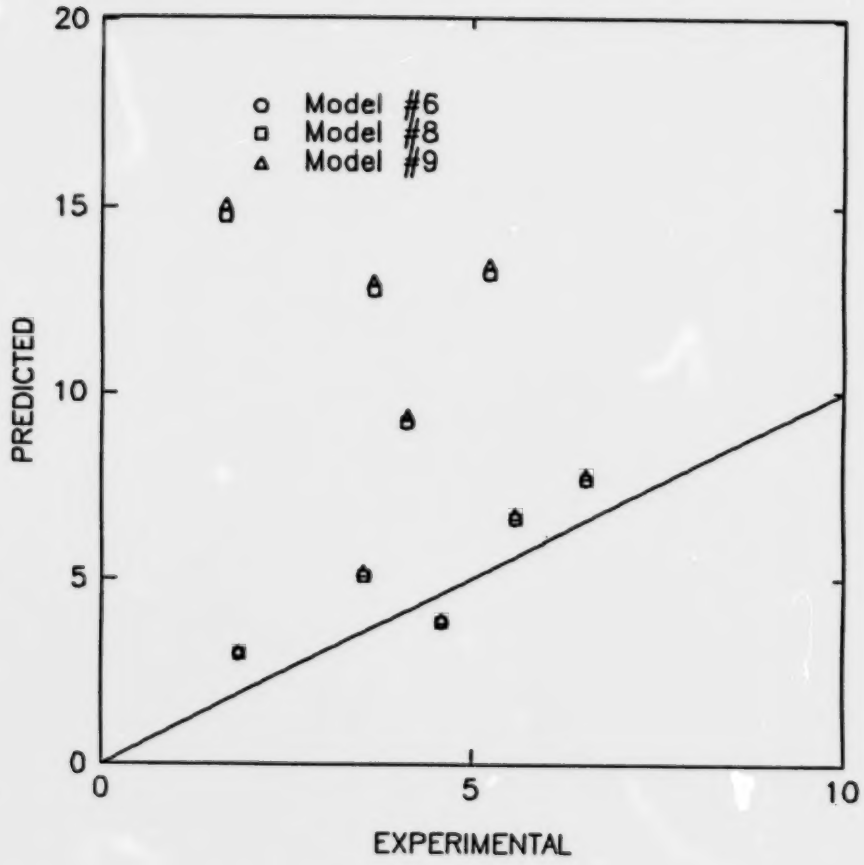

Figure 16. PREASPHALTENES YIELD

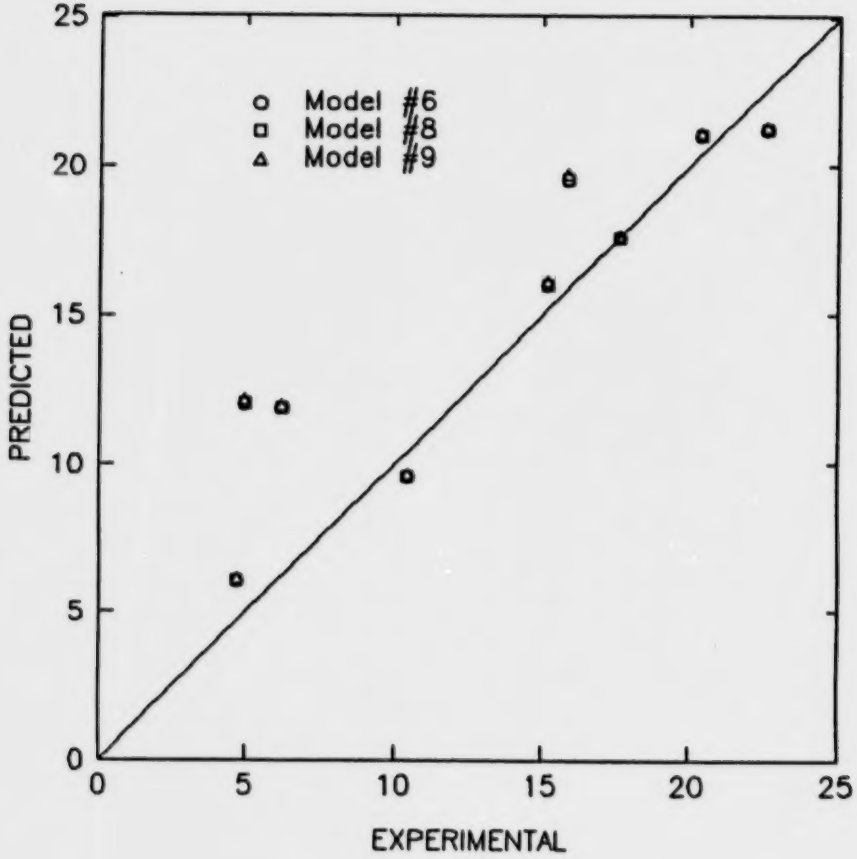

Figure 17. ASPHALTENES YIELD

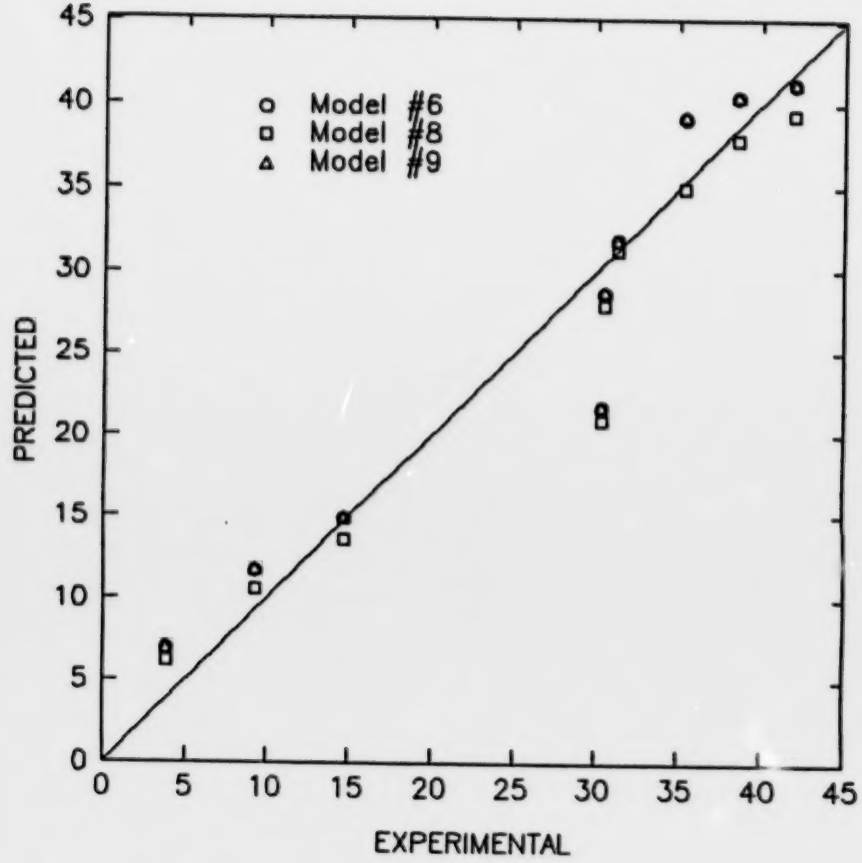

Figure 18. OIL YIELD

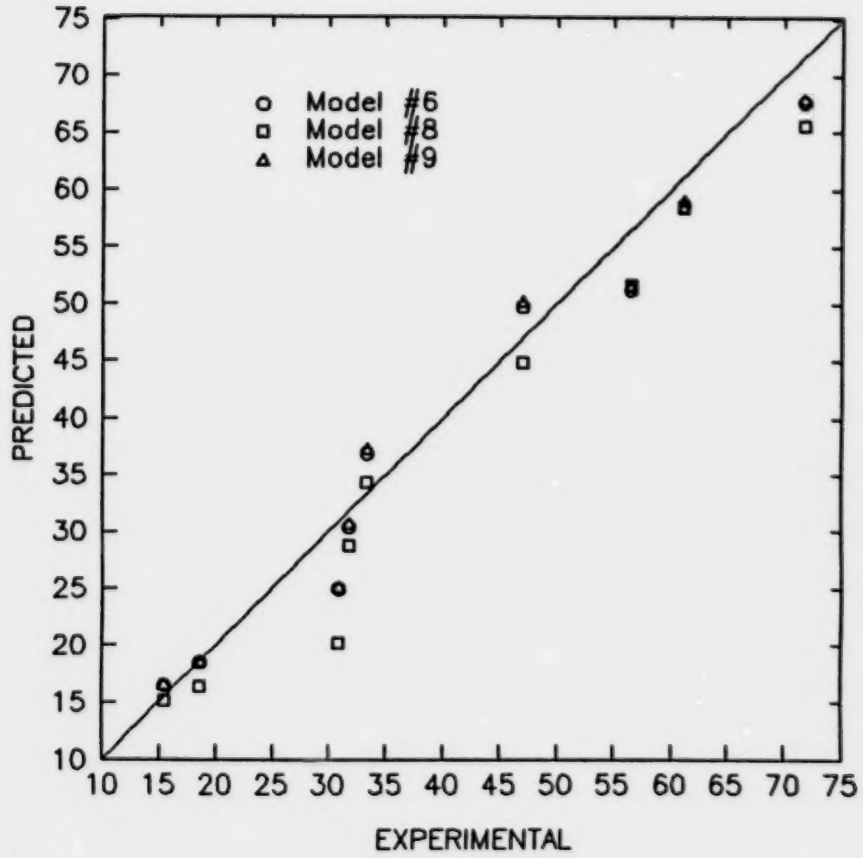

Figure 19. DISTILLATES YIELD

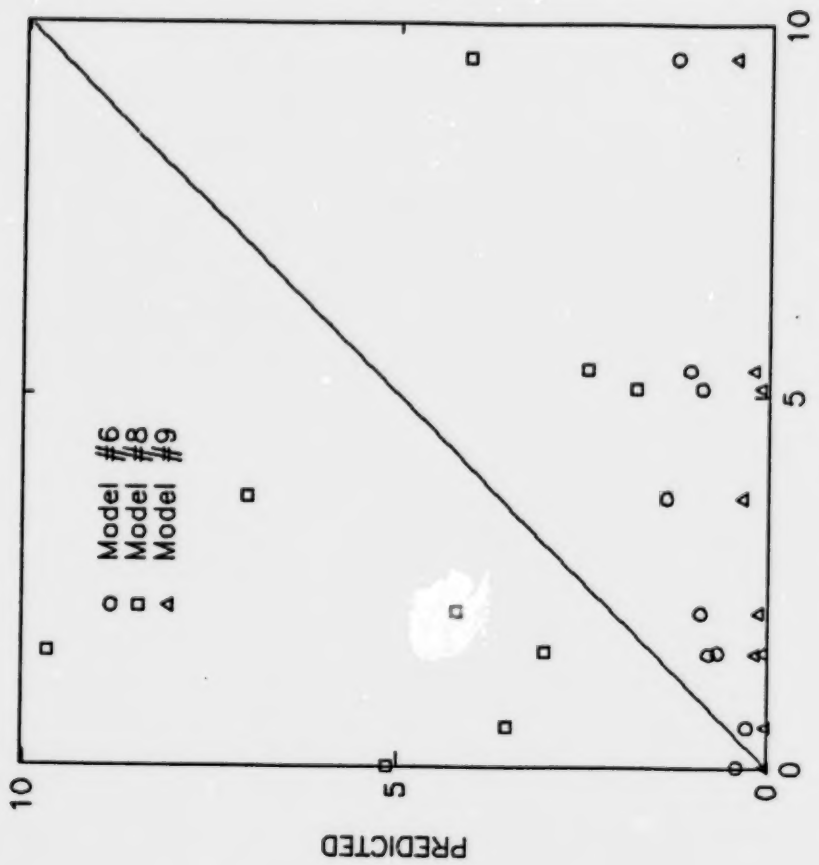

Figure 20. C1-C4 YIELD

5.3. Special Difficulties in Modelling Coprocessing Kinetics

Based on the Multiple Classification Analysis in Section 4.1, some difficulties were expected in modelling the yield of preasphaltenes. Figure 21 depicts the effect of temperature levels on the yield of preasphaltenes. As temperature increases from 400 to 425°C the yield increases; however, as temperature further increased from 425 to 450°C, the yield decreases indicating a change in the sign of the temperature coefficient (activation energy). This led us to believe that two mechanisms are responsible for this apparent anomaly, one being essentially a chemical reaction mechanism with the rate increasing with temperature, and the second mechanism representing an adduct formation for which the rate decreases with temperature. Such an adduct formation may be possible between preasphaltenes and heavy oil.

Cronauer, et al., (1979) and Sato (1976) reported similar rate effects for coal liquefaction. They observed a net negative yield of oil at low space time, suggesting an adduct formation between the solvent and primary liquefaction products. Our discussion with CANMET concerning the adduct formation revealed that other coals also exhibit similar "reverse" temperature effects, (Figure 21) at lower temperatures. At higher temperatures, the adduct seems to disintegrate.

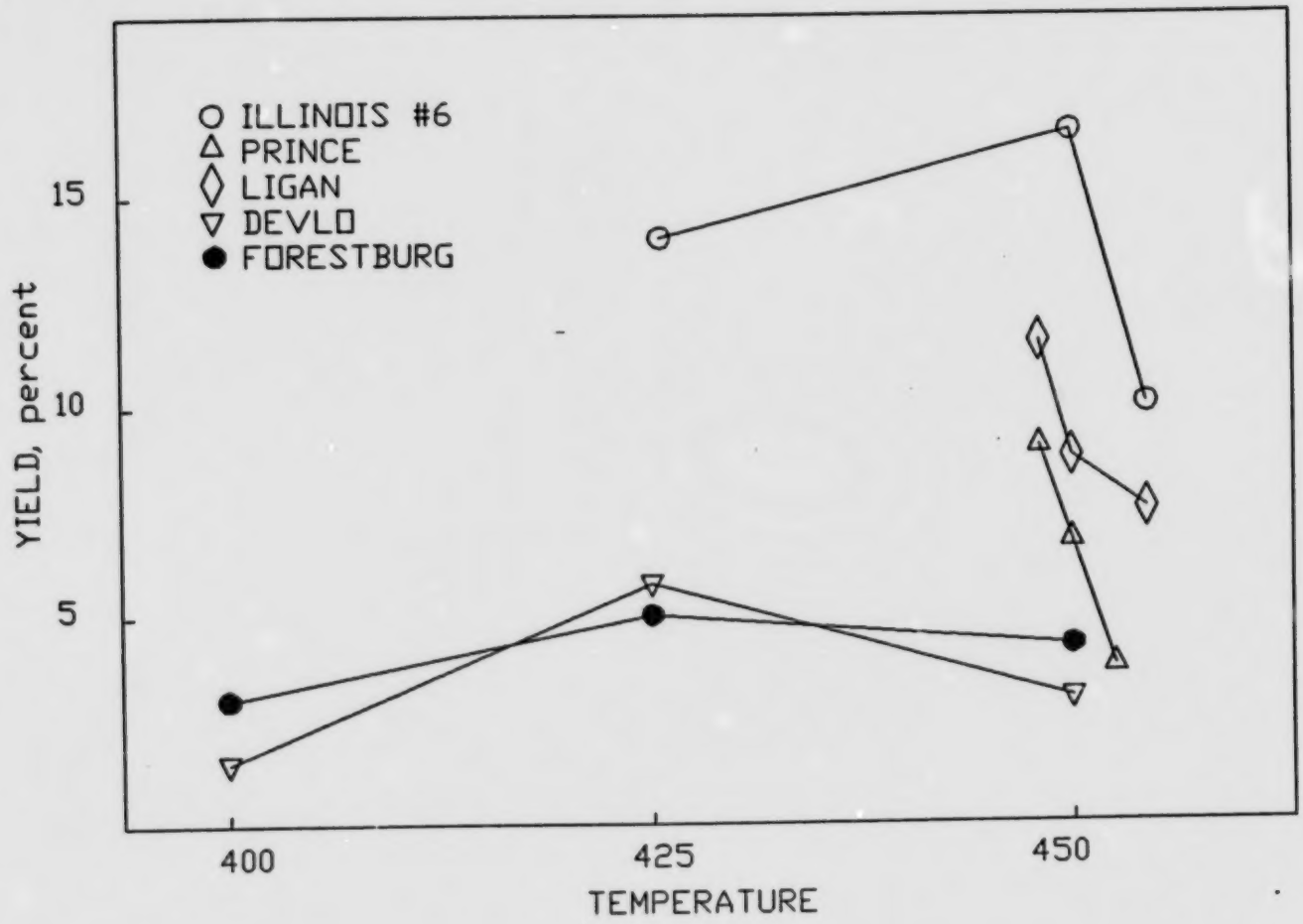

Figure 21. EFFECT OF TEMPERATURE ON PREASPHALTENES

Discussions with CANMET also revealed that on several occasions, a negative yield of oil was observed in coprocessing. The reasons for this apparent anomalous behaviour is better understood in view of the two opposing mechanisms of preasphaltene formation.

It still remains to ascertain the approach to modelling the yield structure of preasphaltenes. To account for the two opposed mechanisms, one would have to postulate independent rate equations for chemical formation and disappearance parts, with an Arrhenius form for rate expressions, and special rate equations which would account for formation of adduct, with the rate decreasing with temperature. The functional form of the adduct rate equation would have to be determined by regressing the rate coefficients based on specially written computer codes. Considering that such effort could not be accomplished within the given manpower effort for this program, and since preasphaltenes constitute only a small fraction of the total product (5 to 10%), we have decided to retain the parallel structure for preasphaltenes with only one reaction path leading to its formation. This approach will not permit modelling preasphaltenes in an accurate way, but it should not significantly affect modelling of the remaining coprocessing fractions.

It is recommended that follow-up work be undertaken to derive rate expressions for adduct formation for preasphaltenes, and to incorporate the adduct rate expressions in the coprocessing reaction networks. This recommendation is further elaborated in Section 6.

The second difficulty in modelling coprocessing products concerned the yield of C1-C4 hydrocarbon gases. The predicted yield structure based on regressed constants consistently gave lower C1-C4 yield than the experimentally derived values. Provision for parallel structures (Model 8) somewhat improved the C1-C4 yield, but it did not correct the problem sufficiently to yield accurate data at higher temperatures. It was, therefore, concluded that a better understanding of C1-C4 formation mechanisms is essential in order to formulate adequate models.

Table 14 depicts the relative distribution of C1-C4 hydrocarbon gases for CANMET coprocessing data. It is somewhat surprising to see the molar ratio of methane to ethane substantially higher than what would be expected for by-products of hydrotreating or hydrocracking (usually less than 1). The C1/C2 ratio varies between 1.38 and 2.60, clearly indicating that C1 may be formed not only from naphtha, but also from other groups of coprocessing products and reactants.

Table 14. YIELD AND DISTRIBUTION OF C1-C4 HYDROCARBON GASES

Temperature	400	400	400	425	425	425	450	450	450
Space Velocity	0.1	1.0	1.5	0.5	1.0	1.5	0.5	1.0	1.5
Yield (d.a.f. feed)									
C1	0.54	0.07	0.21	1.34	0.81	0.59	3.28	2.12	1.86
C2	0.73	0.07	0.25	1.56	0.71	0.57	3.29	1.54	1.34
C3	0.15	0.01	0.04	0.55	0.38	.029	2.29	1.16	1.11
C4	0.12	0.01	0.05	0.19	0.20	0.11	0.75	0.54	0.80

Recently, Gray, et al., (1986) reported results of their study on the distribution of C1-C6 products from hydrotreating of Syncrude coker gas oil. They showed that methane was likely formed from primary thermal decomposition reactions of the oil. Gray, et al., (1986) also concluded that the structural precursors of the C1-C6 group were present in the hydroprocessed oil.

The above analysis suggests that the reaction paths for the C1-C4 group in coprocessing can originate from heavy oil and/or distillate fractions. The completed ANOVA analysis for the C1-C4 group (see Section 3.6) also suggests that two or more initial lumps for C1-C4 formation may be required. It is conjectured, therefore, that modelling of the C1-C4 formation reactions may be possible by extending the analysis of the reaction networks through incorporation of the distillate fractions, and by postulating more than one source for the formation of the C1-C4 group.

5.4. Modelling the Yield and Distribution of Distillate Fractions

Over twenty different reaction networks were tested for correlating the yield structure of distillate fractions (Appendix 9). Most of these models encountered difficulties in accurately correlating the CANMET data, or meeting the physical constraints on rate constant coefficients, i.e., to

yield positive pre-exponential factors and activation energies.

The principal differences between the tested models were their sequential or parallel characteristics, or the grouping of Heavy Gas Oil 1 and Heavy Gas Oil 2 fractions. Based on Section 3.8, we felt that since the HGO1 yield curve resembled the LGO more than the HGO2 yield, HGO1 and LGO should be grouped together. This lumping did not work well, however, and all models based on HOG1 + LGO grouping had difficulties in predicting the yield structure for Heavy Gas Oil 1 (Models 10 - 33). On the other hand, the same reaction networks correlated the yield of distillate fractions much better when HGO2 was lumped together with HGO1. The final choices made were models 52 and 61 (Figures 22 and 23). Model 52 has strong parallel characteristics for the yield of distillate fractions with the prime coprocessing products (light gas oil, naphtha and hydrocarbon gases), constituting the termination lumps for the coprocessing network. Table 15 shows the regressed rate constants and Table 16 shows the percent of variance explained by Model 52. The model shows excellent accuracy for predicting the yield structure for naphtha, C1-C4, OIL and THFI (Figures 24-31). The total explained variance is 84.4 percent, which is close to the target of 92.5 percent (Table 16).

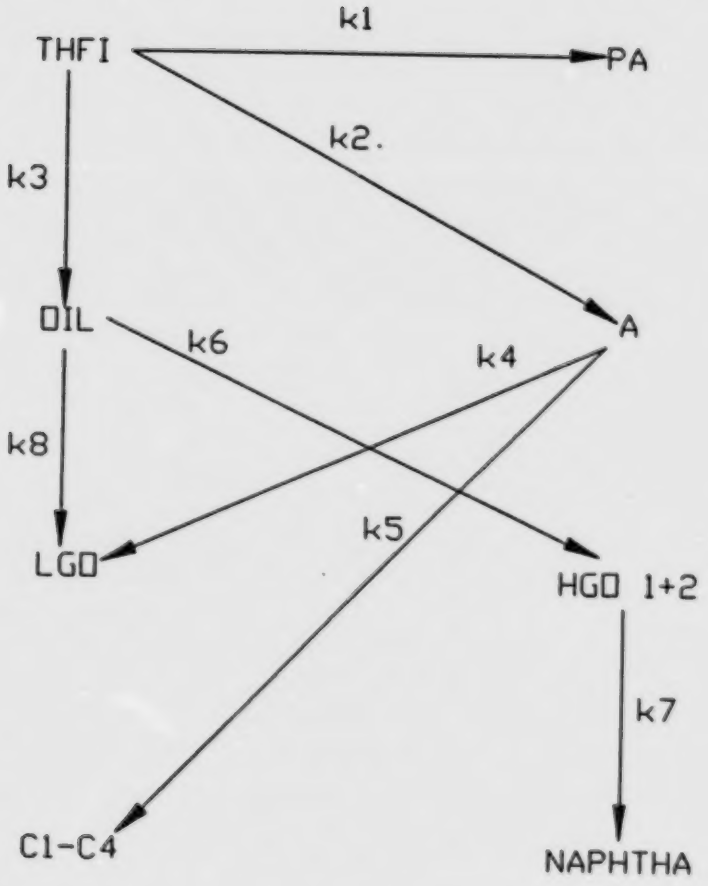

Figure 22. MODEL 52

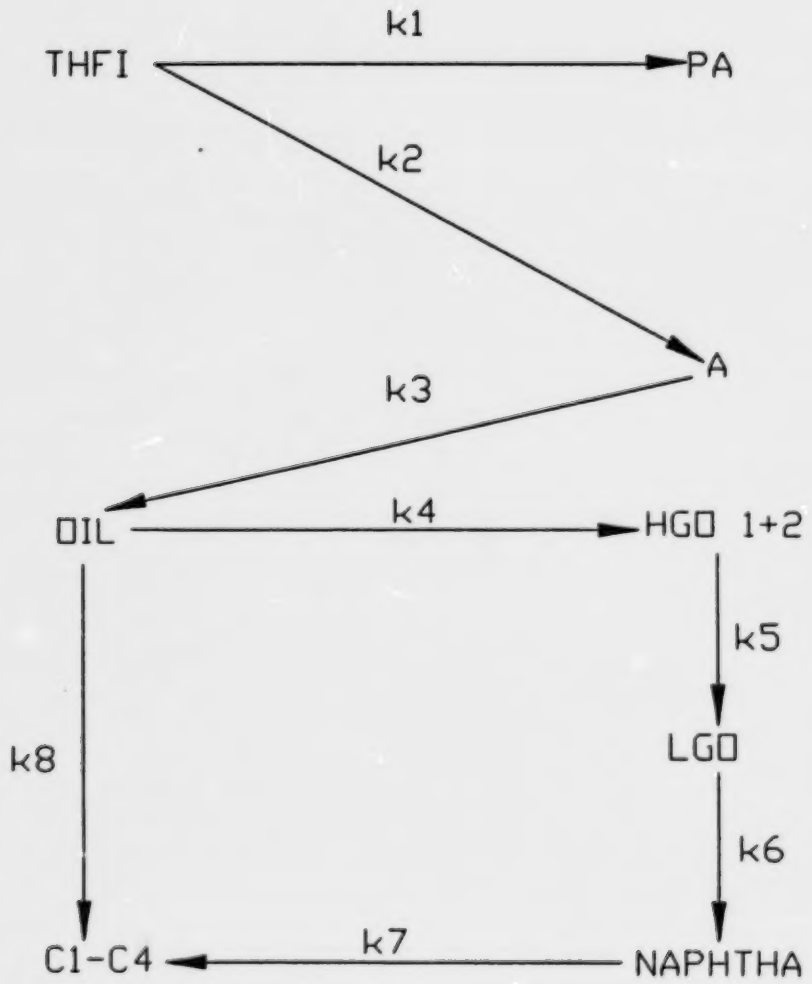

Figure 23. MODEL 61

Table 15. RATE CONSTANT COEFFICIENTS FOR MODEL 52 AND 61

Rate Constant	MODEL 52 Ai	MODEL 52 Ei	MODEL 61 Ai	MODEL 61 Ei
1	1.24E10	33,020	5.33E13	44,040
2	8.31E23	76,180	5.23E03	12,030
3	1.84E12	39,030	8.33E08	29,390
4	1.72E12	40,000	9.48E18	61,030
5	4.97E17	58,910	5.56E09	31,990
6	4.06E19	63,400	7.90E06	23,310
7	7.90E06	23,510	6.53E02	13,860
8	2.28E14	47,470	1.50E06	55,000

Model 61 (Figure 23) has a sequential characteristic with the exception of the formation path for C1-C4 group. Table 15 shows the rate constants and percent of variance explained by Model 61 . Again, similar to Model 52, Model 61 shows good accuracy in predicting the yield structure for naphtha, C1-C4, OIL and THFI (Figures 24-31). It also performs better than Model 52 in predicting the light gas oil fraction; however, it performs less effectively in terms of explaining the yield structure for all coprocessing products, i.e., 81.4 percent explained of total variance vs. the target of 92.5 percent.

We have further tested Model 61 by removing reaction path number 8. As a result, the new Model 63 (Figure 32) could not correlate the yield of C1-C4 products at higher temperatures, (Figure 33). It was concluded, therefore, that it is not possible to postulate and confirm a purely sequential model. The coprocessing reactions maintain both sequential and parallel reaction path characteristics, with the resultant models closely approximating the actual yield structure for CANMET data.

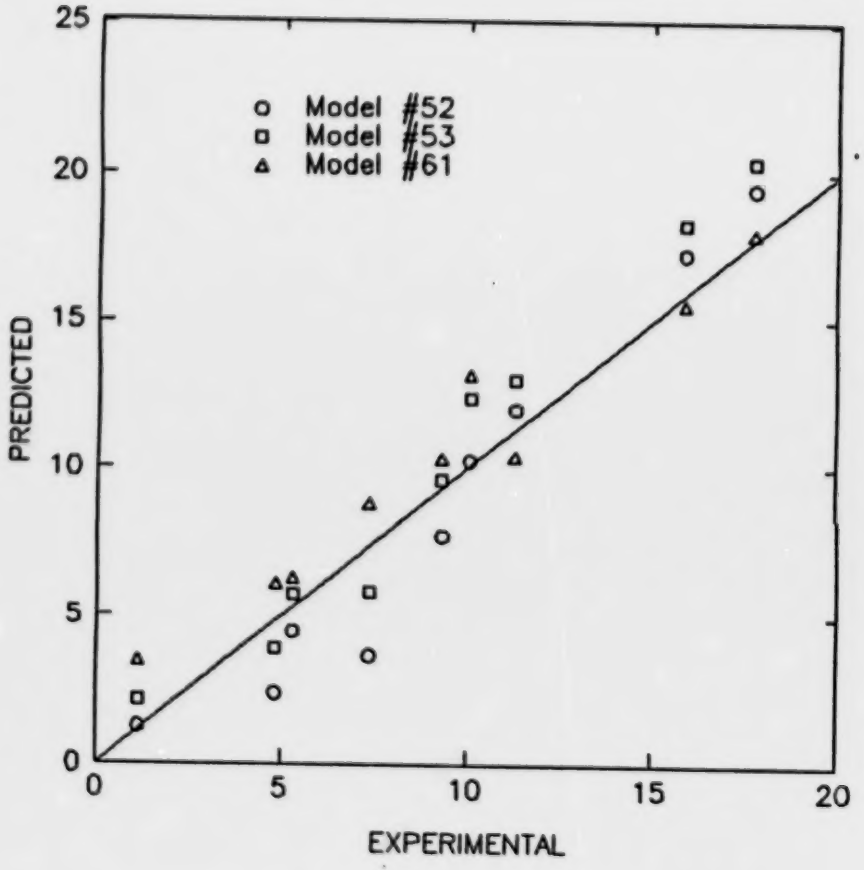

Figure 24. THFI YIELD

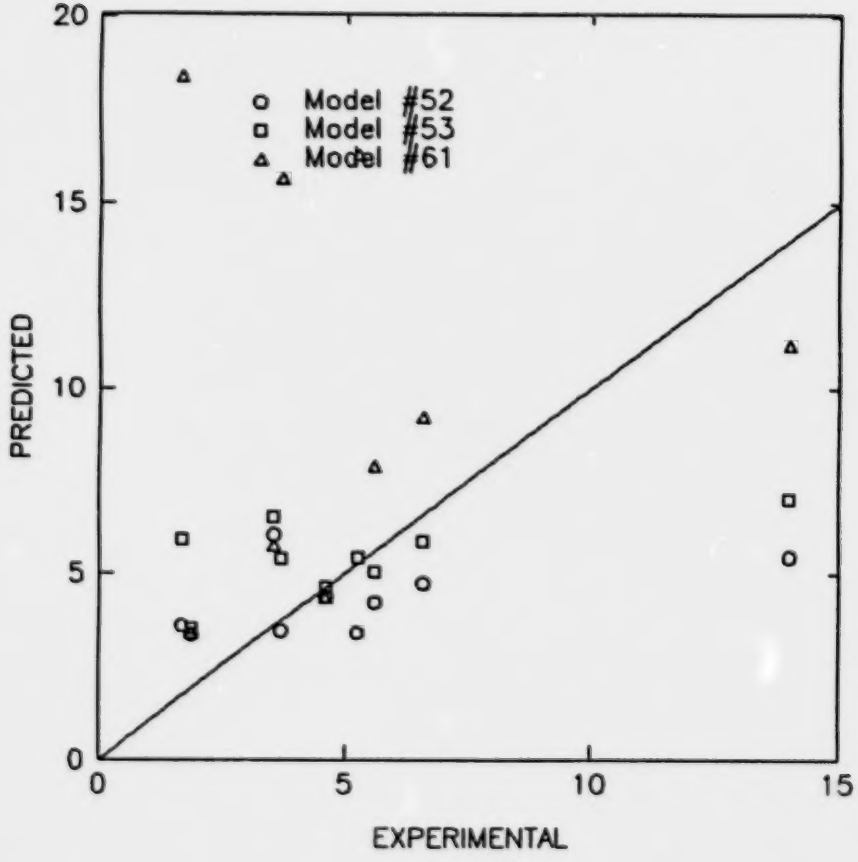

Figure 25. PREASPHALTENES YIELD

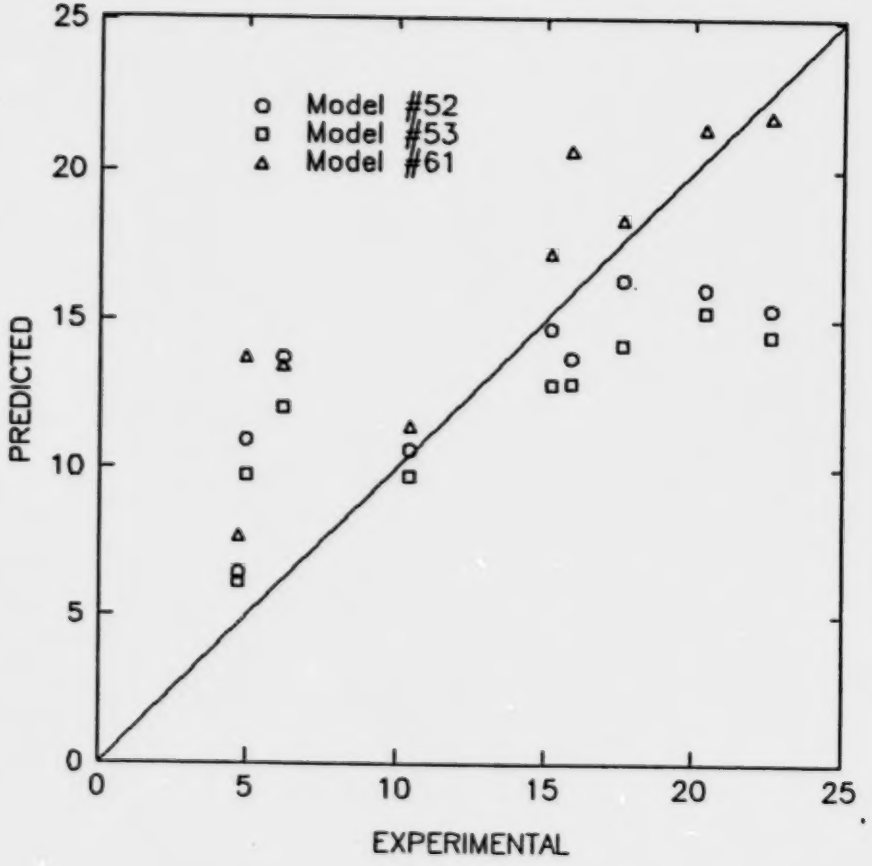

Figure 26. ASPHALTENES YIELD

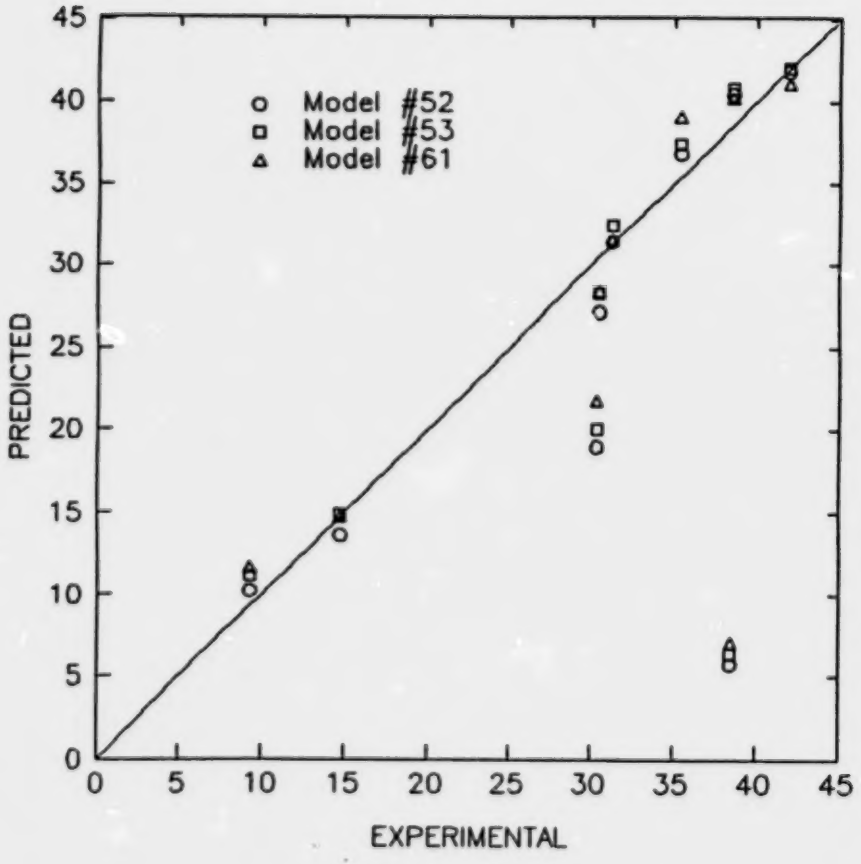

Figure 27. OIL YIELD

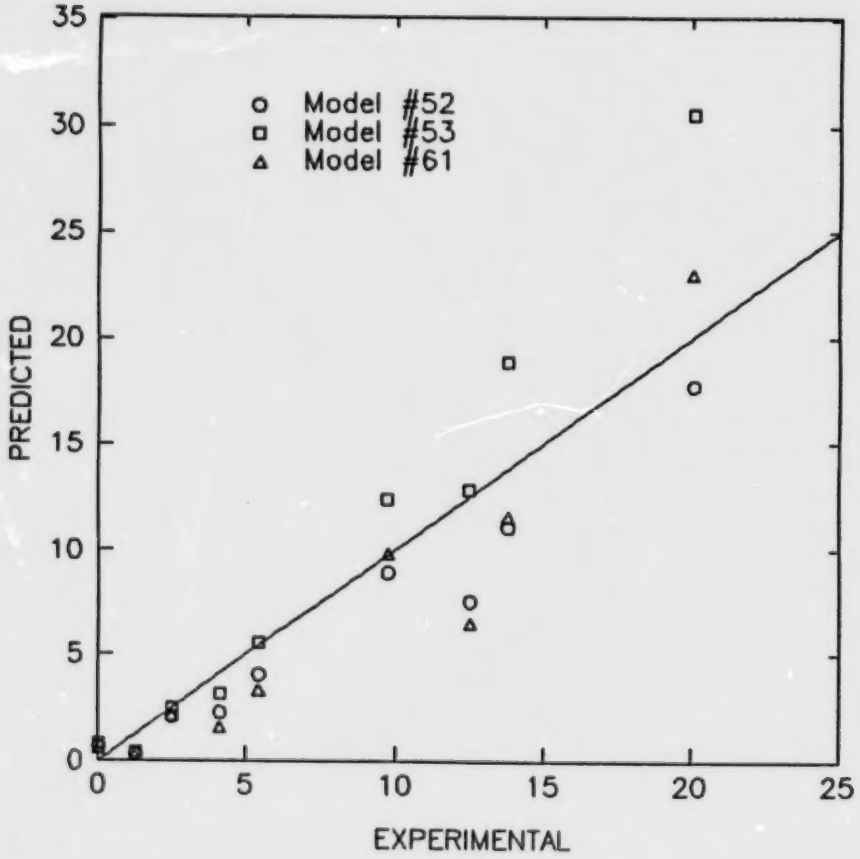

Figure 28. HEAVY GAS OIL 1 AND 2 YIELD

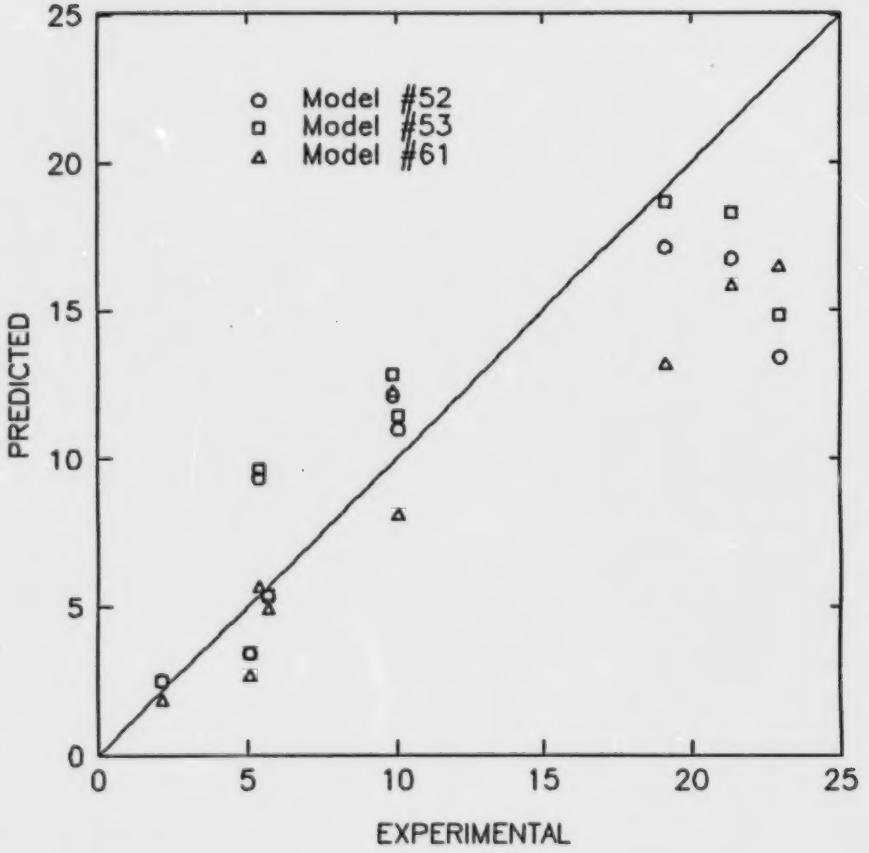

Figure 29. LIGHT GAS OIL YIELD

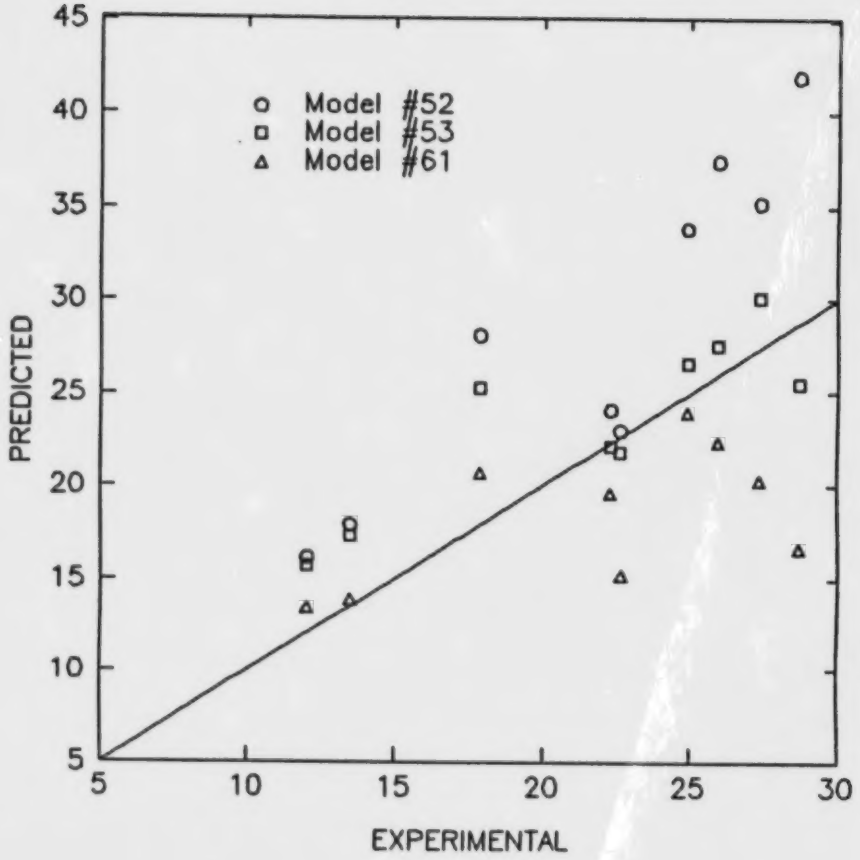

Figure 30. NAPHTHA YIELD

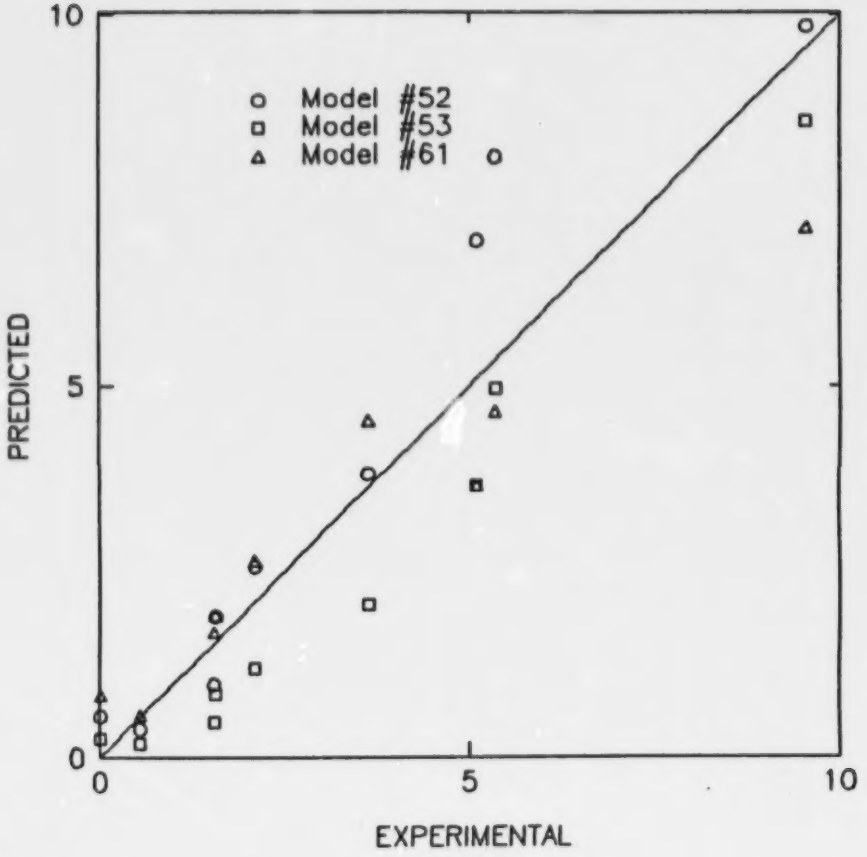

Figure 31. C1-C4 YIELD

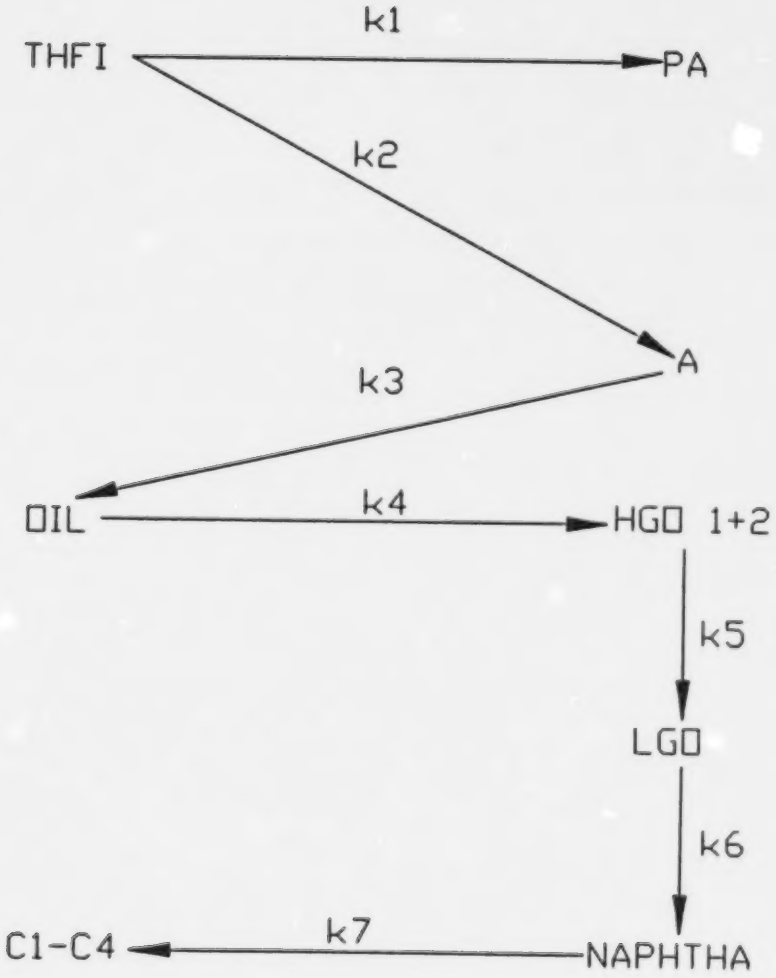

Figure 32. MODEL 63

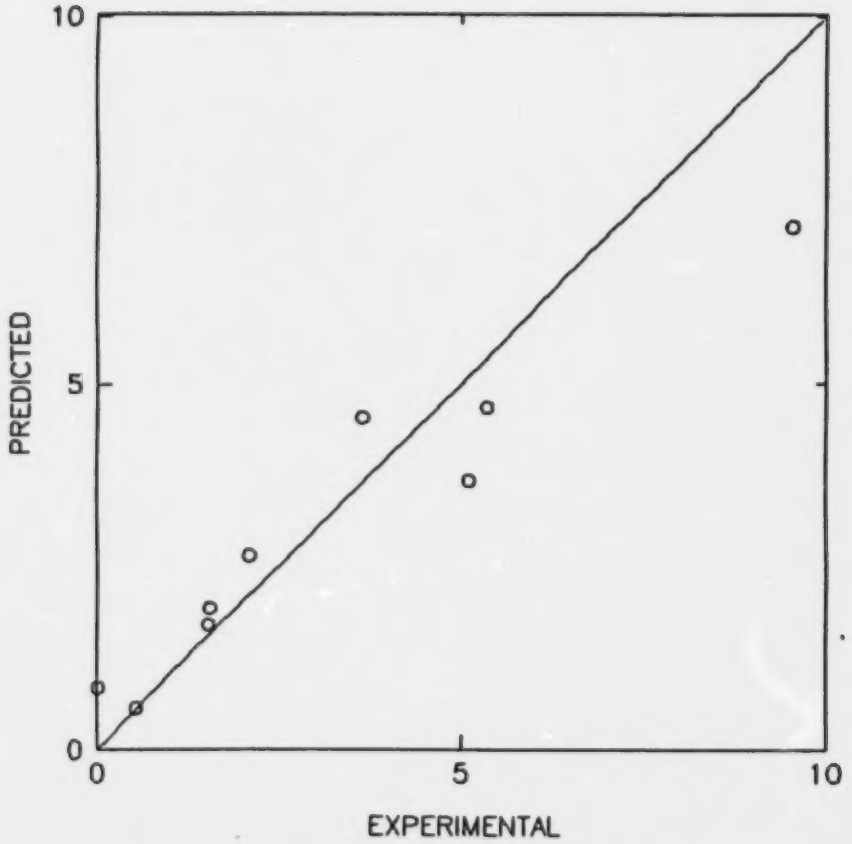

Figure 33. C1-C4 YIELD FOR MODEL 63

The final step was to improve on Model 52 by adding two more reaction paths in order to meet the limiting conditions on coprocessing products, i.e., at infinite time all distillate fractions should be converted to hydrocarbon gases. Model 53 is depicted in Figure 34 and the predicted yield of processing products is given in Appendix 10.

Table 16 presents the theoretical "expected" explanation of variance for each component and total variance, and the percent of variance explained by Model 53. With the exception of preasphaltenes, which were discussed previously (Section 5.3), Model 53 explained most of the variance due to process variables. It also is close to meeting the criterion of 92.5 percent for explaining the total variance due to process independent variables.

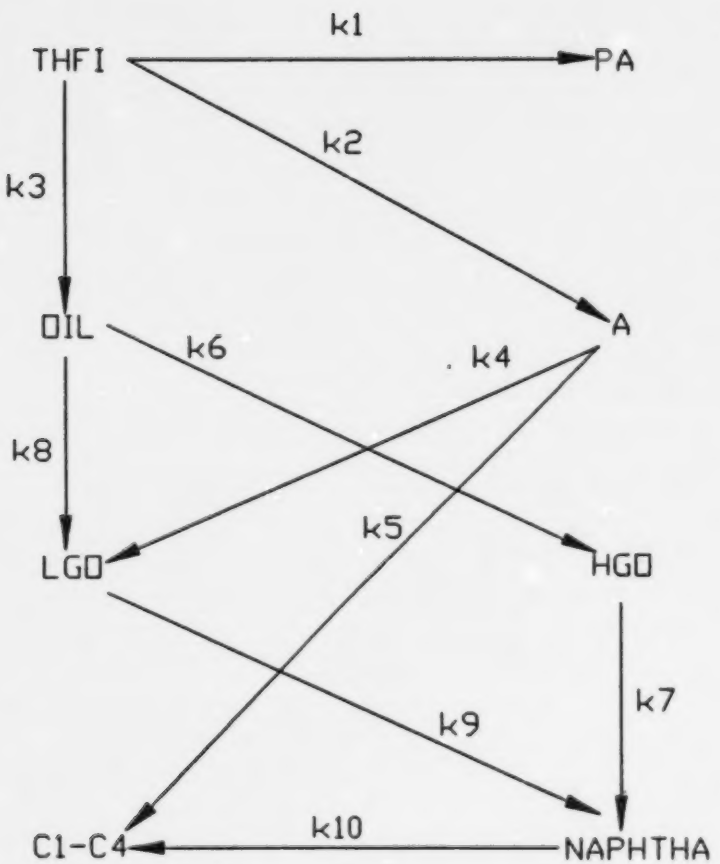

Figure 34. MODEL 53

Table 16. PERCENT OF VARIANCE EXPLAINED BY MODELS 52, 61 AND 53

	STAT[1]	MODEL 52	MODEL 61	MODEL 53
THF	92.1	90.4	92.8	91.5
PA	91.7	96.3	<0	93.1
A	52.4	54.0	55.3	52.6
OIL	65.9	95.4	96.6	96.0
HGO 1+2	94.1	47.2	75.1	90.6
LGO	98.8	71.5	75.2	78.4
NAPHT	99.4	91.6	88.4	72.7
C1-C4	99.7	98.5	98.7	98.9
TOTAL	92.5	84.4	81.4	90.0

[1]based on standard deviation

5.5. Sensitivity of the Developed Models to Assumptions

One of the key issues in ascertaining the developed models was whether the choice of the models was affected by the assumptions made during the derivation of the CSTR equations. Specifically, these are the assumptions of gas holdup and fraction of products and feed flashed off at the reactor T and P. The objective of this section is to look at the sensitivity of models with respect to the assumption or approximation made for process and reactor conditions.

Table 17 depicts the percent of variance explained by Model 52 for various levels of gas holdup (ϵ = 0.0 to 0.2) and fraction of product flashed (ϕ = 0.05 to 0.20). As is apparent, the capability of the model to explain the variance of coprocessing products remained virtually unchanged over the range of variables tested. The change of ϵ and ϕ values affects the numerical values of rate constants and, specifically, affects the values of pre-exponential factors. It does not, however, as stressed above, enhance or diminish the model's capability to predict the yield structure of coprocessing products.

We find this conclusion very important in modelling of coprocessing kinetics. The above discussion shows that the assumption relating to the actual contact time measurement for coprocessing reactions does not affect the choice of

reaction paths for coprocessing. The choice of reaction paths is determined primarily by the yield structure of the coprocessing products.

Table 17. EFFECT OF ASSUMPTIONS ON MODEL 52

GAS HOLDUP ϵ	FEED FLASHED ϕ	PERCENT OF VARIANCE EXPLAINED
0.03	0.05	84.35
0.03	0.10	84.35
0.03	0.20	84.36
0.00	0.10	84.35
0.10	0.10	84.36
0.20	0.10	84.35

6. CONCLUSIONS AND RECOMMENDATIONS

Review of the state-of-the-art of coal liquefaction and heavy oil upgrading kinetics pointed out the many common features in both processes. Because of similar chemical reactions, such as bond scission, hydrocracking and thermal cracking, the key variable in both processes is temperature with the degree and rate of bond cleavage determined predominantly by the temperature levels. This results in a lesser effect of hydrogen addition on the product yield structure, or the effect of vehicle solvent on coal conversion, with the overall coal conversion yield being similar for coal liquefaction and coprocessing. The products of both coal liquefaction and coprocessing can be classified by solubility or distillation points. This classification can be used to model the process dynamics although special emphasis must be given to the analysis of reaction networks and kinetic models.

The thirteen sets of data provided by CANMET were very good as judged by the mass balances and standard deviations for individual product components. This permitted development of the statistical criteria for goodness of fit, which were stringent enough to discriminate between various models. The expected total variance in the coprocessing data to be explained by the models was 92.5 percent for

eight-component models and 98.7 percent for six-component models.

The individual component variance was dependent on the type of product, reflecting its significance (magnitude of yield) and its standard deviation. The expected explained variance varied between 52.4 percent for asphaltenes and 99.7 percent for hydrocarbon gases.

Comparison of CANMET data to other studies revealed many similarities and common features. Matching the relative yields and hydrogen consumption for the products, CANMET data compared favorably with those of HRI. The final conclusion calls for a more detailed evaluation of CANMET and HRI or other coprocessing data in order to provide for more scientific assessment of various processes. It is felt, however, based on the data quality and consistency, that CANMET data will match or surpass those of other developers. We also recommend that CANMET undertakes an experimental program to evaluate gas holdup in the stirred-tank reactors before a detailed comparison with data generated in tubular reactors is made.

Analysis of variance (ANOVA) of CANMET data shows the yields of coprocessing products to be a strong function of temperature. On average, 64 to 97 percent of variance can be explained by temperature effects, 2 to 39 percent can be

explained by space velocity effects, and a small percentage is explained by the two-way effects. Exceptions are hydrogen consumption and carbon oxides formation with up to 96 and 81 percent, respectively, of variance explained by the space velocity, and preasphaltenes and HG02, with 28 to 61 percent of variance, respectively, explained by the two-way effects. The major part of the component variance is determined primarily by the temperature, confirming that coprocessing products are formed via temperature-sensitive reactions, i.e., bond scission, thermal cracking and hydrocracking.

Statistical analysis of reaction paths for coprocessing was performed on CANMET data processed as a Latin Square factorial design. Since one observation was missing in the 3 x 3 experimental matrix, the Yates method was applied successfully to correct for the missing cell observation. The Yates method was preferred over other statistical methods because it gives good estimated treatment effects and the residuals for the calculated observations are equal to zero.

Analysis of the effects of process variables (T and SV) on the product yield and selectivity showed the product yield structure to be determined primarily by the severity of the process, or in other words, by temperature and the extent of thermal cracking. This explains why the effect of

the quality of solvent, hydrogen consumption, or space velocity is weak in the study of coprocessing conditions. It also explains why simple correlations can be obtained between the yield of coprocessing products and severity of the process, as measured by pitch conversion.

The understanding of coprocessing reactions was greatly aided by the Multiple Classification Analysis, which depicted the overall effects of temperature and space velocity on the yield structure of coprocessing products. Several reaction paths were formulated based on the Multiple Classification Analysis, from which coprocessing models were postulated. It was also shown, by performing a factor analysis and ANOVA, that coprocessing products are independent of, and as exemplified by the OIL group, do not change with, the severity of the process. This requirement is essential for development of sound kinetic structures based on CANMET product definitions. Analysis of reaction networks for THFI also showed that one initial lump is sufficient for modelling coal conversion.

The derived reactor equations and kinetic rate expressions were those for a CSTR, with the rate equations written in terms of dimensionless yields of coprocessing products, on a moisture-and ash-free slurry feed basis. The rate constants were regressed by using the Least Squares method to minimize the residuals between the predicted and

experimental rate data. The rate constant coefficients were later calculated from the regressed rate constants. This approach provided additional understanding of the physical meaning of the regressed rate constants and how the rate constants are affected by the alternative reaction paths.

Two types of models were examined for modelling the yield structure of coprocessing products: a sequential model, where intermediate products are sequentially converted to lighter fractions and a parallel model where coprocessing products are formed via parallel reactions directly from the feed and major intermediate products. The difference between the models is exemplified by the difference in their optimization strategies, with the strategy for the parallel model being less complex but more dependent on the relative economic value for the coprocessing products and byproducts.

A number of reaction networks were evaluated for the two types of models. The principal criterion for evaluation was the percent of variance explained by the studied models. Another criterion was how accurately the model explains the yield structure of coprocessing products. The target for variance explained was 92.5 percent for the eight-component model. The best model (Model 53) explained 90.0 percent of the total variance, which was considered satisfactory, in view of the difficulties with modelling preasphaltenes.

Multiple Classification Analysis showed a change in sign for the temperature coefficient for preasphaltenes. This led us to postulate that two mechanisms are responsible for reaction paths for preasphaltenes, i.e., a chemical mechanism with an Arrhenius rate expression and an adduct formation mechanism with a rate which decreases with temperature. This pattern of preasphaltene yield behaviour was confirmed for other coals and coprocessing runs, underscoring its significance to an understanding of the coprocessing mechanism. Heavy oil upgrading and coal conversion reaction paths are coupled via the preasphaltene adduct formation. To model the preasphaltene group, we would have to derive equations for adduct formation and incorporate these equations in the tested models. This could not be accomplished, however, within the scope of this work. Therefore, it is recommended that CANMET undertake a further study to derive rate equations predicting the adduct formation for preasphaltenes.

It is felt that understanding the mechanism and kinetics of adduct formation may help greatly in the development of an improved process design strategy for CANMET coprocessing, especially in view of the potential interest in application of homogeneous catalysis to the conversion of pitch. The adduct is most likely to be formed from pitch generating heavy oil fractions and it may

influence pitch conversion kinetics through optimized process design.

Some difficulties were also experienced in modelling the C1-C4 group in sequential models. Review of the mechanism of C1-C4 formation, and the C1/C2 ratio for CANMET data, strongly indicate that the C1-C4 group has at least two reaction paths, e.g., one via thermal cracking of the heavy oil precursor structures and another via hydrotreating of light distillates. Incorporation of a parallel structure for modelling the C1-C4 group permitted an accurate modelling of C1-C4 yield in the tested models.

Over twenty different reaction networks were tested for prediction of the yield structure of distillate fractions. In the end two models - one sequential and one parallel - were evaluated in detail, with the sequential model (Model 61) explaining 81.4 percent of total variance and the parallel model (Model 52) explaining 84.4 percent of variance. Our final recommendation is based on a parallel model (Model 53) which incorporates some sequential characteristics. Model 53 can explain 90.0 percent of total variance vs. the 92.5 percent target, which is very good considering that preasphaltenes are modelled without correcting for adduct formation.

The final step in testing kinetic models for coprocessing was evaluation of the model sensitivity to the assumptions made, specifically to the assumptions of gas holdup, ϵ, and the fraction of feed flashed at the reactor T and P. Our sensitivity studies for Model 52 show that model predictive capabilities did not change with the selection of different ϵ and ϕ values. This conclusion is very important to modelling coprocessing kinetics since it reveals that the choice of reaction network is determined, in principle, by the yield structure of the coprocessing products and not by the assumptions made about ϵ or ϕ.

In view of the limited experimental data set evaluated in the course of this program, we recommend that the remaining coprocessing data at CANMET be reviewed in the context of this project's findings and developed statistical analysis methods. The additional review will provide CANMET with an assessment of whether the reported observations would apply to a wide range of coals and experimental conditions. The additional analysis will also provide CANMET with a more detailed understanding of the effects of coal, catalyst and coal properties, etc. through review of a larger set of data.

Finally, we recommend that CANMET undertake a further comprehensive experimental program which will address the effect of catalyst, heavy oil, and coal concentration and

hydrogen uptake on coprocessing product yield and selectivity. We also suggest a new factorial design for these experiments, with a temperature range of 425 - 475°C.

7. REFERENCES

Aczel, T., ERDA Contract No. E(46-1)8007, 1976.

Aris, R. and Gavalas, G. R., Phil Trans Royal Soc, London, 260, 351, 1966.

Attar, A., ACS Dev, 23, 169, 1978.

Audehn, C. A., U.S. Patent 4379045, 1984.

Bailey, J. E., Chem Eng J, 3, 52-61, 1972.

Baltanas, M., Vansina, H. and Frement, G.F., I&EC, Prod Res Dev, 22, 531, 1983.

Banerjee, D. K., Laidler, K.J., Nandi, B.N. and Patmore, D.J., Fuel, 65, 480, 1986.

Beecher, R., Voorhies, A. and Eberly, P., I&EC, Prod Res Dev, 7, 203, 1968.

Belinko, K. and Denis, J., CANMET Report 77-43, September, 1976.

Bottom, R. and Cosserat, D., Chem. Eng. J., 16, 107, 1978.

Constant, W. G., et al., Fuel, 65(1), 8-16, 1986.

Cronauer, D.C., Shah, Y.T., Ruberto, R.G., I&EC, Proc Des Dev, 17, 281, 1978.

Cronauer, D.C. and Ruberto, R.G., EPRI Report AF913, 1979.

Curran, G.P., Struck, R.T. and Gorin, E., I&EC, Proc Des Dev, 6, 166, 1967.

Curtis, C., Guin, J.A., Pass, M. and Tsai, K.J., Presented at Amer Chem Soc, Philadelphia, Aug 26, 1984.

deBruijn, et al., Presented at the Synfuels 2nd Worldwide Symposium, Brussels, October 11-13, 1982.

Falcum, et al., Fuel, 31, 133, 1952.

Flock, et al., Chem Technol, 28, 138, 1976.

Fouda, S.A., Kelly, J.F. and Rahimi, P.M., ERP/ERL 82-52, CANMET, 1982.

Gallakota, S.V., Guin, J.A., Curtis, C.W., I&EC, Proc Des Dev, 24, 1149, 1985.

Gates J. G., Canadian Patent 1174626, 1982.

Gertenbach, D.D., Baldwin, R.M. and Bain, R.L., I&EC, Proc Des Dev, 21, 490, 1982.

Gray, M.R., Khorasheh, F. and Dalla Lana, I.G., Paper presented at 1986 AIChE Meeting, Miami Beach, Fla..

Heredy, L., "Coal Science", 1966, Chapter 28.

Hikita, H. and Kikukawa, H., Chem., Eng. J., 8, 191, 1974.

Hus, M., Oil & Gas J, 109-120, April 13, 1981.

Ignasiak, B., Lewkowicz, L., Kovacik, G., Ohuchi, T. and DU PLeassis, M.P., "Catalysis on Energy Scene", 593-600, 1984.

Kang, D., Ying, D.H.S. and Givens, E.N., Impact of Hydrodynamics On Liquefaction, Final Report, DOE/OR/03054-63, 1983.

Kelly, J. F., Fouda, S.A., Rahimi, P.M. and Ikura, M., Paper presented at the CANMET Coal Conversion Contractors Meeting, Calgary, November, 1984.

Khulbe, K. C., Sachdev, A.K., Mann, R.S. and Davis, S., Fuel Proc Technology, 8, 259, 1984.

Lee, H., AIChE J, 23, 166, 1977.

Leibenberd, B.J. and Potgieter, H.G., Fuel, 62, 133, 1972.

Li, A. and Lin, D., Presented at the 2nd World Congress of Chemical Engineering, Montreal, October 4-9, 1981.

Liu, D., et al., CSChE Conference, Calgary, October, 1985a.

Liu, D., et al., AIChE 1985 Winter Meeting, Chicago, November, 1985b.

Liu, Y.A. and Lapidus, L., AIChE J, 19, 467, 1973.

Lozano, A., et al., I&EC, Prod Res Dev, 17(1), 71, 1978.

Luss, D. and Hutchinson, Y., Chem Eng J, 2, 172, 1971.

MacAurthur, J., Boehm, F., Liron, A. and Shannon, R.H., Presented at 10th Annual EPRI Contractors' Conference on Clean Liquid and Solid Fuel, Palo Alto, Calif., April 23, 1985.

Mohan, G. and Silla, H., I&EC, Proc Des Dev, 20, 349, 1981.

Moschopedis, S., Hawkins, R.W. and Speight, J.G., Fuel Proc Tech, 5, 213-228, 1982.

Moschopedis, S., Canadian Patent 1160586, 1984.

Moschopedis, S., and Ozum, B., Liq Fuel Tech, 2, 177-191, 193-209, 1984.

Neavel, R., Fuel, 55, 237, 1976.

Parulekar, S. J. and Shah Y. Y., Chem. Eng. J. 20, 21, 1980.

Pelipetz, M.G., et al., I&EC, Proc Des Dev, 47, 1201, 1955.

Prasad, G.N., Witmann, C.V., Agnew, J.B. and Sridhar, T., AIChE J, 32, 1277, 1986a.

Prasad, G.N., Agnew, J.B. and Sridhar, T., AIChE J, 32, 1288, 1986b.

Prater, et al., Chem Eng Sci, 22, 1587, 1967.

Sato, S., ACS Div Fuel Chem, Preprints, 24, 270, 1976.

Shalabi, M.A., Baldwin, R.M., Bain, R.L., Gary, J.H. and Golden, J.O., I&EC, Proc Des Dev, 18, 474, 1979.

Shah, Y., Cronauer, D.C., McIlvried, H.G. and Paraskos, J.A., I&EC, Proc Des Dev, 17, 288, 1978.

Shu, W. and Venkatesank, V., J Can Petro, page 60, March-April, 1984.

Sosnowski, J., Turner, D.W. and Eng, J., Chem Eng Progr, 51, February, 1981.

Speight, J.G., "The Desulphurization of Heavy Oils and Residue", Marcel Dekker, Inc., 1981.

Squires, A., Applied Energy, 4, 181, 1978.

Stangeland, B., I&EC, Prod Res Dev, 13, 71-76, 1974.

Steijns, M. and Froment, G., IE&C, Prod Res Dev, 20, 660, 1981.

Szladow, A. and Given, P., I&EC, Proc Des Dev, 20, 27, 1981.

Szladow, A. and Given, P., Chem Eng Comm, 19, 115, 1982.

Wei, J. and K., AIChE J, 9 297, 1969.

Whitehurst, D.D., Farcasiu, M., Mitchel,T.O. and Dickert, J.J., EPRI Report AP480, 1977.

Wiser, W., Fuel, 47, 475, 1968.

Yoshida, R., Yoshida, T., Nakata, Y., Fuel, 55, 337, 1976.

Yoshida, R., Yoshida, T., Nakata, Y., Hasegawa, Y.,Hino, M., Fuel Proc Tech, 7, 161-171, 1983.

APPENDIX 1

CANMET COPROCESSING DATA

RUN NUMBER	SFCF070385-1	SPCF070385-2	SFCF280285-1	SF020683-1	SF070185-1
RUN ORDER	1	2	3	4	5
I. Operating Conditions					
coal type	Forrestburg	Forrestburg	Forrestburg	Forrestburg	Forrestburg
heavy oil type	Cold Lake VB	Cold Lake VB	Cold Lake VB	Cold Lake VB	Cold Lake VB
reactor temperature, C	400.00	425.00	450.00	425.00	425.00
room temperature, C	22.00	22.00	22.00	24.00	15.00
reactor pressure, PSIG	2000.00	2000.00	2000.00	2000.00	2000.00
barometer pressure, mm Hg	760.00	760.00	760.00	760.00	760.00
run duration, min	80.00	80.00	180.00	120.00	120.00
feed toal weight, g	600.00	548.00	402.00	448.00	584.00
hydrogen flow, l/min	6.06	6.06	4.00	8.10	4.00
space velocity, Kg/l/hr	1.54	1.40	0.76	0.76	1.00
coal conc. (maf), wt%	29.71	29.71	30.83	30.73	29.50
II. Analysis					
2.1 Feed Analysis, wt%					
thfi	32.00	32.00	33.20	33.30	31.80
ash	3.25	3.25	3.42	3.65	3.18
carbon	76.43	76.43	76.36	74.64	76.41
hydrogen	8.00	8.00	7.95	7.82	7.98
nitrogen	0.82	0.82	0.96	1.11	0.80
sulphur	4.29	4.29	3.96	3.85	3.91
oxygen	7.20	7.20	7.35	8.93	7.72
water	0.00	0.00	0.00	0.00	0.00
total	100.00	100.00	100.00	100.00	100.00
2.2 Metal Analysis, wt%					
iron	0.472	0.472	0.499	0.356	0.416
nickle	0.008	0.008	0.008	0.007	0.007
vanadium	0.019	0.018	0.018	0.017	0.018
2.3 Prop., heavy oil, gms wt%	408.02	372.66	268.54	299.00	398.65
spe. gravity	1.04	1.04	1.04	1.04	1.04
preasphaltene	0.20	0.20	0.20	0.20	0.20
asphaltene	23.48	23.48	23.48	23.48	23.48
distillation					
420-525	16.75	16.75	16.75	16.75	16.75

CANMET COPROCESSING DATA

RUN NUMBER	SFCF070385-1	SPCF070385-2	SFCF280285-1	SF020683-1	SF070185-1
RUN ORDER	1	2	3	4	5
residue	83.25	83.25	83.25	83.25	83.25
205-420	0.00	0.00	0.00	0.00	0.00
IBP-205	0.00	0.00	0.00	0.00	0.00

III. Products

3.1 Gas Products. grams

hydrogen	22.99	18.46	42.13	61.05	26.37
hydrogen sulfide	0.24	2.27	7.31	3.22	2.87
COx	11.96	11.02	10.54	13.09	9.54
C1 - C4	3.21	8.26	37.07	14.80	11.88
C5 + C6	2.27	2.24	4.66	4.53	1.11
other	0.00	0.00	0.00	0.00	0.00
total	40.68	42.24	101.72	96.69	51.77

3.2 Liquid Yields, grams	599.38	545.81	359.78	431.09	572.86
wt%					
distillate	14.76	30.86	77.22	41.59	32.77
residue	83.04	66.22	14.47	53.46	64.15
water	2.20	2.91	8.31	4.95	3.08
total	100.00	100.00	100.00	100.00	100.00

3.3 Distillate Prop. wt%

gravity	0.95	0.93	0.89	0.89	0.92
carbon	84.43	84.17	85.27	84.26	84.43
hydrogen	11.07	11.30	11.55	11.29	11.42
nitrogen	0.34	0.40	0.57	0.44	0.44
sulphur	2.97	2.74	1.30	2.20	2.30
oxygen	1.19	1.40	1.32	1.81	1.40
total	100.00	100.00	100.00	100.00	100.00

3.4 Distillate Frac. wt%

IBP - 205 C	8.20	12.80	27.70	11.90	15.80
205 - 315 C	13.60	17.00	32.10	27.20	30.30
315 - 435 C	30.60	27.00	26.30	23.90	32.70
435 - 525 C	47.60	43.20	13.80	37.00	21.20

RUN NUMBER RUN ORDER	SFCF070385-1 1	SPCF070385-2 2	SFCF280285-1 3	SF020683-1 4	SF070185-1 5
total	100.00	100.00	99.90	100.00	100.00
3.5 Residue Analysis, wt%					
ash	4.28	5.23	15.10	6.86	5.17
carbon	78.08	80.00	74.20	77.02	79.77
hydrogen	7.95	7.92	5.79	7.24	8.07
nitrogen	1.26	1.46	1.37	1.31	1.26
sulphur	4.08	3.99	3.87	3.64	3.95
oxygen	4.44	4.00	3.98	3.93	3.06
total	100.08	102.60	104.31	100.00	101.28
petane insoluable, wt%	51.00	54.10	71.30	51.70	53.00
toluene insoluable, wt%	27.20	28.20	36.20	26.30	29.60
THFI	25.00	20.00	23.60	22.70	19.50
IV. Data Workout					
4.1 Inlet Conditions					
feed rate gm/min	7.50	6.85	2.23	3.73	4.87
feed rate, wt% (maf)	7.26	6.63	2.16	3.60	4.71
total weight, gm (maf)	580.48	530.17	388.24	431.64	565.45
total coal wight,gm (maf)	172.46	157.51	119.69	132.64	166.81
ash, grams	19.52	17.83	13.76	16.36	18.55
Feed Concentration, grams					
coal (maf)	172.46	157.51	119.69	132.64	166.81
preasphaltene	0.82	0.75	0.54	0.60	0.80
asphaltene	95.80	87.50	63.05	70.21	93.60
oil	243.06	221.99	159.97	178.11	237.47
HGO	68.34	62.42	44.98	50.08	66.77
LGO	0.00	0.00	0.00	0.00	0.00
Naphtha	0.00	0.00	0.00	0.00	0.00
total	580.48	530.17	388.24	431.64	565.45
total feed pitch	512.14	467.75	343.26	381.56	498.68
4.2 Product Yields, grams	622.96				

CANMET COPROCESSING DATA

RUN NUMBER	SFCF070385-1	SPCF070385-2	SFCF280285-1	SF020683-1	SF070185-1
RUN ORDER	1	2	3	4	5
Distillate + C5 + C6	90.76	170.70	282.48	183.83	188.81
Residue (maf)	476.41	342.54	44.21	214.65	348.50
Water	13.19	15.90	29.89	21.33	17.65
coal	124.43	72.29	12.29	52.31	71.66
ash	21.30	18.90	7.86	15.80	19.00
coal (maf)	103.13	53.39	4.43	36.51	52.66
preahaltene	10.95	29.64	6.56	8.30	37.12
asphaltene	118.45	93.61	18.28	58.53	86.00
oil	243.88	165.90	14.94	111.31	172.73
HGO [Fraction 4]	42.12	72.78	38.34	66.34	39.79
LGO2 [Fraction 3]	27.08	45.49	73.07	42.85	61.38
LGO1 [Fraction 2]	12.03	28.64	89.18	48.77	56.87
Naph [Fract. 1 + C5-6]	9.53	23.80	81.89	25.86	30.77
sub-total	588.47	532.15	334.55	414.28	556.32
water	13.19	15.90	29.89	21.33	17.65
ash	21.30	18.90	7.86	15.80	19.00
total	622.96	566.96	372.30	451.41	592.97
4.3 Conversion					
total product pitch, g	476.41	342.54	44.21	214.65	348.50
Coal Conversion, wt%	40.20	66.11	96.30	72.47	68.43
Pitch Conversion, wt%	6.98	26.77	87.12	43.75	30.12
4.4 H2 consumption					
H2 in, grams	40.06	40.06	59.49	79.77	40.63
H2 out, grams	22.99	18.46	42.13	61.05	26.37
Net H2 consumed, gms	17.07	21.60	17.36	18.72	14.25
H2 consumption as wt% of feed (maf)	2.94	4.07	4.47	4.34	2.52
V. SUMMARY (BASE:MAF FEED)					
Reactor temp., C	400	425	450	425	425
Space velocity,Kg/l/hr	1.54	1.40	0.76	0.76	1.00
FEEDS	WT%	WT%	WT%	WT%	WT%

CANMET COPROCESSING DATA

RUN NUMBER	SFCF070385-1	SPCF070385-2	SFCF280285-1	SF020683-1	SF070185-1
RUN ORDER	1	2	3	4	5
coal	29.71	29.71	30.83	30.73	29.50
preasphaltene	0.14	0.14	0.14	0.14	0.14
asphaltene	16.50	16.50	16.24	16.26	16.55
oil	41.87	41.87	41.20	41.26	42.00
HGO [Fraction 4]	11.77	11.77	11.59	11.60	11.81
LGO2 [Fraction 3]	0.00	0.00	0.00	0.00	0.00
Naph [Fract. 1 + C5-6]	0.00	0.00	0.00	0.00	0.00
sub-total	100.00	100.00	100.00	100.00	100.00
H2 consumed	2.94	4.07	4.47	4.34	2.52
ash in	3.36	3.36	3.55	3.79	3.28
Total	106.30	107.44	108.02	108.13	105.80
PRODUCTS:					
coal	17.77	10.07	1.14	8.46	9.31
preasphaltene	1.89	5.59	1.69	1.92	6.56
asphaltene	20.41	17.66	4.71	13.56	15.21
oil	42.01	31.29	3.85	25.79	30.55
HGO [Fraction 4]	7.26	13.73	9.88	15.37	7.04
LGO2 [Fraction 3]	4.66	8.58	18.82	9.93	10.85
LGO1 [Fraction 2]	2.07	5.40	22.97	11.30	10.06
Naph [Fract. 1 + C5-6]	1.64	4.49	21.09	5.99	5.44
gas [H2S + COx + C1-4]	2.65	4.06	14.15	7.21	4.30
sub-total	100.36	100.87	98.29	99.52	99.32
water	2.27	3.00	7.70	4.94	3.12
ash out	3.67	3.57	2.03	3.66	3.36
Total	106.30	107.44	108.02	108.13	105.80
CONVERSIONS					
coal	40.20	66.11	96.30	72.47	68.43
pitch	6.98	26.77	87.12	43.75	30.12

CANMET COPROCESSING DATA

RUN NUMBER RUN ORDER	SF160683-2 6	SF250383-2 7	SPCF040385-1 8	SF070185-2 9	SF261083-2 10
I. Operating Conditions					
coal type	Forrestburg	Forrestburg	Forrestburg	Forrestburg	Forrestburg
heavy oil type	Cold Lake VB	Cold Lake VB	Cold Lake VB	Cold Lake VB	Cold Lake VB
reactor temperature, C	450.00	400.00	425.00	450.00	450.00
room temperature, C	30.00	22.00	19.00	26.00	21.00
reactor pressure, PSIG	2000.00	2000.00	2000.00	2000.00	2000.00
barometer pressure, mm Hg	760.00	760.00	760.00	760.00	760.00
run duration, min	80.00	120.00	180.00	120.00	120.00
feed coal weight, g	565.60	452.00	454.00	576.00	568.00
hydrogen flow, l/min	7.85	8.00	3.99	4.00	4.00
space velocity, Kg/l/hr	1.45	0.77	0.52	0.98	0.97
coal conc. (maf), wt%	32.10	30.20	29.71	29.55	31.20
II. Analysis					
2.1 Feed Analysis, wt%					
thfi	34.60	32.74	32.00	31.80	33.80
ash	3.62	3.57	3.25	3.18	3.73
carbon	75.29	76.27	76.43	76.41	76.30
hydrogen	7.77	7.36	8.00	7.98	7.73
nitrogen	0.81	1.04	0.82	0.89	0.47
sulphur	3.78	4.00	4.29	3.91	3.86
oxygen	8.73	7.76	7.20	7.72	7.90
water	0.00	0.00	0.00	0.00	0.00
total	100.00	100.00	100.00	100.09	100.00
2.2 Metal Analysis, wt%					
iron	0.266	0.360	0.472	0.416	0.356
nickle	0.012	0.008	0.008	0.007	0.007
vanadium	0.017	0.019	0.019	0.018	0.017
2.3 Prop., heavy oil, gms	370.13	304.23	308.74	392.93	376.20
wt%					
spe. gravity	1.04	1.04	1.04	1.04	1.04
preasphaltene	0.20	0.20	0.20	0.20	0.20
asphaltene	23.48	23.48	23.48	23.48	23.48
distillation					
420-525	16.75	16.75	16.75	16.75	16.75

CANMET COPROCESSING DATA

RUN NUMBER RUN ORDER	SF160683-2 6	SF250383-2 7	SPCF040385-1 8	SF070185-2 9	SF261083-2 10
residue	83.25	83.25	83.25	83.25	83.25
205-420	0.00	0.00	0.00	0.00	0.00
IBP-205	0.00	0.00	0.00	0.00	0.00
III. Products					
3.1 Gas Products. grams					
hydrogen	31.17	66.63	47.93	20.37	17.42
hydrogen sulfide	3.80	0.80	4.27	6.11	7.33
COx	13.65	7.57	11.55	9.93	13.40
C1 - C4	27.85	5.12	16.01	27.94	31.08
C5 + C6	4.23	2.56	2.98	1.30	2.42
other	0.00	0.00	0.00	0.00	0.00
total	80.70	82.69	82.74	65.66	71.65
3.2 Liquid Yields, grams	535.42	448.63	431.21	550.76	536.14
wt%					
distillate	56.79	25.67	47.21	61.67	62.01
residue	36.90	69.90	49.08	34.51	31.84
water	6.31	4.43	3.71	3.82	6.15
total	100.00	100.00	100.00	100.00	100.00
3.3 Distillate Prop. wt%					
gravity	0.90	0.89	0.91	0.90	0.89
carbon	84.66	84.60	83.56	85.17	85.08
hydrogen	11.56	10.20	11.30	11.22	11.63
nitrogen	0.45	0.49	0.50	0.50	0.44
sulphur	1.70	2.71	3.09	1.65	1.50
oxygen	1.63	2.00	1.55	1.47	1.35
total	100.00	100.00	100.00	100.00	100.00
3.4 Distillate Frac. wt%					
IBP - 205 C	21.00	9.40	19.60	23.20	21.90
205 - 315 C	34.30	15.10	21.30	35.40	34.90
315 - 435 C	24.30	23.70	26.20	22.00	23.20
435 - 525 C	20.40	51.80	32.90	19.40	20.80

CANMET COPROCESSING DATA

RUN NUMBER	SF160683-2	SF290383-2	SPCF040385-1	SF070185-2	SF261083-2
RUN ORDER	6	7	8	9	10
total	100.00	100.00	100.00	100.00	100.80
3.5 Residue Analysis, wt%					
ash	11.63	5.22	7.09	8.42	9.03
carbon	76.52	78.51	76.73	77.68	77.50
hydrogen	5.86	6.99	7.67	5.55	5.91
nitrogen	1.56	1.38	1.20	1.75	1.22
sulphur	3.78	4.05	3.52	3.53	3.63
oxygen	3.19	3.85	3.78	3.07	2.71
total	102.54	100.00	100.00	100.00	100.00
petane insoluable, wt%	59.30	47.32	37.00	80.90	61.20
toluene insoluable, wt%	42.20	28.22	26.70	43.80	34.90
THFI	32.00	25.71	18.10	20.50	26.80
IV. Data Workout					
4.1 Inlet Conditions					
feed rate gm/min	7.07	3.77	2.52	4.80	4.73
feed rate, wt% (maf)	6.81	3.63	2.44	4.65	4.56
total weight, gm (maf)	545.13	435.86	439.23	557.71	546.80
total coal wight,gm (maf)	174.99	131.63	130.50	164.78	170.60
ash, grams	20.47	16.14	14.77	18.29	21.20
Feed Concentration, grams					
coal (maf)	174.99	131.63	130.50	164.78	170.60
preasphaltene	0.74	0.61	0.62	0.79	0.75
asphaltene	86.91	71.43	72.49	92.26	88.33
oil	220.49	181.23	183.91	234.07	224.10
HGO	62.00	50.96	51.71	65.82	63.01
LGO	0.00	0.00	0.00	0.00	0.00
Naphtha	0.00	0.00	0.00	0.00	0.00
total	545.13	435.86	439.23	557.71	546.80
total feed pitch	483.13	304.90	387.52	491.89	483.79
4.2 Product Yields, grams					

CANMET COPROCESSING DATA

RUN NUMBER	SF160683-2	SF250383-2	SPCF040385-1	SF070185-2	SF261083-2
RUN ORDER	6	7	8	9	10
Distillate + C5 + C6	308.27	117.74	206.54	340.92	334.90
Residue (maf)	174.61	297.21	196.65	174.08	155.27
Water	33.79	19.87	16.00	21.04	32.98
coal	63.23	80.63	38.31	38.97	45.74
ash	22.98	16.38	15.01	16.01	15.41
coal (maf)	40.25	64.24	23.30	22.96	30.33
preahaltene	20.15	7.87	18.20	44.29	13.83
asphaltene	33.79	59.90	21.80	70.52	44.89
oil	80.42	165.20	133.35	36.31	66.22
HGO [Fraction 4]	62.02	59.66	66.97	65.89	69.16
LGO2 [Fraction 3]	73.88	27.30	53.33	74.72	77.14
LGO1 [Fraction 2]	104.29	17.39	43.36	120.23	116.04
Naph [Fract. 1 + C5-6]	68.08	13.39	42.88	80.09	72.57
sub-total	505.86	431.33	418.20	531.01	505.58
water	33.79	19.87	16.00	21.04	32.98
ash	22.98	16.38	15.01	16.01	132.28
total	562.63	467.58	449.21	568.06	670.83
4.3 Conversion					
total product pitch, g	174.61	297.21	196.65	174.08	155.27
Coal Conversion, wt%	77.00	51.19	82.15	86.07	82.22
Pitch Conversion, wt%	63.86	22.78	49.25	64.61	67.91
4.4 H2 consumption					
H2 in, grams	50.52	79.32	59.95	39.13	39.80
H2 out, grams	31.17	66.63	47.93	20.37	17.42
Net H2 consumed, gms	19.35	12.69	12.02	18.76	22.38
H2 consumption as wt% of feed (maf)	3.55	2.91	2.74	3.36	4.09
V. SUMMARY (BASE:MAF FEED)					
Reactor temp., C	450	400	425	450	450
Space velocity,Kg/l/hr	1.45	0.77	0.52	0.98	0.97
FEEDS	WT%	WT%	WT%	WT%	WT%

CANMET COPROCESSING DATA

RUN NUMBER	SF160683-2	SF250383-2	SPCF040385-1	SF070185-2	SF261083-2
RUN ORDER	6	7	8	9	10
coal	32.10	30.20	29.71	29.55	31.20
preasphaltene	0.14	0.14	0.14	0.14	0.14
asphaltene	15.94	16.39	16.50	16.54	16.15
oil	40.45	41.58	41.87	41.97	40.98
HGO [Fraction 4]	11.37	11.69	11.77	11.80	11.52
LGO2 [Fraction 3]	0.00	0.00	0.00	0.00	0.00
Naph [Fract. 1 + C5-6]	0.00	0.00	0.00	0.00	0.00
sub-total	100.00	100.00	100.00	100.00	100.00
H2 consumed	3.55	2.91	2.74	3.36	4.09
ash in	3.76	3.70	3.36	3.28	3.88
Total	107.31	106.61	106.10	106.64	107.97
PRODUCTS					
coal	7.38	14.74	5.30	4.12	5.55
preasphaltene	3.70	1.81	4.14	7.94	2.53
asphaltene	6.20	13.74	4.96	12.64	8.21
oil	14.75	37.90	30.36	6.51	12.11
HGO [Fraction 4]	11.38	13.69	15.25	11.81	12.65
LGO2 [Fraction 3]	13.55	6.26	12.14	13.40	14.11
LGO1 [Fraction 2]	19.13	3.99	9.87	21.56	21.22
Naph [Fract. 1 + C5-6]	12.49	3.07	9.76	14.36	13.27
gas [H2S + COx + C1-4]	8.31	3.10	7.25	7.89	9.48
sub-total	96.89	98.30	99.04	100.23	99.12
water	6.20	4.56	3.64	3.77	6.03
ash out	4.22	3.76	3.42	2.87	2.82
Total	107.31	106.61	106.10	106.87	107.97
CONVERSIONS					
coal	77.00	51.19	82.15	86.07	82.22
pitch	63.86	22.78	49.25	64.61	67.91

CANMET COPROCESSING DATA

RUN NUMBER	SPCF210285-1	SF230185-2	SF090683-2
RUN ORDER	11	12	13

I. Operating Conditions

coal type	Forrestburg	Forrestburg	Forrestburg
heavy oil type	Cold Lake VB	Cold Lake VB	Cold Lake VB
reactor temperature, C	400.00	450.00	455.00
room temperature, C	21.00	21.00	24.00
reactor pressure, PSIG	2000.00	2500.00	2000.00
barometer pressure, mm Hg	760.00	760.00	760.00
run duration, min	180.00	120.00	120.00
feed toal weight, g	442.00	586.00	535.00
hydrogen flow, l/min	4.03	4.02	7.92
space velocity, Kg/l/hr	0.50	1.00	0.91
coal conc. (maf), wt%	30.83	33.88	32.10

II. Analysis

2.1 Feed Analysis, wt%

thfi	33.20	35.90	34.60
ash	3.42	3.05	3.62
carbon	76.36	77.05	75.29
hydrogen	7.95	7.98	7.77
nitrogen	0.96	0.64	0.81
sulphur	3.96	3.95	3.78
oxygen	7.35	7.34	8.74
water	0.00	0.00	0.00
total	100.00	100.00	100.00

2.2 Metal Analysis, wt%

iron	0.499	0.000	0.270
nickle	0.008	0.000	0.012
vanadium	0.018	0.000	0.017

2.3 Prop., heavy oil, gms	295.26	375.66	350.11
wt%			
spe. gravity	1.04	1.04	1.04
preasphaltene	0.20	0.20	0.20
asphaltene	23.48	23.48	23.48
distillation			
420-525	16.75	16.75	16.75

CANMET COPROCESSING DATA

RUN NUMBER	SPCF210285-1	SF230185-2	SF090683-2
RUN ORDER	11	12	13
residue	83.25	83.25	83.25
205-420	0.00	0.00	0.00
IBP-205	0.00	0.00	0.00

III. Products

3.1 Gas Products. grams

hydrogen	46.51	23.91	59.81
hydrogen sulfide	0.08	1.94	5.25
COx	11.32	8.39	13.20
C1 - C4	6.59	32.26	38.20
C5 + C6	1.78	2.42	4.54
other	0.00	0.00	0.00
total	66.27	68.92	120.99

3.2 Liquid Yields, grams	435.87	557.08	492.00
wt%			
distillate	29.84	65.02	72.93
residue	68.27	31.06	21.28
water	1.89	3.92	5.78
total	100.00	100.00	100.00

3.3 Distillate Prop. wt%

gravity	0.96	0.90	0.90
carbon	84.38	84.89	84.37
hydrogen	10.99	11.49	11.64
nitrogen	0.45	0.51	0.55
sulphur	2.72	1.60	1.37
oxygen	1.46	1.51	2.07
total	100.00	100.00	100.00

3.4 Distillate Frac. wt%

IBP - 205 C	7.00	26.40	22.00
205 - 315 C	18.70	30.10	35.60
315 - 435 C	25.10	19.10	26.60
435 - 525 C	49.20	24.40	15.80

CANMET COPROCESSING DATA

RUN NUMBER	SPCF210285-1	SF230185-2	SF090683-2
RUN ORDER	11	12	13
total	100.00	100.00	100.00
3.5 Residue Analysis, wt%			
ash	5.10	11.08	11.77
carbon	77.20	75.38	74.74
hydrogen	8.00	5.65	5.60
nitrogen	1.52	1.40	1.56
sulphur	3.89	3.83	3.16
oxygen	4.28	2.66	3.17
total	100.00	100.00	100.00
petane insoluable, wt%	49.20	86.40	52.60
toluene insoluable, wt%	26.40	52.20	36.30
THFI	21.30	28.20	28.10
IV. Data Workout			
4.1 Inlet Conditions			
feed rate gm/min	2.46	4.88	4.46
feed rate, wt% (maf)	2.37	4.73	4.30
total weight, gm (maf)	426.87	568.15	515.63
total coal wight,gm (maf)	131.60	192.49	165.53
ash, grams	15.13	17.85	19.37
Feed Concentration, grams			
coal (maf)	131.60	192.49	165.53
preasphaltene	0.59	0.75	0.70
asphaltene	69.33	88.21	82.21
oil	175.89	223.78	208.56
HGO	49.46	62.92	58.64
LGO	0.00	0.00	0.00
Naphtha	0.00	0.00	0.00
total	426.87	568.15	515.63
total feed pitch	377.41	505.23	456.99
4.2 Product Yields, grams			

CANMET COPROCESSING DATA

RUN NUMBER	SPCF210285-1	SF230185-2	SF090683-2
RUN ORDER	11	12	13
Distillate + C5 + C6	131.82	364.61	363.38
Residue (maf)	282.38	153.85	92.39
Water	8.26	21.86	28.45
coal	63.38	48.79	29.43
ash	15.19	19.18	12.33
coal (maf)	48.19	29.62	17.10
preahaltene	15.18	41.53	8.59
asphaltene	67.84	59.17	17.07
oil	151.16	23.53	49.64
HGO [Fraction 4]	63.98	88.37	56.70
LGO2 [Fraction 3]	32.64	69.18	95.45
LGO1 [Fraction 2]	24.32	109.02	127.75
Naph [Fract. 1 + C5-6]	10.88	98.04	83.49
sub-total	429.39	537.64	468.10
water	8.26	21.86	28.45
ash	229.72	130.42	78.27
total	667.36	689.92	574.81
4.3 Conversion			
total product pitch, g	282.38	153.85	92.39
Coal Conversion, wt%	63.38	84.61	89.67
Pitch Conversion, wt%	25.18	69.55	79.78
4.4 H2 consumption			
H2 in, grams	60.14	39.99	78.00
H2 out, grams	46.51	23.91	59.81
Net H2 consumed, gms	13.63	16.09	18.19
H2 consumption as wt% of feed (maf)	3.19	2.83	3.53
V. SUMMARY (BASE:MAF FEED)			
Reactor temp., C	400	450	455
Space velocity,Kg/l/hr	0.50	1.00	0.91
FEEDS	WT%	WT%	WT%

CANMET COPROCESSING DATA

RUN NUMBER	SPCF210285-1	SF230185-2	SF090683-2
RUN ORDER	11	12	13
coal	30.83	33.88	32.10
preasphaltene	0.14	0.13	0.14
asphaltene	16.24	15.52	15.94
oil	41.20	39.39	40.45
HGO [Fraction 4]	11.59	11.08	11.37
LGO2 [Fraction 3]	0.00	0.00	0.00
Naph [Fract. 1 + C5-6]	0.00	0.00	0.00
sub-total	100.00	100.00	100.00
H2 consumed	3.19	2.83	3.53
ash in	3.55	3.14	3.76
Total	106.74	105.97	107.28
PRODUCTS			
coal	11.29	5.21	3.32
preasphaltene	3.56	7.31	1.67
asphaltene	15.89	10.42	3.31
oil	35.41	4.14	9.63
HGO [Fraction 4]	14.99	15.55	11.00
LGO2 [Fraction 3]	7.65	12.18	18.51
LGO1 [Fraction 2]	5.70	19.19	24.77
Naph [Fract. 1 + C5-6]	2.55	17.26	16.19
gas [H2S + COx + C1-4]	4.21	7.50	10.99
sub-total	101.25	98.75	99.38
water	1.93	3.85	5.52
ash out	3.56	3.38	2.39
Total	106.74	105.97	107.28
CONVERSIONS			
coal	63.38	84.61	89.67
pitch	25.18	69.55	79.78

APPENDIX 2

TWO-FACTOR ANOVA FOR REPLICATES

	REPLICATES									
	1	2	3	4	5	6	R(i)	TVR(i)	SR(i)	RSR(i)
THFI	4.3	6.1	5.5	4.1	5.2	4.6	4.967	2.953	0.7685	0.09324
PA	3.5	1.6	2.5	7.9	6.2	6.5	4.700	31.62	2.515	0.3224
A	7.4	5.7	8.2	12.6	11.4	12.7	9.667	43.83	2.961	0.1846
OIL	15.5	11.2	12.1	6.5	7.9	5.8	9.833	70.23	3.748	0.2297
DIST	62.7	64.4	61.2	61.1	57.8	58.2	60.90	32.52	2.550	0.02523
C1-C4	5.0	6.6	5.7	5.0	5.5	6.1	56.50	1.975	0.6285	0.06703
C(j)	16.4	15.9	15.8	16.2	15.7	15.6	**15.9**			
							GMEAN			
TV(j)	2668	2865	2518	2464	2156	2213				
Sc(j)	23.10	23.94	22.44	22.20	20.77	21.04				
CSC(j)	0.848	0.905	0.852	0.825	0.798	0.810				

Two-Factor ANOVA for Replicates: Basic Equations

$$R(i) = \frac{1}{6} \sum_{j=1}^{6} X(i,j)$$ mean value for Row i

$$TVR(i) = \sum_{j=1}^{6} [X(i,j) - R(i)]^2$$ total variance for Row i

$$SR(i) = [TVR(i) / (6-1)]^{1/2}$$ standard deviation for Row i

$$RSR(i) = (t_{\alpha/2} SR(i))/(R(i)*6^{1/2})$$ t-statistic for estimation of μ from $\overline{X}$

$t_{\alpha/2} = 1.476$ for $\alpha = 0.2$ => 80% confidence interval.

$$C(j) = \frac{1}{6} \sum_{i=1}^{6} X(i,j)$$ mean value for Column j

$$TVC(j) = \sum_{i=1}^{6} [X(i,j) - C(j)]^2$$ total variance for Column j

$$SC(j) = [TVC(j) / (6-1)]^{1/2}$$ standard deviation for Column j

$$CSC(j) = (t_{\alpha/2} SC(j))/(C(j)*6^{1/2})$$

$$GMEAN = \frac{1}{6} \sum_{i=1}^{6} R(i) = \frac{1}{6} \sum_{j=1}^{6} C(j)$$ Grand Mean

$$VR = 6 \sum_{i=1}^{6} [R(i) - GMEAN]^2$$ variation between rows

$$VC = 6 \sum_{j=1}^{6} [C(j) - GMEAN]^2$$ variation between columns

$$VE = \sum_{i=1}^{6} \sum_{j=1}^{6} [X(i,j) - R(I) - C(j) + GMEAN]^2$$ Variation due to error

$$VT = \sum_{i=1}^{6} \sum_{j=1}^{6} [X(i,j) - GMEAN]^2$$ Total variation

$$VT = VR + VC + VE$$

BASED ON SIX REPLICATES

$$\frac{VR}{VT} = \frac{14700}{14990} = 98.06\%$$

or 98.72 percent of variance should be explained by the "best" model, based on the set of six replicate data.

APPENDIX 3

SAMPLE CALCULATIONS FOR GAS HOLDUPS

Run No. SFCF070385-1

Hydrogen Velocity = $6.06^{l}/_{min}$

$= 6.06 \times 10^{3}/60\ cm^{3}/sec$

$= 1.01 \times 10^{2}\ cm^{3}/sec$

$= 1.01 \times 10^{-4}/\ m^{3}/sec$

$= 1.01 \times 10^{-4}\ m^{3}/sec$

Assume hydrogen flow follows PV = nRT (Z = 1.02)

$$V_1/V_2 = T_1\ P_2/t_2\ P1$$

To calculate hydrogen flow at reaction conditions.

$T_1 = 20^{o}C = 293^{o}K$

$T_2 = 400^{oC} = 673^{o}K$

$P_1 = 1\ atm = 14.7\ psia$

$P_2 = 2000\ psig + 14.7 = 2014.7\ psia$

$= 137\ atm$

$V_2 = V_1\ T_2\ P_1/T_1\ P_2$

$= 1.01 \times 10^{-4}\ (673 \times 1)/(293 \times 137)$

$= 1.69 \times 10^{-6}\ m^{3}/sec$

It is very difficult to estimate the physical properties of co-processing liquids. For this reason, physical properties of fhydrocracking reactor liquids are used here.

$\mu_i = 10\ cp$

$\sigma = 100\ dyne/cm$

Let d be reactor diameter 3" = 7.56 cm

$Ug = 1.69 \times 10^{-6}/\ (\pi/4(7.56/100)^{2}) = 3.72 \times 10^{-4}\ m/sec$

Bottom et al (Chem Eng J, 16, 107, 1978)

$\epsilon g = 0.88\ Ug^{0.6}$ for d = 2 - 10 cm

$= 0.88\ (3.72 \times 10^{-4})\ 0.6$

$= 0.77 \times 10^{-2}$

Hikita and Kikukawa (Chem Eng J, 8, 191 (1974))

$\epsilon g = 0.8 \times Ug^{0.47}\ (72/\sigma)^{2/3} (1/\mu_g)^{0.05}$

$= 0.8 * (3.72 \times 10^{-4})^{0.47}\ (72/100)^{2/3}\ (1/10)^{0.05}$

$= 0.93 \times 10^{-2}$

The gas holdup as calculated for the co-processing reactor is in a range 0.7 to 1.4 % of reactor volume.

Reactor diameter, cm	7.62	7.62	7.62	7.62	7.62
Reactor Height, cm	28.3	28.3	28.3	28.3	28.3
RUN NUMBER	SFCF070385-1	SPCF070385-2	SFCF280285-1	SF020683-1	SF070185-1
RUN ORDER	1	2	3	4	5
reactor temperature, C	400.00	425.00	450.00	425.00	425.00
room temperature, C	22.00	22.00	22.00	24.00	15.00
reactor pressure, PSIG	2000.00	2000.00	2000.00	2000.00	2000.00
barometer pressure, mm Hg	760.00	760.00	760.00	760.00	760.00
hydrogen flow, l/min	6.06	6.06	4.00	8.10	4.00
space velocity, Kg/l/hr	1.54	1.40	0.76	0.76	1.00
vol. flow @STD, m3/sec	1.01E-04	1.01E-04	6.67E-05	1.35E-04	6.67E-05
vol. flow @cond. m3/sec	1.69E-06	1.76E-06	1.20E-06	2.33E-06	1.19E-06
s'ficial vel. @STD m/sec	1.74E-02	1.74E-02	1.15E-02	2.33E-02	1.15E-02
s'ficial vel @cond. m/sec	3.71E-04	3.85E-04	2.63E-04	5.11E-04	2.60E-04
BOTTOM & COSSERAT					
VOID = K * (Ug)**a K=0.88 a=0.6	7.70E-03	7.87E-03	6.26E-03	9.33E-03	6.22E-03
HIKITA and KIKUKAWA					
liq.viscosity, cp	10	10	10	10	10
surf. tension dyne/cm	100	100	100	100	100
VOID=0.8*Ug**0.4	2.12E-02	2.15E-02	1.85E-02	2.41E-02	1.84E-02
VOID=Void*(72/a)**0.6666	1.71E-02	1.73E-02	1.49E-02	1.94E-02	1.48E-02
Void=void*MU**-0.05	1.52E-02	1.54E-02	1.32E-02	1.73E-02	1.32E-02

7.62	7.62	7.62	7.62	7.62	7.62	7.62
28.3	28.3	28.3	28.3	28.3	28.3	28.3
SF160683-2	SF250383-2	SPCF040385-1	SF070185-2	SF261083-2	SPCF210285-1	SF230185-2
6	7	8	9	10	11	12
450.00	400.00	425.00	450.00	450.00	400.00	450.00
30.00	22.00	19.00	26.00	21.00	21.00	21.00
2000.00	2000.00	2000.00	2000.00	2000.00	2000.00	2500.00
760.00	760.00	760.00	760.00	760.00	760.00	760.00
7.85	8.00	3.99	4.00	4.00	4.03	4.02
1.45	0.77	0.52	0.98	0.97	0.50	1.00
1.31E-04	1.33E-04	6.65E-05	6.67E-05	6.67E-05	6.72E-05	6.70E-05
2.29E-06	2.24E-06	1.17E-06	1.18E-06	1.21E-06	1.13E-06	9.69E-07
2.25E-02	2.30E-02	1.15E-02	1.15E-02	1.15E-02	1.16E-02	1.15E-02
5.03E-04	4.90E-04	2.56E-04	2.60E-04	2.64E-04	2.48E-04	2.12E-04
9.24E-03	9.09E-03	6.16E-03	6.21E-03	6.28E-03	6.04E-03	5.51E-03
10	10	10	10	10	10	10
100	100	100	100	100	100	100
2.40E-02	2.37E-02	1.83E-02	1.84E-02	1.85E-02	1.81E-02	1.70E-02
1.93E-02	1.91E-02	1.47E-02	1.48E-02	1.49E-02	1.45E-02	1.36E-02
1.72E-02	1.70E-02	1.31E-02	1.32E-02	1.33E-02	1.29E-02	1.22E-02

	7.62
	28.3
	SF090683-2
	13
	455.00
	24.00
	2000.00
	760.00
	7.92
	0.91
	1.32E-04
	2.38E-06
	2.27E-02
	5.21E-04
	9.44E-03
	10
	100
	2.43E-02
	1.95E-02
	1.74E-02

APPENDIX 4

CALCULATED DATA FOR A MISSING COPROCESSING RUN AT 400°C AND SPACE VELOCITY OF 1.0

DATA	400°C Sv=1.0	Excluding run 070385-2 Sv= 1.4
Coal Conversion	47.9	63.1
Pitch Conversion	7.4	14.0
Gas Yields		
H_2	3.8	4.7
H_2S	0.0	0.0
CO_x	1.8	2.3
C1-C4	0.0	0.2
Distillates		
Total	17.4	24.0
Distillates Type		
[1]	0.0	1.0
[2]	5.1	6.6
[3]	5.2	7.3
[4]	8.3	11.8
Oils	38.6	46.4
Asphaltenes	22.6	27.0
Preasphaltenes	4.6	6.0
THFI	15.9	18.4
Water	1.3	2.0

CANMET COPROCESSING DATA
Experiments Selected for Latin Square Design

Product Yield, %daf	211285-1	Yates(1)	070385-1	040385-1	070185-1	070385-2	280285-1	Ave.(2)	160683-2
TEMPERATURE deg C	400	400	400	425	425	425	450	450	450
SPACE VELOCITY	0.50	1.00	1.50	0.50	1.00	1.50	0.50	1.00	1.50
THFI	11.29	15.90	17.77	5.30	9.31	10.07	1.14	4.84	7.38
OILS	35.41	38.60	42.01	30.36	30.55	31.29	3.85	9.31	14.75
PREASPHALTENES	3.56	4.60	1.89	4.14	6.56	5.59	1.69	5.24	3.70
ASPHALTENES	15.89	22.60	20.41	4.96	15.21	17.66	4.71	10.43	6.20
DISTILLATES									
Fraction 1 + C5-C6	2.55	0.01	1.28	9.76	5.44	4.12	20.09	13.79	12.49
Fraction 2	5.70	5.10	2.17	9.87	10.06	5.40	22.97	21.39	19.14
Fraction 3	7.65	5.20	4.78	12.14	10.85	8.58	18.82	13.76	13.55
Fraction 4	14.99	8.30	7.26	15.25	7.04	13.73	9.88	12.23	11.38
Total	30.89	18.61	15.49	47.02	33.39	31.83	71.76	61.17	56.56
GAS YIELD									
Carbon Oxides	2.65	1.80	2.06	2.63	1.69	2.08	2.71	2.12	2.50
Hydrogen Sulphide	0.02	0.01	0.04	0.97	0.51	0.43	1.88	1.22	0.70
C1-C4	1.54	0.01	0.55	3.64	2.10	1.56	9.55	5.35	5.11
Hydrogen	10.90	3.80	3.96	10.91	4.66	3.48	10.85	3.42	5.72
Total	15.11	5.62	6.61	18.15	8.96	7.55	24.99	12.11	14.03
COAL CONVERSION	63.38	47.90	40.20	82.15	68.43	66.11	96.30	84.15	77.00
PITCH CONVERSION	25.18	7.40	6.98	49.25	30.12	26.77	87.12	66.26	63.86

Note: (1) Missing Values - Calculated using Yates' Method
(2) Average of Runs 070185-2 and 261083-2

APPENDIX 5

he raw data or transformation pass is proceeding
9 cases are written to the uncompressed active file.

'ANOVA' PROBLEM REQUIRES 1136 BYTES OF MEMORY.

---

ge 2

*** ANALYSIS OF VARIANCE ***

HYGEN hydrogen consumption
BY TEMP temperature C
SV space velocity

Source of Variation	Sum of Squares	DF	Mean Square	F	Signif of F
Main Effects	82.091	4	20.523		
TEMP	1.716	2	.858		
SV	80.376	2	40.188		
2-way Interactions	1.911	4	.478		
TEMP SV	1.911	4	.478		
Explained	84.002	8	10.500		
Residual	0.0	0	0.0		
Total	84.002	8	10.500		

Page 3

9 Cases were processed.
0 CASES (.0 PCT) were missing.

Page 4

This procedure was completed at 13:31:48

The raw data or transformation pass is proceeding
9 cases are written to the uncompressed active file.

'ANOVA' PROBLEM REQUIRES 1136 BYTES OF MEMORY.

---

ge 2

* * * A N A L Y S I S O F V A R I A N C E * * *

COGAS carbon oxides
BY TEMP temperature C
SV space velocity

Source of Variation	Sum of Squares	DF	Mean Square	F	Signif of F
Main Effects	1.131	4	.283		
TEMP	.162	2	.081		
SV	.969	2	.484		
2-way Interactions	.071	4	.018		
TEMP SV	.071	4	.018		
Explained	1.202	8	.150		
Residual	0.0	0	0.0		
Total	1.202	8	.150		

Page 3

9 Cases were processed.
0 CASES (.0 PCT) were missing.

Page 4

This procedure was completed at 13:19:15

The raw data or transformation pass is proceeding
9 cases are written to the uncompressed active file.

'ANOVA' PROBLEM REQUIRES 1136 BYTES OF MEMORY.

---

ge 5

* * * A N A L Y S I S O F V A R I A N C E * * *

HGAS hydrocarbon gases
BY TEMP temperature C
SV space velocity

Source of Variation	Sum of Squares	DF	Mean Square	F	Signif of F
Main Effects	67.864	4	16.966		
TEMP	56.016	2	28.008		
SV	11.849	2	5.924		
2-way Interactions	4.251	4	1.063		
TEMP SV	4.251	4	1.063		
Explained	72.116	8	9.014		
Residual	0.0	0	0.0		
Total	72.116	8	9.014		

Page 6

9 Cases were processed.
0 CASES (.0 PCT) were missing.

Page 7

This procedure was completed at 13:25:16

The raw data or transformation pass is proceeding
     9 cases are written to the uncompressed active file.

'ANOVA' PROBLEM REQUIRES   1136 BYTES OF MEMORY.

Page   2

*** ANALYSIS OF VARIANCE ***

H2O water
BY TEMP temperature C
SV space velocity

Source of Variation	Sum of Squares	DF	Mean Square	F	Signif of F
Main Effects	28.698	4	7.174		
TEMP	27.536	2	13.768		
SV	1.162	2	.581		
2-way Interactions	3.138	4	.784		
TEMP SV	3.138	4	.784		
Explained	31.836	8	3.979		
Residual	0.0	0	0.0		
Total	31.836	8	3.979		

Page   3

     9 Cases were processed.
     0 CASES (.0 PCT) were missing.

Page   4

This procedure was completed at 13:15:25

he raw data or transformation pass is proceeding
9 cases are written to the uncompressed active file.

ANOVA' PROBLEM REQUIRES 1136 BYTES OF MEMORY.

---

* * * A N A L Y S I S O F V A R I A N C E * * *

H2S hydrogen sulphide
BY TEMP temperature C
SV space velocity

Source of Variation	Sum of Squares	DF	Mean Square	F	Signif of F
ain Effects	2.607	4	.652		
TEMP	2.047	2	1.023		
SV	.560	2	.280		
2-way Interactions	.373	4	.093		
TEMP SV	.373	4	.093		
xplained	2.980	8	.373		
esidual	0.0	0	0.0		
Total	2.980	8	.373		

---

9 Cases were processed.
0 CASES (.0 PCT) were missing.

This procedure was completed at 13:28:22

he raw data or transformation pass is proceeding
9 cases are written to the uncompressed active file.

ANOVA' PROBLEM REQUIRES 1136 BYTES OF MEMORY.

---

* * * A N A L Y S I S O F V A R I A N C E * * *

DIST distillates
BY TEMP temperature C
SV space velocity

Source of Variation	Sum of Squares	DF	Mean Square	F	Signif of F
ain Effects	3398.813	4	849.703		
TEMP	2908.687	2	1454.343		
SV	490.127	2	245.063		
-way Interactions	9.067	4	2.267		
TEMP SV	9.067	4	2.267		
xplained	3407.880	8	425.985		
Residual	0.0	0	0.0		
otal	3407.880	8	425.985		

---

9 Cases were processed.
0 CASES (.0 PCT) were missing.

---

his procedure was completed at 12:59:13

he raw data or transformation pass is proceeding
9 cases are written to the uncompressed active file.

ANOVA' PROBLEM REQUIRES 1136 BYTES OF MEMORY.

---

ge 2

*** A N A L Y S I S O F V A R I A N C E ***

ASP asphaltenes
BY TEMP temperature C
SV space velocity

Source of Variation	Sum of Squares	DF	Mean Square	F	Signif of F
ain Effects	333.998	4	83.499		
TEMP	236.702	2	118.351		
SV	97.296	2	48.648		
-way Interactions	34.018	4	8.504		
TEMP SV	34.018	4	8.504		
xplained	368.016	8	46.002		
esidual	0.0	0	0.0		
otal	368.016	8	46.002		

-ge 3

9 Cases were processed.
0 CASES (.0 PCT) were missing.

Page 4

his procedure was completed at 13:06:42

he raw data or transformation pass is proceeding
9 cases are written to the uncompressed active file.

ANOVA' PROBLEM REQUIRES 1136 BYTES OF MEMORY.

---

* * * A N A L Y S I S O F V A R I A N C E * * *

PASP preasphaltenes
BY TEMP temperature C
SV space velocity

Source of Variation	Sum of Squares	DF	Mean Square	F	Signif of F
lain Effects	15.251	4	3.813		
TEMP	6.976	2	3.488		
SV	8.276	2	4.138		
-way Interactions	5.784	4	1.446		
TEMP SV	5.784	4	1.446		
xplained	21.036	8	2.629		
Residual	0.0	0	0.0		
Total	21.036	8	2.629		

---

9 Cases were processed.
0 CASES (.0 PCT) were missing.

---

his procedure was completed at 13:09:28

```
WARNING   420, Text: TFHI
UNDEFINED VARIABLE NAME--Check for a misspelled variable name.

The raw data or transformation pass is proceeding
     9 cases are written to the uncompressed active file.

'ONOVA' PROBLEM REQUIRES     1136 BYTES OF MEMORY.
```


* * * A N A L Y S I S O F V A R I A N C E * * *

BY THFI
TEMP temperature C
SV space velocity

Source of Variation	Sum of Squares	DF	Mean Square	F	Signif of F
Main Effects	226.178	4	56.544		
TEMP	169.976	2	84.988		
SV	56.202	2	28.101		
2-way Interactions	1.351	4	.338		
TEMP SV	1.351	4	.338		
Explained	227.529	8	28.441		
Residual	0.0	0	0.0		
Total	227.529	8	28.441		

9 Cases were processed.
0 CASES (.0 PCT) were missing.

This procedure was completed at 13:12:23

The raw data or transformation pass is proceeding
9 cases are written to the uncompressed active file.

'ANOVA' PROBLEM REQUIRES 1136 BYTES OF MEMORY.

---

* * * A N A L Y S I S O F V A R I A N C E * * *

BY COAL
TEMP temperature C
SV space velocity

Source of Variation	Sum of Squares	DF	Mean Square	F	Signif of F
Main Effects	1956.707	4	489.177		
TEMP	1364.460	2	682.230		
SV	592.247	2	296.123		
2-way Interactions	118.973	4	29.743		
TEMP SV	118.973	4	29.743		
Explained	2075.680	8	259.460		
Residual	0.0	0	0.0		
Total	2075.680	8	259.460		

---

9 Cases were processed.
0 CASES (.0 PCT) were missing.

This procedure was completed at 13:34:21

The raw data or transformation pass is proceeding
9 cases are written to the uncompressed active file.

'ANOVA' PROBLEM REQUIRES 1136 BYTES OF MEMORY.

Page 2

* * * A N A L Y S I S O F V A R I A N C E * * *

OILS oils
BY TEMP temperature C
SV space velocity

Source of Variation	Sum of Squares	DF	Mean Square	F	Signif of F
Main Effects	1604.071	4	401.018		
TEMP	1575.109	2	787.554		
SV	28.962	2	14.481		
2-way Interactions	12.711	4	3.178		
TEMP SV	12.711	4	3.178		
Explained	1616.782	8	202.098		
Residual	0.0	0	0.0		
Total	1616.782	8	202.098		

Page 3

9 Cases were processed.
0 CASES (.0 PCT) were missing.

Page 4

This procedure was completed at 13:03:42

The raw data or transformation pass is proceeding
9 cases are written to the uncompressed active file.

NOVA' PROBLEM REQUIRES 1136 BYTES OF MEMORY.

---

* * * A N A L Y S I S O F V A R I A N C E * * *

C1 methane
BY TEMP temperature C
SV space velocity

Source of Variation	Sum of Squares	DF	Mean Square	F	Signif of F
Main Effects	8.514	4	2.128		
TEMP	7.288	2	3.644		
SV	1.226	2	.613		
2-way Interactions	.331	4	.083		
TEMP SV	.331	4	.083		
Explained	8.845	8	1.106		
Residual	0.0	0	0.0		
Total	8.845	8	1.106		

---

9 Cases were processed.
0 CASES (.0 PCT) were missing.

The raw data or transformation pass is proceeding
9 cases are written to the uncompressed active file.

NOVA' PROBLEM REQUIRES 1136 BYTES OF MEMORY.

---

* * * A N A L Y S I S O F V A R I A N C E * * *

C2 ethane
BY TEMP temperature C
SV space velocity

Source of Variation	Sum of Squares	DF	Mean Square	F	Signif of F
Main Effects	6.984	4	1.746		
TEMP	4.501	2	2.250		
SV	2.483	2	1.242		
2-way Interactions	.625	4	.156		
TEMP SV	.625	4	.156		
Explained	7.609	8	.951		
Residual	0.0	0	0.0		
tal	7.609	8	.951		

---

9 Cases were processed.
0 CASES (.0 PCT) were missing.

---

he raw data or transformation pass is proceeding
9 cases are written to the uncompressed active file.

ANOVA' PROBLEM REQUIRES 1136 BYTES OF MEMORY.

---

* * * A N A L Y S I S O F V A R I A N C E * * *

C3 propane
BY TEMP temperature C
SV space velocity

Source of Variation	Sum of Squares	DF	Mean Square	F	Signif of F
ain Effects	3.825	4	.956		
TEMP	3.365	2	1.683		
SV	.460	2	.230		
2-way Interactions	.387	4	.097		
TEMP SV	.387	4	.097		
Explained	4.212	8	.526		
sidual	0.0	0	0.0		
Total	4.212	8	.526		

---

9 Cases were processed.
0 CASES (.0 PCT) were missing.

The raw data or transformation pass is proceeding
9 cases are written to the uncompressed active file.

NOVA' PROBLEM REQUIRES 1136 BYTES OF MEMORY.

* * * A N A L Y S I S O F V A R I A N C E * * *

C4 butane
BY TEMP temperature C
SV space velocity

Source of Variation	Sum of Squares	DF	Mean Square	F	Signif of F
Main Effects	.714	4	.179		
TEMP	.698	2	.349		
SV	.017	2	.008		
2-way Interactions	.032	4	.008		
TEMP SV	.032	4	.008		
Explained	.747	8	.093		
Residual	0.0	0	0.0		
Total	.747	8	.093		

9 Cases were processed.
0 CASES (.0 PCT) were missing.

The raw data or transformation pass is proceeding
9 cases are written to the uncompressed active file.

'ANOVA' PROBLEM REQUIRES 1136 BYTES OF MEMORY.

---

* * * A N A L Y S I S O F V A R I A N C E * * *

F4 fraction 4
BY TEMP temperature C
SV space velocity

Source of Variation	Sum of Squares	DF	Mean Square	F	Signif of F
Main Effects	31.730	4	7.933		
TEMP	4.996	2	2.498		
SV	26.734	2	13.367		
2-way Interactions	49.452	4	12.363		
TEMP SV	49.452	4	12.363		
Explained	81.182	8	10.148		
Residual	.000	0	0.0		
Total	81.182	8	10.148		

---

9 Cases were processed.
0 CASES (.0 PCT) were missing.

The raw data or transformation pass is proceeding
9 cases are written to the uncompressed active file.

ANOVA' PROBLEM REQUIRES 1136 BYTES OF MEMORY.

* * * A N A L Y S I S O F V A R I A N C E * * *

F3 fraction 3
BY TEMP temperature C
SV space velocity

Source of Variation	Sum of Squares	DF	Mean Square	F	Signif of F
Main Effects	160.145	4	40.036		
TEMP	135.396	2	67.698		
SV	24.749	2	12.374		
2-way Interactions	4.360	4	1.090		
TEMP SV	4.360	4	1.090		
Explained	164.505	8	20.563		
Residual	.000	0	0.0		
Total	164.505	8	20.563		

9 Cases were processed.
0 CASES (.0 PCT) were missing.

The raw data or transformation pass is proceeding
9 cases are written to the uncompressed active file.

'ANOVA' PROBLEM REQUIRES 1136 BYTES OF MEMORY.

---

* * * A N A L Y S I S O F V A R I A N C E * * *

F2 fraction 2
BY TEMP temperature C
SV space velocity

Source of Variation	Sum of Squares	DF	Mean Square	F	Signif of F
Main Effects	489.304	4	122.326		
TEMP	462.555	2	231.278		
SV	26.748	2	13.374		
2-way Interactions	1.707	4	.427		
TEMP SV	1.707	4	.427		
Explained	491.011	8	61.376		
Residual	0.0	0	0.0		
Total	491.011	8	61.376		

---

9 Cases were processed.
0 CASES (.0 PCT) were missing.

The raw data or transformation pass is proceeding
9 cases are written to the uncompressed active file.

'ANOVA' PROBLEM REQUIRES 1136 BYTES OF MEMORY.

* * * A N A L Y S I S O F V A R I A N C E * * *

F1 fraction 1 + C5-C6
BY TEMP temperature C
SV space velocity

Source of Variation	Sum of Squares	DF	Mean Square	F	Signif of F
Main Effects	351.742	4	87.936		
TEMP	308.904	2	154.452		
SV	42.839	2	21.419		
2-way Interactions	10.839	4	2.710		
TEMP SV	10.839	4	2.710		
Explained	362.581	8	45.323		
Residual	0.0	0	0.0		
Total	362.581	8	45.323		

9 Cases were processed.
0 CASES (.0 PCT) were missing.

9 cases are written to the uncompressed active file.

This procedure was completed at 22:13:51

'ANOVA' PROBLEM REQUIRES 528 BYTES OF MEMORY.

---

* * * A N A L Y S I S O F V A R I A N C E * * *

THFI TETRAHYDROFURAN INSOLUBLES
BY TEMP TEMPERATURE C
SV SPACE VELOCITY

Source of Variation	Sum of Squares	DF	Mean Square	F	Signif of F
Main Effects	226.178	4	56.544	167.401	.000
TEMP	169.976	2	84.988	251.609	.000
SV	56.202	2	28.101	83.194	.001
Explained	226.178	4	56.544	167.401	.000
Residual	1.351	4	.338		
Total	227.529	8	28.441		

9 Cases were processed.
0 CASES (.0 PCT) were missing.

The raw data or transformation pass is proceeding
9 cases are written to the uncompressed active file.

'ANOVA' PROBLEM REQUIRES 1136 BYTES OF MEMORY.

---

* * * A N A L Y S I S O F V A R I A N C E * * *

F5 fraction 5
BY TEMP temperature C
SV space velocity

Source of Variation	Sum of Squares	DF	Mean Square	F	Signif of F
Main Effects	260.853	4	65.213		
TEMP	167.771	2	83.886		
SV	93.082	2	46.541		
2-way Interactions	25.687	4	6.422		
TEMP SV	25.687	4	6.422		
Explained	286.540	8	35.817		
Residual	0.0	0	0.0		
Total	286.540	8	35.817		

---

9 Cases were processed.
0 CASES (.0 PCT) were missing.

The raw data or transformation pass is proceeding
6 cases are written to the uncompressed active file.

Correlations:

	PITCH	COAL	DIST	OILS	ASP	PASP
PITCH	1.0000	.9317*	.9975**	-.9237*	-.8083	-.8281
COAL	.9317*	1.0000	.9392*	-.7384	-.8154	-.8881*
DIST	.9975**	.9392*	1.0000	-.9229*	-.7754	-.8346
OILS	-.9237*	-.7384	-.9229*	1.0000	.5901	.6183
ASP	-.8083	-.8154	-.7754	.5901	1.0000	.7723
PASP	-.8281	-.8881*	-.8346	.6183	.7723	1.0000
THFI	-.9065*	-.9975**	-.9174*	.7008	.7884	.8845*
H2O	.9196*	.7763	.9131*	-.9198*	-.6835	-.7702
COGAS	.7051	.7208	.6865	-.4886	-.8626	-.8780
HGAS	.9699**	.9319*	.9765**	-.8798	-.7373	-.8871*
H2S	.8985*	.9819**	.9173*	-.7209	-.7033	-.8850*
HYGEN	.3537	.5593	.3512	-.0155	-.6145	-.7843

N of cases: 6 1-tailed Signif: * - .01 ** - .001

" . " is printed if a coefficient cannot be computed

Correlations:

	THFI	H2O	COGAS	HGAS	H2S	HYGEN
PITCH	-.9065*	.9196*	.7051	.9699**	.8985*	.3537
COAL	-.9975**	.7763	.7208	.9319*	.9819**	.5593
DIST	-.9174*	.9131*	.6865	.9765**	.9173*	.3512
OILS	.7008	-.9198*	-.4886	-.8798	-.7209	-.0155
ASP	.7884	-.6835	-.8626	-.7373	-.7033	-.6145
PASP	.8845*	-.7702	-.8780	-.8871*	-.8850*	-.7843
THFI	1.0000	-.7460	-.6970	-.9176*	-.9881**	-.5777
H2O	-.7460	1.0000	.6060	.9431*	.7718	.2890
COGAS	-.6970	.6060	1.0000	.6791	.6384	.7761
HGAS	-.9176*	.9431*	.6791	1.0000	.9375*	.4436
H2S	-.9881**	.7718	.6384	.9375*	1.0000	.5437
HYGEN	-.5777	.2890	.7761	.4436	.5437	1.0000

N of cases: 6 1-tailed Signif: * - .01 ** - .001

" . " is printed if a coefficient cannot be computed

This procedure was completed at 15:33:38

TEMPERATURE RANGE 425 to 450 deg. C

The raw data or transformation pass is proceeding
6 cases are written to the uncompressed active file.

Correlations:

	PITCH	COAL	DIST	OILS	ASP	PASP
PITCH	1.0000	.8537	.9973**	-.8701	-.9572*	.3679
COAL	.8537	1.0000	.8698	-.8590	-.7509	.5959
DIST	.9973**	.8698	1.0000	-.8903*	-.9372*	.4001
OILS	-.8701	-.8590	-.8903*	1.0000	.6963	-.7602
ASP	-.9572*	-.7509	-.9372*	.6963	1.0000	-.1206
PASP	.3679	.5959	.4001	-.7602	-.1206	1.0000
THFI	-.9835**	-.9017*	-.9916**	.9385*	.8916*	-.5140
H2O	.7462	.5906	.7239	-.7928	-.6778	.5832
COGAS	.5357	.3508	.5462	-.2005	-.6084	-.3914
HGAS	.9849**	.7693	.9705**	-.8093	-.9779**	.2782
H2S	.9090*	.7833	.8859*	-.7655	-.9110*	.3342
HYGEN	.7313	.5882	.7448	-.4579	-.7555	-.1230

N of cases: 6 1-tailed Signif: * - .01 ** - .001

" . " is printed if a coefficient cannot be computed

Correlations:

	THFI	H2O	COGAS	HGAS	H2S	HYGEN
PITCH	-.9835**	.7462	.5357	.9849**	.9090*	.7313
COAL	-.9017*	.5906	.3508	.7693	.7833	.5882
DIST	-.9916**	.7239	.5462	.9705**	.8859*	.7448
OILS	.9385*	-.7928	-.2005	-.8093	-.7655	-.4579
ASP	.8916*	-.6778	-.6084	-.9779**	-.9110*	-.7555
PASP	-.5140	.5832	-.3914	.2782	.3342	-.1230
THFI	1.0000	-.7469	-.4657	-.9434*	-.8686	-.6890
H2O	-.7469	1.0000	-.1184	.7855	.8603	.1051
COGAS	-.4657	-.1184	1.0000	.5111	.2854	.9527*
HGAS	-.9434*	.7855	.5111	1.0000	.9294*	.6900
H2S	-.8686	.8603	.2854	.9294*	1.0000	.4660
HYGEN	-.6890	.1051	.9527*	.6900	.4660	1.0000

N of cases: 6 1-tailed Signif: * - .01 ** - .001

" . " is printed if a coefficient cannot be computed

This procedure was completed at 15:30:41

TEMPERATURE RANGE 400 to 425 deg. C

The raw data or transformation pass is proceeding
9 cases are written to the uncompressed active file.

Correlations:	PITCH	COAL	DIST	OILS	ASP	PASP
PITCH	1.0000	.9076**	.9987**	-.9560**	-.9133**	-.1415
COAL	.9076**	1.0000	.9161**	-.8316*	-.8342*	.0521
DIST	.9987**	.9161**	1.0000	-.9552**	-.8982**	-.1407
OILS	-.9560**	-.8316*	-.9552**	1.0000	.7872*	.0591
ASP	-.9133**	-.8342*	-.8982**	.7872*	1.0000	.1417
PASP	-.1415	.0521	-.1407	.0591	.1417	1.0000
THFI	-.9425**	-.9549**	-.9481**	.8398*	.9000**	-.0203
H2O	.9344**	.7891*	.9272**	-.9449**	-.8126*	-.1911
COGAS	.5809	.4991	.5783	-.4277	-.6950	-.5148
HGAS	.9709**	.8598*	.9727**	-.9266**	-.8511*	-.3113
H2S	.9323**	.8914**	.9382**	-.8495*	-.8278*	-.2429
HYGEN	.3821	.4516	.3898	-.1510	-.5421	-.4153

N of cases: 9 1-tailed Signif: * - .01 ** - .001

" . " is printed if a coefficient cannot be computed

Correlations:	THFI	H2O	COGAS	HGAS	H2S	HYGEN
PITCH	-.9425**	.9344**	.5809	.9709**	.9323**	.3821
COAL	-.9549**	.7891*	.4991	.8598*	.8914**	.4516
DIST	-.9481**	.9272**	.5783	.9727**	.9382**	.3898
OILS	.8398*	-.9449**	-.4277	-.9266**	-.8495*	-.1510
ASP	.9000**	-.8126*	-.6950	-.8511*	-.8278*	-.5421
PASP	-.0203	-.1911	-.5148	-.3113	-.2429	-.4153
THFI	1.0000	-.8132*	-.5602	-.8899**	-.9135**	-.5053
H2O	-.8132*	1.0000	.4253	.9551**	.8816**	.2201
COGAS	-.5602	.4253	1.0000	.5702	.4614	.8580*
HGAS	-.8899**	.9551**	.5702	1.0000	.9559**	.4062
H2S	-.9135**	.8816**	.4614	.9559**	1.0000	.3839
HYGEN	-.5053	.2201	.8580*	.4062	.3839	1.0000

N of cases: 9 1-tailed Signif: * - .01 ** - .001

" . " is printed if a coefficient cannot be computed

This procedure was completed at 9:31:43

- - - - F A C T O R A N A L Y S I S - - - -

Varimax Rotation 1, Extraction 1, Analysis 1 - Kaiser Normalization.

Varimax converged in 3 iterations.

Rotated Factor Matrix:

	FACTOR 1	FACTOR 2
DIST	-.98987	-.09794
OILS	.93561	.02026
ASP	.93192	.11114
PASP	.04120	.99867
THFI	.96751	-.06513

Factor Transformation Matrix:

	FACTOR 1	FACTOR 2
FACTOR 1	.99724	.07430
FACTOR 2	-.07430	.99724

The case limit is set to: 9
Matrix input has been written to the active file

This procedure was completed at 20:51:03

This FACTOR analysis requires 6124 (6.0K) BYTES of memory.

- - - - F A C T O R A N A L Y S I S - - - -

Analysis Number 1 Matrix input

Extraction 1 for Analysis 1, Principal-Components Analysis (PC)

Initial Statistics:

Variable	Communality	*	Factor	Eigenvalue	Pct of Var	Cum Pct
DIST	1.00000	*	1	3.67617	73.5	73.5
OILS	1.00000	*	2	1.00922	20.2	93.7
ASP	1.00000	*	3	.23280	4.7	98.4
PASP	1.00000	*	4	.08157	1.6	100.0
THFI	1.00000	*	5	.00025	.0	100.0

PC Extracted 2 factors.

- - - - F A C T O R A N A L Y S I S - - - -

Factor Matrix:

	FACTOR 1	FACTOR 2
DIST	-.99441	-.02412
OILS	.93453	-.04931
ASP	.93760	.04160
PASP	.11528	.99285
THFI	.96000	-.13683

Final Statistics:

Variable	Communality	*	Factor	Eigenvalue	Pct of Var	Cum Pct
DIST	.98943	*	1	3.67617	73.5	73.5
OILS	.87577	*	2	1.00922	20.2	93.7
ASP	.88082	*				
PASP	.99904	*				
THFI	.94032	*				

- - - - F A C T O R A N A L Y S I S - - - -

Final Statistics:

Variable	Communality	*	Factor	Eigenvalue	Pct of Var	Cum Pct
		*				
H2O	.95376	*	1	3.49598	69.9	69.9
COGAS	.92756	*	2	1.25714	25.1	95.1
HGAS	.99448	*				
H2S	.93083	*				
HYGEN	.94650	*				

Reproduced Correlation Matrix:

	H2O	COGAS	HGAS	H2S	HYGEN
H2O	.95376*	.02351	-.00161	-.05213	-.01425
COGAS	.40179	.92756*	.00471	-.04452	-.06174
HGAS	.95671	.56549	.99448*	-.00484	-.00478
H2S	.93373	.50592	.96074	.93083*	.03259
HYGEN	.23435	.91974	.41098	.35131	.94650*

The lower left triangle contains the reproduced correlation matrix; The diagonal, communalities; and the upper right triangle, residuals between the observed correlations and the reproduced correlations.

- - - - F A C T O R A N A L Y S I S - - - -

There are 2 (20.0%) residuals (above diagonal) that are > 0.05

- - - - F A C T O R A N A L Y S I S - - - -

Extraction 1 for Analysis 2, Principal-Components Analysis (PC)

Initial Statistics:

Variable	Communality	*	Factor	Eigenvalue	Pct of Var	Cum Pct
H2O	1.00000	*	1	3.49598	69.9	69.9
COGAS	1.00000	*	2	1.25714	25.1	95.1
HGAS	1.00000	*	3	.17950	3.6	98.7
H2S	1.00000	*	4	.05990	1.2	99.9
HYGEN	1.00000	*	5	.00748	.1	100.0

PC Extracted 2 factors.

- - - - F A C T O R A N A L Y S I S - - - -

Factor Matrix:

	FACTOR 1	FACTOR 2
HGAS	.96057	
H2S	.91404	
2O	.87501	
COGAS	.75535	.59750
HYGEN	.63373	.73817

- - - - F A C T O R A N A L Y S I S - - - -

Anti-Image Covariance Matrix:

	H2O	COGAS	HGAS	H2S	HYGEN
H2O	.03774				
COGAS	.02108	.11700			
HGAS	-.01776	-.02145	.01107		
H2S	.02080	.04378	-.01804	.03838	
HYGEN	.01229	-.11299	.00628	-.02945	.17881

Anti-Image Correlation Matrix:

	H2O	COGAS	HGAS	H2S	HYGEN
H2O	.61991				
COGAS	.31725	.49354			
HGAS	-.86872	-.59608	.54995		
H2S	.54658	.65343	-.87490	.55910	
HYGEN	.14954	-.78117	.14112	-.35549	.58479

Measures of sampling adequacy (MSA) are printed on the diagonal.

- - - - F A C T O R A N A L Y S I S - - - -

Correlation 1-tailed Significance Matrix:
' . ' is printed for diagonal elements.

	H2O	COGAS	HGAS	H2S	HYGEN
H2O	.				
COGAS	.12689	.			
HGAS	.00003	.05446	.		
H2S	.00084	.10562	.00003	.	
HYGEN	.28466	.00154	.13900	.15386	.

- - - - F A C T O R A N A L Y S I S - - - -

Analysis Number 2 Matrix input

Correlation Matrix:

	H2O	COGAS	HGAS	H2S	HYGEN
H2O	1.00000				
COGAS	.42530	1.00000			
HGAS	.95510	.57020	1.00000		
H2S	.88160	.46140	.95590	1.00000	
HYGEN	.22010	.85800	.40620	.38390	1.00000

Determinant of Correlation Matrix = .0003535

- - - - F A C T O R A N A L Y S I S - - - -

Inverse of Correlation Matrix:

	H2O	COGAS	HGAS	H2S	HYGEN
H2O	26.49399				
COGAS	4.77406	8.54731			
HGAS	-42.49396	-16.56123	90.31151		
H2S	14.36133	9.75173	-42.44230	26.05766	
HYGEN	1.82026	-5.40089	3.17152	-4.29139	5.59252

Kaiser-Meyer-Olkin Measure of Sampling Adequacy = .55939

Bartlett Test of Sphericity = 43.71119, Significance = .00000

There are 2 (10.0%) off-diagonal elements of AIC Matrix > 0.09

- - - - F A C T O R A N A L Y S I S - - - -

inal Statistics:

Variable	Communality	*	Factor	Eigenvalue	Pct of Var	Cum Pct
		*				
DIST	.98943	*	1	3.67617	73.5	73.5
OILS	.87577	*	2	1.00922	20.2	93.7
ASP	.88082	*				
PASP	.99904	*				
THFI	.94032	*				

Reproduced Correlation Matrix:

	DIST	OILS	ASP	PASP	THFI
DIST	.98943*	-.02709	.03516	-.00212	.00323
OILS	-.92811	.87577*	-.08696	.00032	-.06409
ASP	-.93336	.87416	.88082*	-.00769	.00560
PASP	-.13858	.05878	.14939	.99904*	.00489
THFI	-.95133	.90389	.89440	-.02519	.94032*

The lower left triangle contains the reproduced correlation matrix; The diagonal, communalities; and the upper right triangle, residuals between the observed correlations and the reproduced correlations.

- - - - F A C T O R A N A L Y S I S - - - -

There are 2 (20.0%) residuals (above diagonal) that are > 0.05

- - - - F A C T O R A N A L Y S I S - - - -

Extraction 1 for Analysis 1, Principal-Components Analysis (PC)

Initial Statistics:

Variable	Communality	*	Factor	Eigenvalue	Pct of Var	Cum Pct
		*				
DIST	1.00000	*	1	3.67617	73.5	73.5
OILS	1.00000	*	2	1.00922	20.2	93.7
ASP	1.00000	*	3	.23280	4.7	98.4
PASP	1.00000	*	4	.08157	1.6	100.0
THFI	1.00000	*	5	.00025	.0	100.0

PC Extracted 2 factors.

- - - - F A C T O R A N A L Y S I S - - - -

Factor Matrix:

	FACTOR 1	FACTOR 2
DIST	-.99441	
THFI	.96000	
ASP	.93760	
OILS	.93453	
PASP		.99285

- - - - F A C T O R A N A L Y S I S - - - -

Anti-Image Covariance Matrix:

	DIST	OILS	ASP	PASP	THFI
DIST	.00037				
OILS	.00072	.00143			
ASP	.00378	.00742	.06450		
PASP	.00316	.00623	.03086	.02814	
THFI	.00076	.00150	.00733	.00662	.00161

Anti-Image Correlation Matrix:

	DIST	OILS	ASP	PASP	THFI
DIST	.42601				
OILS	.99749	.38864			
ASP	.77755	.77169	.50156		
PASP	.98343	.97969	.72419	.01264	
THFI	.99366	.98727	.71970	.98424	.41181

Measures of sampling adequacy (MSA) are printed on the diagonal.

- - - - F A C T O R A N A L Y S I S - - - -

Correlation 1-tailed Significance Matrix:
' . ' is printed for diagonal elements.

	DIST	OILS	ASP	PASP	THFI
DIST	.				
OILS	.00003	.			
ASP	.00050	.00590	.		
PASP	.35903	.43998	.35806	.	
THFI	.00005	.00231	.00047	.47933	.

The case limit is set to: 9
Matrix input has been written to the active file

This procedure was completed at 21:12:03

This FACTOR analysis requires 6006 (5.9K) BYTES of memory.

- - - - F A C T O R A N A L Y S I S - - - -

Analysis Number 1 Matrix input

Correlation Matrix:

	DIST	OILS	ASP	PASP	THFI
DIST	1.00000				
OILS	-.95520	1.00000			
ASP	-.89820	.78720	1.00000		
PASP	-.14070	.05910	.14170	1.00000	
THFI	-.94810	.83980	.90000	-.02030	1.00000

Determinant of Correlation Matrix = .0000173

- - - - F A C T O R A N A L Y S I S - - - -

Inverse of Correlation Matrix:

	DIST	OILS	ASP	PASP	THFI
DIST	2728.47422				
OILS	1375.64926	697.06648			
ASP	159.92114	80.22223	15.50359		
PASP	306.20045	154.18040	16.99695	35.53079	
THFI	1293.88299	649.78649	70.64241	146.25197	621.43052

Kaiser-Meyer-Olkin Measure of Sampling Adequacy = .37207

Bartlett Test of Sphericity = 60.31689, Significance = .00000

There are 0 (0.0%) off-diagonal elements of AIC Matrix > 0.09

APPENDIX 6

EQUATIONS FOR CSTR

From mass balance for *i* component.

$$F_i^{in}\,\Delta t - F_i^{out}\Delta t = r_i V'_R \Delta t \tag{1}$$

$$F_i^{in} - F_i^{out} = r_i V'_R \tag{2}$$

$$F_i^{in}\,(X_{i0} - X_i) = r_i V'_R \tag{3}$$

Defining

$$r_i = \sum_{i=1}^{n} \sum_{j=1}^{l} k_{ij}\ (M_{ir}/V'_R) \tag{4}$$

$$M_{ir} = M_{i\ total} / N \tag{5}$$

$$M_{i\ total} = X_i F^{in} \Delta t \tag{6}$$

$$N = (\text{total volume of products}) / V'_R = V_p / V'_R \tag{7}$$

$$V_p = M_{p\ total} / \rho_p \tag{8}$$

$$M_{p\ total} = F^{in}\,(1 - \phi)\,\Delta t \tag{9}$$

$$N = F^{in}\,(1 - \phi)\,\Delta t / \rho_p V'_R \tag{10}$$

Combining equations (5) - (10):

$$M_{ir} = \frac{X_i F^{in} \Delta t}{F^{in}\,(1 - \phi)\,\Delta t}\ \rho_p V'_R = \frac{\rho_p V'_R}{(1 - \phi)}\ X_i \tag{11}$$

Combining equations (4) and (11):

$$r_i = \frac{\rho_p V'_R}{(1 - \phi)}\ \frac{1}{V'_R}\ \Sigma\Sigma\, k_{ij} X_i \tag{12}$$

$$r_i = \frac{\rho_p}{(1 - \phi)}\ \Sigma\Sigma\, k_{ij} X_i = \frac{\rho_p}{(1 - \phi)}\ r'_i \tag{13}$$

Combining equations (3) - (13):

$$F_i^{in}\ (X_{i0} - X_i) = \frac{\rho_p V'_R}{(1 - \phi)}\ r'_i \qquad (14)$$

$$\frac{F_i^{in}(1 - \phi)}{\rho_p V'_R}\ (X_{i0} - X_i) = r_i \qquad (15)$$

or if $V'_R = (1 - \epsilon)\ V_R$ (16)

$$\frac{F_i^{in}(1 - \phi)}{(1 - \epsilon)\rho_p V_R}\ (X_{i0} - X_i) = r'_i \qquad (17)$$

Symbols

F = rate of mass, kg/hr

V_R = volume of reactants

$X_i = F_i^{out} / F^{in}$

$X_{i0} = F_i^{in}/F^{in}$

M_{ir} = mass of i component in the reaction volume V'_R, kg

$M_{i,total}$ = Total mass of i component over time Δt, kg

ρ_p = average mass density of products, kg/*l*

ϕ = traction of the feed or products flashed at reactor T,P

r'_i = dimensionless rate in terms of fractional conversion

ϵ = gas holdup

V_R = reactor volume, *l*

N = number of changes of reactor volume over time Δt

APPENDIX 7

THE LEAST-SQUARES

Denote: NS = number of states, ie, NS = 6 for the case under investigation.
NK = number of k values, ie., NK = 7 for the model #1.

There are NS govering equations in the form of:

$$X_1 = f_1(k,X)$$
$$X_2 = f_2(k,X), \text{ etc.}$$

It should be mentioned that f_1, f_2 and so on are "linear" functions.

Define:
$$e_1 = f1(k,X) - r_1$$
$$e_2 = f2(k,X) - r_2, \text{ etc}$$

and
$$E = \sum_{i=1}^{NS} e_i^2$$

The objective is to find the best k_i (i=1 to NK) values such that E is the minimum.

The conditions are, therfore, the so-called normal equations:

$$\frac{\partial E}{\partial k_1} = \frac{\partial E}{\partial k_2} = \cdots = \frac{\partial E}{\partial k_{NK}} = 0$$

That is, there are NK equations for NK unknowns.

The Normal Equations

Define: Term 1 = $T_1 = \Sigma e_1^2 = \Sigma[f_1(k,X) - r_1]^2$

$T_2 = \Sigma e_2^2 = \Sigma[f_2(k,X) - r_2]^2$, etc.

Where Σ is for various space velocities at the same temperature.

It should be mentioned that there are NS terms.

Apendix 8 uses model #1 as an example. With reference to page 1 of Appendix 8, the equations for

$$\frac{\partial T_1}{\partial k_1}, \quad \frac{\partial T_1}{\partial k_2}, \ldots, \frac{\partial T_1}{\partial k_{NK}}$$

are determined.

Page 2 to 8 determine the equations for

$$\frac{\partial T_i}{\partial k_1} \quad , \quad \frac{\partial T_i}{\partial k_2} \quad , \ldots , \quad \frac{\partial T_i}{\partial k_{NS}} \qquad \text{where } i = 2 \text{ to NS}$$

Therefore, with reference to Page 7 to 8

$$\frac{\partial E}{\partial k_1} = \sum_{i=1}^{NS} \frac{\partial T_i}{\partial k_1} = 0$$

$$\frac{\partial E}{\partial k_2} = \sum_{i=1}^{NS} \frac{\partial T_i}{\partial k_2} = 0 \ , \text{ etc.}$$

can be established. That is, the NK k values can be determined from the above NK equations.

APPENDIX 8

```
1000 DIM CA(20,20),CB(20),CY(20),DX(20),DZ(20)
1020 DIM MK(15,20),ZK(20,3),AK(20),EK(20)
1040 DIM X0(15,3,3),X(15,3,3),XDOT(15,3,3)
1060 DIM TC(3),TK(3),SV(3),P(3)
1080 DIM BA(15,15),BB(15,15)
1100 DIM FK(20,3),XP(15,3,3),XBAR(16),FXD(15,3,3)
1120 DIM XPD(15,3,3),FST(16),FSB(16),FR(16)
1140 REM
1160 REM *****  GET MODEL PARAMETER VALUES *****
1180 REM
1200 OPEN "YMOD.DAT" FOR INPUT AS #1
1220 INPUT#1,MN,NS,NK : PRINT MN,NS,NK : INPUT#1,A$ : PRINT A$
1240 FOR I = 1 TO NS
1260 FOR J = 1 TO NK : INPUT#1,MK(I,J)
1280 PRINT USING"###  ";MK(I,J); : NEXT J
1300 PRINT : NEXT I : CLOSE#1
1320 PRINT
1340 REM
1360 REM *****  GET AK(J) & EK(J) WHERE J = 1 TO NK  *****
1380 REM
1400 OPEN "YAE.DAT" FOR INPUT AS #1
1420 FOR J = 1 TO NK
1440 INPUT#1,III,AK(J),EK(J)
1460 PRINT USING"###    ##.###^^^^    ##.###^^^^";III;AK(J);EK(J)
1480 NEXT J : CLOSE#1
1500 PRINT
1520 REM
1540 REM *****  GET EXPERIMENTAL  DATA  *****
1560 REM
1580 OPEN "ZINP.DAT" FOR INPUT AS #1
1600 INPUT#1,TC(1),W,W,TC(2),W,W,TC(3),W,W
1620 INPUT#1,SV(1),SV(2),SV(3),W,W,W,W,W,W
1640 INPUT#1,A$
1660 FOR I = 1 TO NS
1680 INPUT#1,X(I,1,1),X(I,2,1),X(I,3,1)
1700 INPUT#1,X(I,1,2),X(I,2,2),X(I,3,2)
1720 INPUT#1,X(I,1,3),X(I,2,3),X(I,3,3)
1740 NEXT I
1760 INPUT#1,A$
1780 FOR I = 1 TO NS
1800 INPUT#1,X0(I,1,1),X0(I,2,1),X0(I,3,1)
1820 INPUT#1,X0(I,1,2),X0(I,2,2),X0(I,3,2)
1840 INPUT#1,X0(I,1,3),X0(I,2,3),X0(I,3,3)
1860 NEXT I
1880 CLOSE#1
1900 REM
1920 REM *****  SET UP CONSOLIDATION PARAMETERES  *****
1940 REM
1960  PHI = .1 : E = .03 : ROP = 1.05 : R = 1.98
1980 CON1 = ( 1-PHI ) / ( (1-E)*ROP )
2000 FOR J = 1 TO 3 : P(J) = CON1 * SV(J) : NEXT J
2020 FOR K = 1 TO 3 : TK(K) = 1 / ( 273.16 + TC(K) ) : NEXT K
2040 FOR K = 1 TO 3 : FOR J = 1 TO 3 : FOR I = 1 TO NS
2060 XDOT(I,J,K) = P(J) * ( X(I,J,K) - X0(I,J,K) )
2080 NEXT I : NEXT J : NEXT K
2100 REM
2120 REM *****  CALCULATE FK(I,K) FROM AK(I) & EK(I)  *****
2140 REM *****  AND THEN THE GOODNESS OF FIT          *****
2160 REM
2180 FOR K = 1 TO 3 : FOR I = 1 TO NK
2200 FK(I,K) = AK(I) * ( 2.71828 ^ ( -EK(I)*TK(K)/R ) )
2220 NEXT I : NEXT K
2240 FOR K = 1 TO 3 : FOR J = 1 TO 3
2260 FOR KROW = 1 TO NS
2280 FOR KCOL = 1 TO NS : CA(KROW,KCOL) = 0 : NEXT KCOL
```

```
2300 FOR KCOL = 1 TO NK
2320  IP = MK(KROW,KCOL)
2340 IPA = ABS(IP)
2360 IF IP = 0 THEN 2420
2380 IF IP < 0 THEN CA(KROW,IPA) = CA(KROW,IPA) + FK(KCOL,K)
2400 IF IP > 0 THEN CA(KROW,IPA) = CA(KROW,IPA) - FK(KCOL,K)
2420 NEXT KCOL
2440 CA(KROW,KROW) = CA(KROW,KROW) + P(J)
2460       CB(KROW) = P(J) * X0(KROW,J,K)
2480 NEXT KROW
2500 NN = NS : GOSUB 4520 : IF CHECK < 0 THEN 4380
2520 FOR I = 1 TO NN : XP(I,J,K) = CY(I) : NEXT I
2540 NEXT J : NEXT K
2560 FOR I = 1 TO (NS+1) : XBAR(I) = 0 : NEXT I
2580 FOR I = 1 TO NS : FOR J = 1 TO 3
2600 FOR K = 1 TO 3 : XBAR(I) = XBAR(I) + X(I,J,K) : NEXT K
2620 NEXT J : NEXT I
2640 FOR I = 1 TO NS
2660 XBAR(I) = XBAR(I) / 9 : XBAR(NS+1) = XBAR(NS+1) + XBAR(I) / NS
2680 NEXT I
2700 REM
2720 REM ***   DEPENDING ON THE PHYSICAL INTERPRETATION,   ***
2740 REM *** THE XBAR(NS+1) BELOW MAY BE REPLACED BY XBAR(I). ***
2760 REM
2780 FOR K = 1 TO 3 : FOR J = 1 TO 3 : FOR I = 1 TO NS
2800 FXD(I,J,K) = X(I,J,K) - XBAR(NS+1)
2820 XPD(I,J,K) = X(I,J,K) - XP(I,J,K)
2840 NEXT I : NEXT J : NEXT K
2860 FST(NS+1) = 0 : FSB(NS+1) = 0
2880 FOR I = 1 TO NS
2900 FST(I) = 0 : FSB(I) = 0
2920 FOR K = 1 TO 3 : FOR J = 1 TO 3
2940 FST(I) = FST(I) + XPD(I,J,K) ^ 2
2960 FSB(I) = FSB(I) + FXD(I,J,K) ^ 2
2980 NEXT J : NEXT K
3000 FR(I) = 1 - FST(I) / FSB(I)
3020 FST(NS+1) = FST(NS+1) + FST(I) : FSB(NS+1) = FSB(NS+1) + FSB(I)
3040 NEXT I
3060 FR(NS+1) = 1 - FST(NS+1) / FSB(NS+1)
3080 REM
3100 REM *****  STORE ALL THE RESULTS IN A FILE  *****
3120 REM
3140 OPEN "A",#3,"YOUT.DAT"
3160 PRINT#3,"Final results of Model";MN
3180 PRINT#3,
3200 PRINT#3,"# of states or components =";NS
3220 PRINT#3,"             # of k values =";NK
3240 PRINT#3,
3260 PRINT#3,"The model matrix is:"
3280 PRINT#3,
3300 FOR I = 1 TO NS
3320 FOR J = 1 TO NK
3340 PRINT#3,USING"#####";MK(I,J);
3360 NEXT J
3380 PRINT#3,
3400 NEXT I
3420 PRINT#3,
3440 PRINT#3,"The rows below are: i = 1 to";NK
3460 PRINT#3,"  i, AK(i), EK(i), FK(i,1), FK(i,2) & FK(i,3)."
3480 PRINT#3,"***"
3500 FOR I = 1 TO NK : PRINT#3,USING"###";I;
3520 PRINT#3,USING"   ##.###^^^^";AK(I);EK(I);FK(I,1);FK(I,2);FK(I,3)
3540 NEXT I
3560 PRINT#3,
3580 PRINT#3,"The rows below are the correlation values."
3600 PRINT#3,"i=1 to";(NS+1);" & i=last row means grand values."
```

```
3620 PRINT#3, I, FST(I), FSB(I), FR(I) & XBAR(I)
3640 PRINT#3,"***"
3660 FOR I = 1 TO (NS+1) : PRINT#3,USING"###";I;
3680 PRINT#3,USING"    ##.###^^^^";FST(I);FSB(I);FR(I);XBAR(I)
3700 NEXT I
3720 PRINT#3, : PRINT#3,
3740 PRINT#3,"Information below are the intermediate results."
3760 PRINT#3,
3780 PRINT#3,"Col 1 = temperature in degree C"
3800 PRINT#3,"Col 2 = space velocity"
3820 PRINT#3,"Col 3 = experimental value"
3840 PRINT#3,"Col 4 = predicted value"
3860 PRINT#3,"Col 5 = experimental - predicted"
3880 PRINT#3,"Col 6 = ( experimental - predicted ) / experimental"
3900 PRINT#3,"Col 7 = experimental - grand mean"
3920 PRINT#3,
3940 FOR I = 1 TO NS
3960 PRINT#3,
3980 PRINT#3,"State #";I
4000 PRINT#3,
4020 FOR K = 1 TO 3 : FOR J = 1 TO 3
4040 PRINT#3,USING"#####.#   ###.## ";TC(K);SV(J);
4060 PRINT#3,USING"##.###^^^^  ";X(I,J,K);
4080 PRINT#3,USING"##.###^^^^  ";XP(I,J,K);
4100 PRINT#3,USING"##.###^^^^  ";XPD(I,J,K);
4120 COL6 = 10 ^ 38
4140 IF X(I,J,K) <> 0 THEN COL6 = XPD(I,J,K) / X(I,J,K)
4160 PRINT#3,USING"##.###^^^^  ";COL6;
4180 PRINT#3,USING"##.###^^^^  ";FXD(I,J,K)
4200 NEXT J : NEXT K
4220 PRINT#3,
4240 NEXT I
4260 CLOSE#3
4280 GOTO 4480
4300 PRINT
4320 PRINT "PLEASE ALERT & READ THE MESSAGE CAREFULLY"
4340 PRINT "----------------------------------------"
4360 PRINT
4380 PRINT "CHECK is less that 0."
4400 PRINT "This means that a unique solution does not exist."
4420 PRINT "I suggest you to check all the input files carefully."
4440 PRINT "Please press the space bar to continue."
4460 AAA$ = INPUT$(1)
4480 SYSTEM
4500 END
4520 REM
```

NORMAL EQUATIONS FOR MODEL 1

Term 1 = $T_1 = \Sigma(-X_1k_1 - X_1k_3 - r_1)^2$

$$\frac{\partial T_1}{\partial k_2} = \frac{\partial T_1}{\partial k_4} = \frac{\partial T_1}{\partial k_5} = \frac{\partial T_1}{\partial k_6} = \frac{\partial T_1}{\partial k_7} = 0$$

$$\frac{1}{2}\frac{\partial T_1}{\partial k_1} = \Sigma(\bar{}X_1k_1 - X_1k_3 - r_1)\ (\bar{}X_1)$$

$$= (\Sigma X_1^2)k_1 + (\Sigma X_1^2)k_3 + \Sigma X_1r_1$$

$$\frac{1}{2}\frac{\partial T_1}{\partial k_3} = \Sigma(\bar{}X_1k_1 - X_1k_3 - r_1)\ (\bar{}X_1)$$

$$= (\Sigma X_1^2)k_1 + (\Sigma X_1^2)k_3 + \Sigma X_1r_1$$

Term 2 = $T_2 = \Sigma(X_1k_1 - X_2k_2 - r_2)^2$

$$\frac{\partial T_2}{\partial k_3} = \frac{\partial T_2}{\partial k_4} = \frac{\partial T_2}{\partial k_5} = \frac{\partial T_2}{\partial k_6} = \frac{\partial T_2}{\partial k_7} = 0$$

$$\frac{1}{2}\frac{\partial T_2}{\partial k_1} = (\Sigma X_1^2)k_1 - (\Sigma X_1X_2)k_2 - \Sigma X_1r_2$$

$$\frac{1}{2}\frac{\partial T_2}{\partial k_2} = (-\Sigma X_1X_2)k_1 + (\Sigma X_2^2)k_2 + \Sigma X_2r_2$$

Term 3 = $T_3 = (X_2k_2 + X_1k_3 - X_3k_4 - X_3k_6 - r_3)^2$

$$\frac{\partial T_3}{\partial k_1} = \frac{\partial T_3}{\partial k_5} = \frac{\partial T_3}{\partial k_7} = 0$$

$$\frac{1}{2}\frac{\partial T_3}{\partial k_2} = (X_2^2)k_2 + (X_1X_2)k_3 - (X_2X_3)k_4 - (X_2X_3)k_6 - (X_2r_3)$$

$$\frac{1}{2}\frac{\partial T_3}{\partial k_3} = (X_1X_2)k_2 + (X_1^2)k_3 - (X_1X_3)k_4 - (X_1X_3)k_6 - (X_1r_3)$$

$$\frac{1}{2}\frac{\partial T_3}{\partial k_4} = (\bar{}X_2X_3)k_2 - (X_1X_3)k_3 + (X_3^2)k_4 + (X_3^2)k_6 + (X_3r_3)$$

$$\frac{1}{2}\frac{\partial T_3}{\partial k_6} = (\bar{}X_2X_3)k_2 - (X_1X_3)k_3 + (X_3^2)k_4 + (X_3^2)k_6 + (X_3r_3)$$

Term 4 = $T_4 = (X_3k_4 - X_4k_5 - r_4)^2$

$$\frac{\partial T_4}{\partial k_1} = \frac{\partial T_4}{\partial k_2} = \frac{\partial T_4}{\partial k_3} = \frac{\partial T_4}{\partial k_6} = \frac{\partial T_4}{\partial k_7} = 0$$

$$\frac{1}{2}\frac{\partial T_4}{\partial k_4} = (X_3^2)k_4 - (X_3X_4)k_5 - X_3r_4$$

$$\frac{1}{2}\frac{\partial T_4}{\partial k_5} = (-X_3X_4)k_4 + (X_4^2)k_5 + (X_4r_4)$$

Term 5 = $T_5 = (X_4k_5 - X_3k_6 - X_5k_7 - r_5)^2$

$$\frac{\partial T_5}{\partial k_1} = \frac{\partial T_5}{\partial k_2} = \frac{\partial T_5}{\partial k_3} = \frac{\partial T_5}{\partial k_4} = 0$$

$$\frac{1}{2}\frac{\partial T_5}{\partial k_5} = (X_4^2)k_5 + (X_3X_4)k_6 - (X_4X_5)k_7 - (X_4r_5)$$

$$\frac{1}{2}\frac{\partial T_5}{\partial k_6} = (X_3X_4)k_5 + (X_3^2)k_6 - (X_3X_5)k_7 - (X_3r_5)$$

$$\frac{1}{2}\frac{\partial T_5}{\partial k_7} = (-X_4X_5)k_5 - (X_3X_5)k_6 + (X_5^2)k_7 + (X_5r_5)$$

Term 6 = $T_6 = (X_5k_7 - r_6)^2$

$$\frac{\partial T_6}{\partial k_1} = \cdots = \frac{\partial T_6}{\partial k_6} = 0$$

$$\frac{1}{2}\frac{\partial T_6}{\partial k_7} = (X_5^2)k_7 - (X_5X_6)$$

APPENDIX 9

Figure 1 PRELIMINARY MODELS

MODEL 1

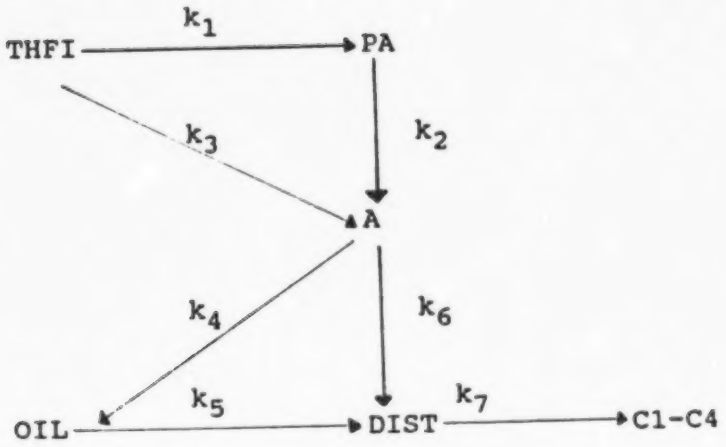

MODEL 2

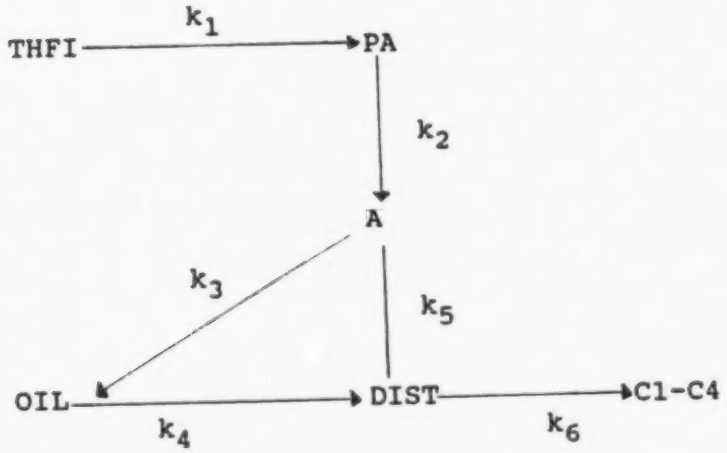

MODEL 3

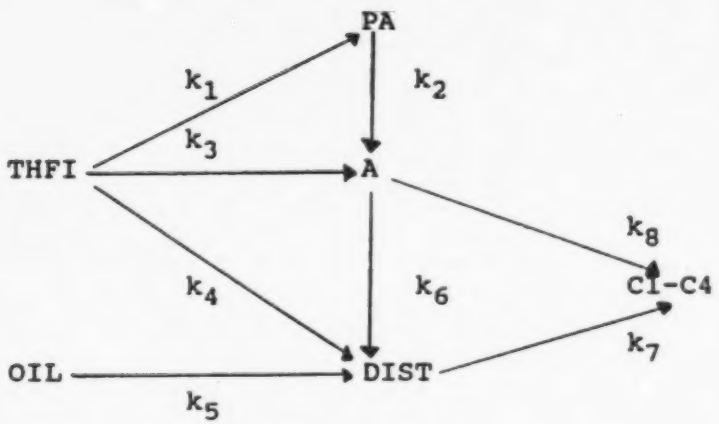

MODEL 4

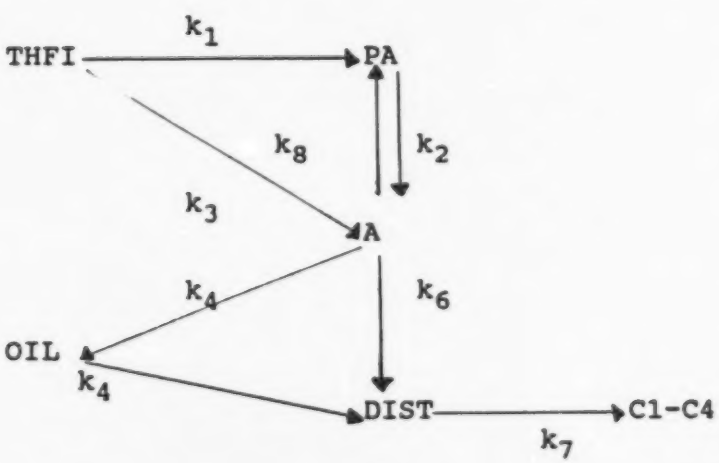

MODEL 5

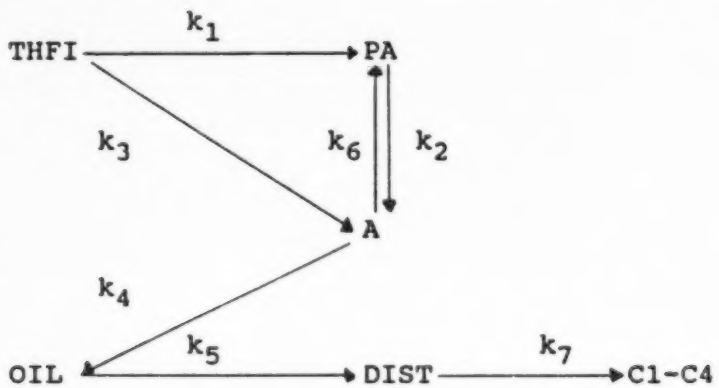

MODEL 6

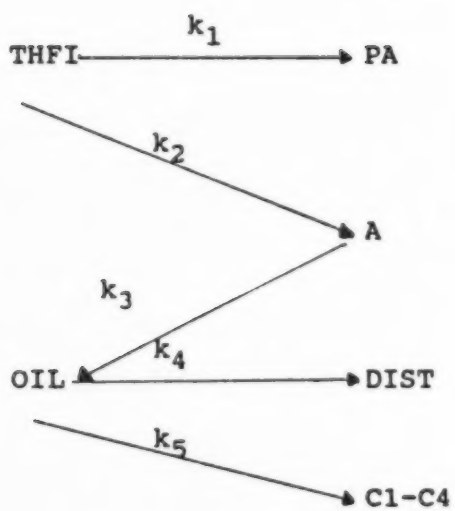

MODEL 7

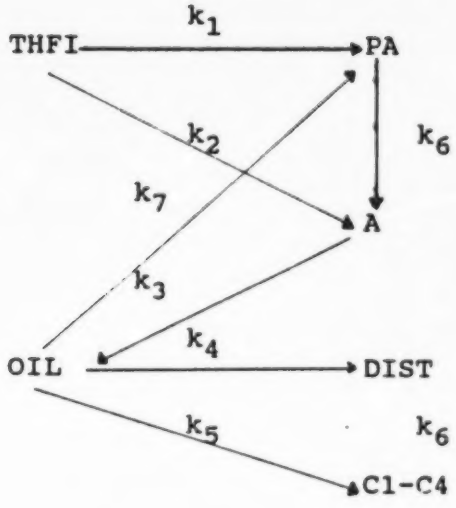

MODEL 8

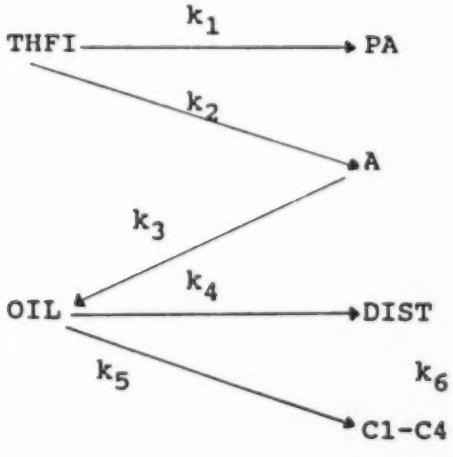

MODEL 9

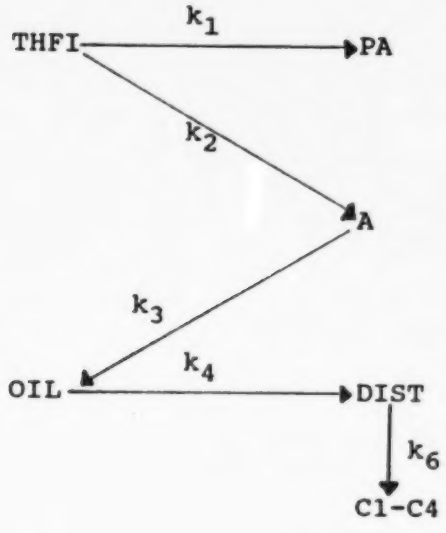

MODEL 10

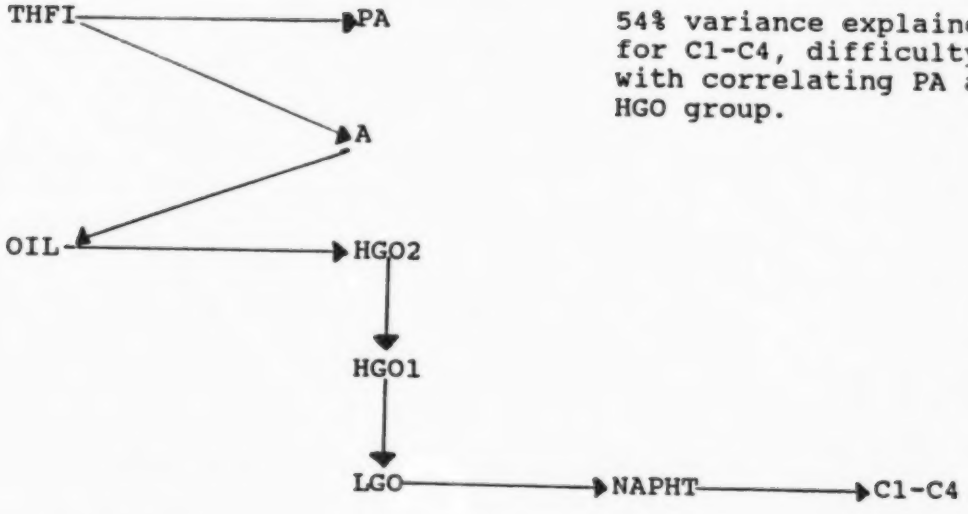

54% variance explained for C1-C4, difficulty with correlating PA and HGO group.

MODEL 11

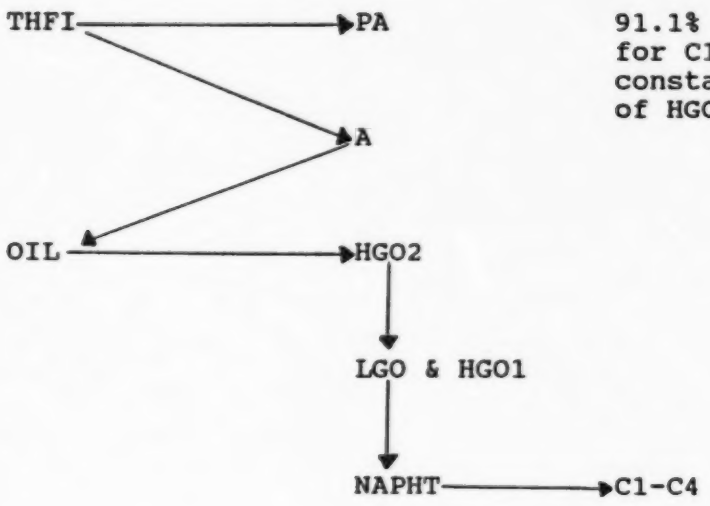

91.1% variance explained for C1-C4, negative rate constants for formation of HGO and LGO.

MODEL 12

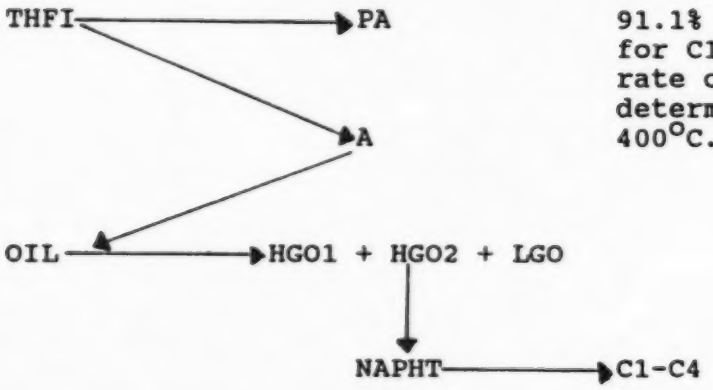

91.1% variance explained for C1-C4, but negative rate constant was determined at temperature 400^{o}C.

MODEL 21

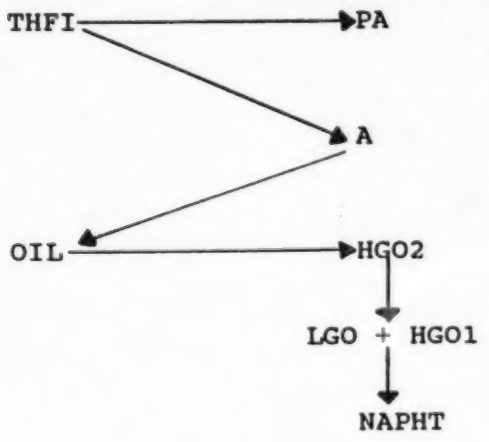

Percent Variance Explained
77.6 For Fractions:

HGO	12.8
LGO2 + LGO1	93.1
NAPHT	40.4

MODEL 25

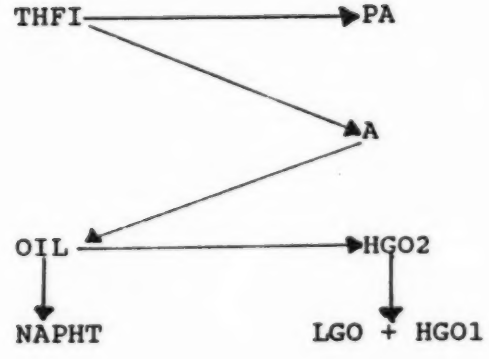

Percent Variance Explained
83.6 For Fractions:

HGO2	11.6
LGO + LGO1	87.6
NAPHT	97.3

MODEL 24

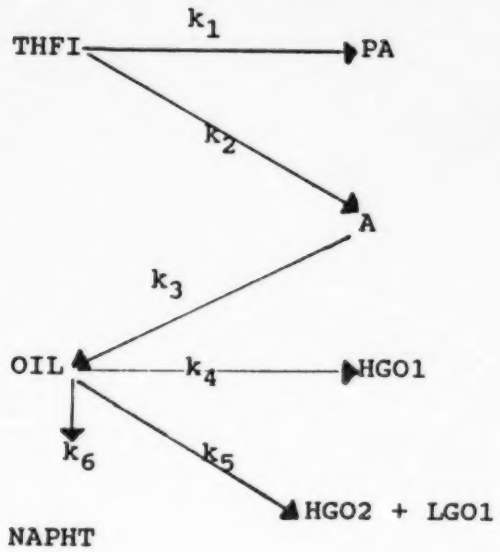

Percent Variance Explained
82.6 For Fractions:

HGO	<0
LGO2 + LGO1	89.0
NAPHT	95.3

MODEL 22

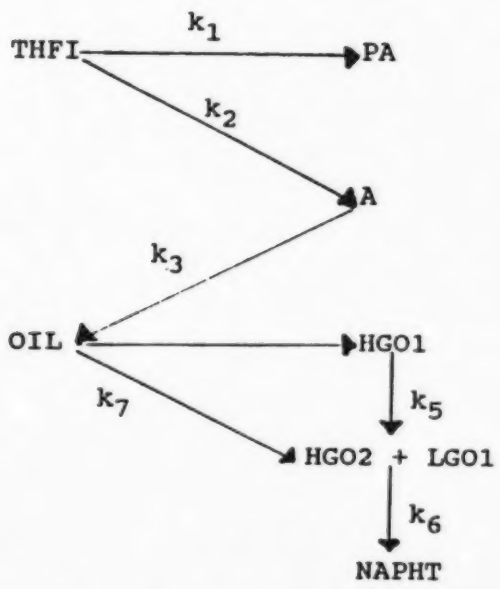

Percent Variance Explained
74.1 For Fractions:

HGO	<0
LGO2 + LGO1	87.1
NAPHT	88.8

MODEL 23

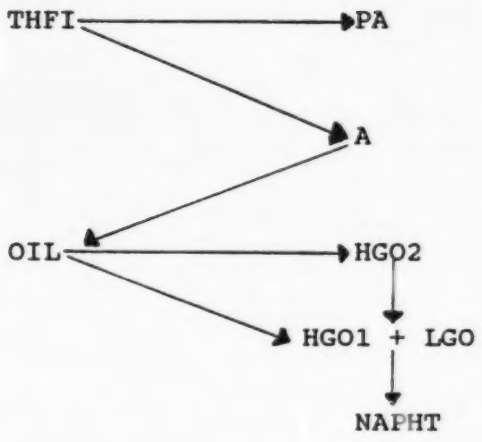

Percent Variance Explained 88.9 Negative k rate constant

MODEL 26

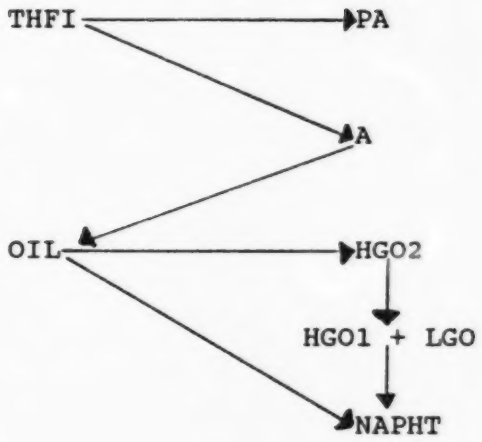

Percent Variance Explained <0

MODEL 27

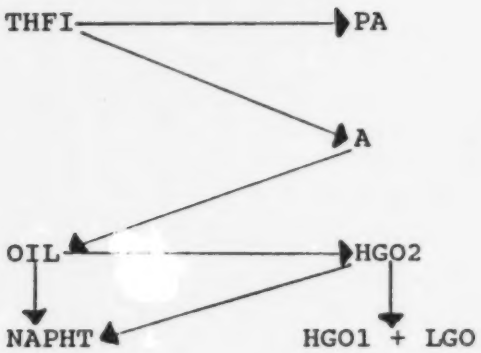

Percent Variance Explained <0

MODEL 28

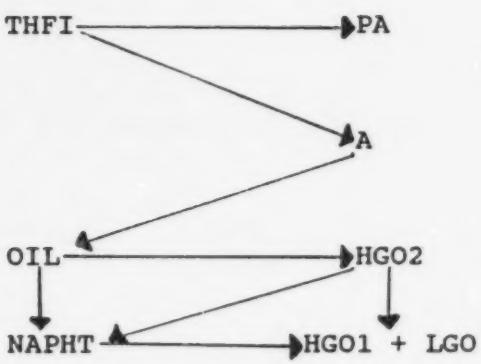

Percent Variance Explained <0

MODEL 30

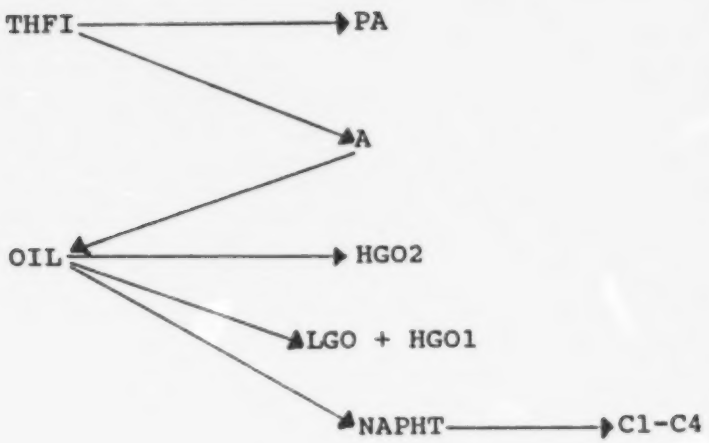

MODEL 31

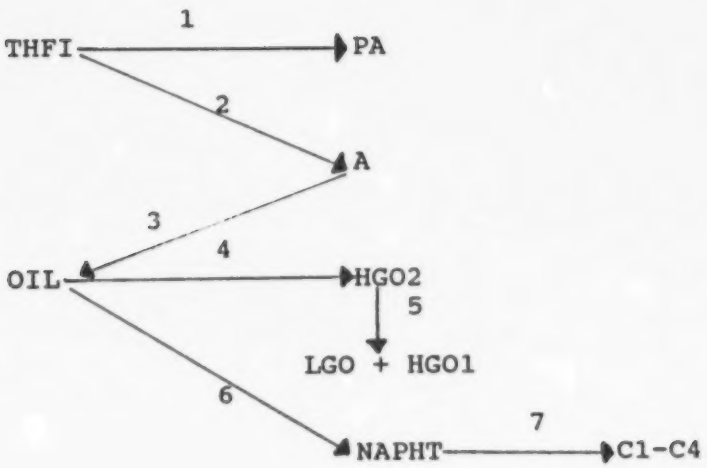

MODEL 32

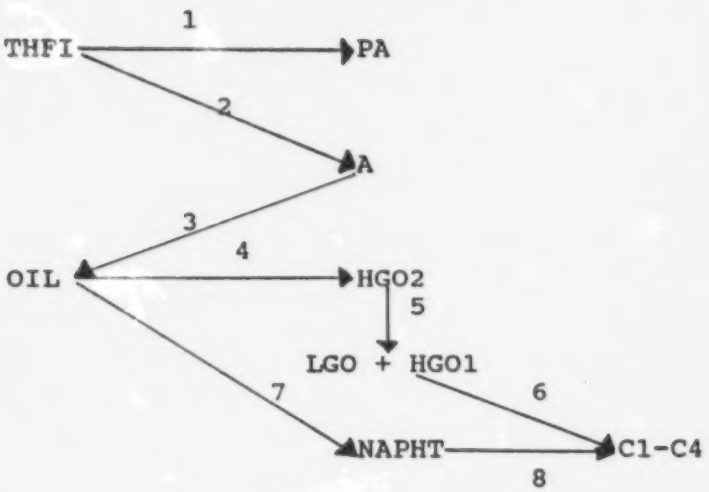

MODEL 33

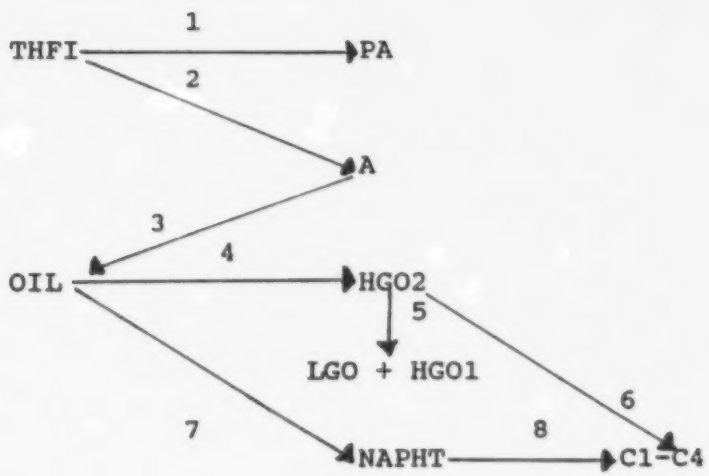

MODEL 34

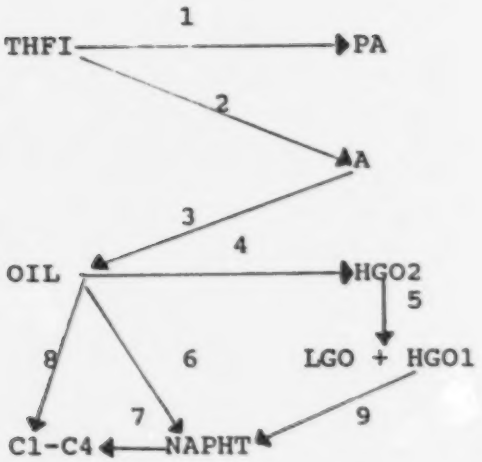

APPENDIX 10

Final results of Model 53

# of states or components = 8
# of k values = 10

The model matrix is:

-1	-1	-1	0	0	0	0	0	0	0
1	0	0	0	0	0	0	0	0	0
0	1	0	-3	-3	0	0	0	0	0
0	0	1	0	0	-4	0	-4	0	0
0	0	0	3	0	0	0	4	-5	0
0	0	0	0	0	4	-6	0	0	0
0	0	0	0	0	0	6	0	5	-7
0	0	0	0	3	0	0	0	0	7

The rows below are: i = 1 to 10
i, AK(i), EK(i), FK(i,1), FK(i,2) & FK(i,3).

***					
1	1.244E+10	3.302E+04	2.166E-01	5.260E-01	1.201E+00
2	9.112E+23	7.773E+04	4.288E-02	3.461E-01	2.418E+00
3	1.835E+12	3.903E+04	3.517E-01	1.004E+00	2.664E+00
4	1.507E+12	4.000E+04	1.395E-01	4.086E-01	1.111E+00
5	4.165E+17	5.961E+04	1.572E-02	7.798E-02	3.463E-01
6	4.063E+19	6.340E+04	8.928E-02	4.904E-01	2.394E+00
7	7.902E+06	2.351E+04	1.727E-01	3.248E-01	5.847E-01
8	2.276E+14	4.747E+04	7.757E-02	2.777E-01	9.102E-01
9	3.514E+19	6.640E+04	8.132E-03	4.841E-02	2.548E-01
10	4.518E+16	5.909E+04	2.519E-03	1.232E-02	5.401E-02

The rows below are the correlation values.
i=1 to 9 & i=last row means grand values.
i, FST(i), FSB(i), FR(i) & XBAR(i)

***				
1	2.471E+01	2.999E+02	9.176E-01	9.222E+00
2	3.743E+01	5.940E+02	9.370E-01	4.108E+00
3	1.809E+02	3.777E+02	5.209E-01	1.312E+01
4	1.321E+02	3.268E+03	9.596E-01	2.624E+01
5	1.077E+02	1.120E+03	9.039E-01	2.171E+01
6	1.105E+02	4.964E+02	7.774E-01	1.131E+01
7	1.442E+02	5.338E+02	7.298E-01	7.726E+00
8	7.469E+00	7.727E+02	9.903E-01	3.268E+00
9	7.451E+02	7.463E+03	9.002E-01	1.209E+01

Information below are the intermediate results.

Col 1 = temperature in degree C
Col 2 = space velocity
Col 3 = experimental value
Col 4 = predicted value
Col 5 = experimental - predicted
Col 6 = (experimental - predicted) / experimental
Col 7 = experimental - grand mean

State # 1

400.0	0.50	1.129E+01	1.294E+01	-1.645E+00	-1.457E-01	-7.975E-01
400.0	1.00	1.590E+01	1.822E+01	-2.324E+00	-1.462E-01	3.813E+00
400.0	1.50	1.777E+01	2.033E+01	-2.563E+00	-1.443E-01	5.683E+00
425.0	0.50	5.300E+00	5.664E+00	-3.639E-01	-6.866E-02	-6.787E+00
425.0	1.00	9.310E+00	9.463E+00	-1.528E-01	-1.641E-02	-2.777E+00
425.0	1.50	1.007E+01	1.224E+01	-2.165E+00	-2.150E-01	-2.017E+00
450.0	0.50	1.140E+00	2.026E+00	-8.856E-01	-7.768E-01	-1.095E+01

450.0	1.00	4.840E+00	5.742E+00	-1.038E+00	-2.268E-01	-7.247E+00
450.0	1.50	7.380E+00	5.592E+00	1.788E+00	2.423E-01	-4.707E+00

State # 2

400.0	0.50	3.560E+00	6.482E+00	-2.922E+00	-8.207E-01	-8.528E+00
400.0	1.00	4.600E+00	4.607E+00	-7.316E-03	-1.590E-03	-7.487E+00
400.0	1.50	1.890E+00	3.463E+00	-1.573E+00	-8.322E-01	-1.020E+01
425.0	0.50	4.140E+00	6.882E+00	-2.742E+00	-6.624E-01	-7.948E+00
425.0	1.00	6.560E+00	5.772E+00	7.877E-01	1.201E-01	-5.527E+00
425.0	1.50	5.590E+00	4.995E+00	5.950E-01	1.064E-01	-6.497E+00
450.0	0.50	1.690E+00	5.646E+00	-3.956E+00	-2.341E+00	-1.040E+01
450.0	1.00	5.240E+00	5.227E+00	1.345E-02	2.567E-03	-6.848E+00
450.0	1.50	3.700E+00	5.207E+00	-1.507E+00	-4.074E-01	-8.388E+00

State # 3

400.0	0.50	1.589E+01	1.295E+01	2.943E+00	1.852E-01	3.803E+00
400.0	1.00	2.260E+01	1.457E+01	8.034E+00	3.555E-01	1.051E+01
400.0	1.50	2.041E+01	1.536E+01	5.051E+00	2.475E-01	8.323E+00
425.0	0.50	4.960E+00	9.963E+00	-5.003E+00	-1.009E+00	-7.127E+00
425.0	1.00	1.521E+01	1.306E+01	2.154E+00	1.416E-01	3.123E+00
425.0	1.50	1.766E+01	1.441E+01	3.254E+00	1.843E-01	5.573E+00
450.0	0.50	4.710E+00	6.357E+00	-1.647E+00	-3.496E-01	-7.377E+00
450.0	1.00	1.043E+01	1.004E+01	3.935E-01	3.772E-02	-1.657E+00
450.0	1.50	6.200E+00	1.245E+01	-6.251E+00	-1.008E+00	-5.888E+00

State # 4

400.0	0.50	3.541E+01	3.738E+01	-1.971E+00	-5.566E-02	2.332E+01
400.0	1.00	3.860E+01	4.076E+01	-2.158E+00	-5.591E-02	2.651E+01
400.0	1.50	4.201E+01	4.198E+01	2.888E-02	6.875E-04	2.992E+01
425.0	0.50	3.036E+01	1.999E+01	1.037E+01	3.416E-01	1.827E+01
425.0	1.00	3.055E+01	2.820E+01	2.346E+00	7.678E-02	1.846E+01
425.0	1.50	3.129E+01	3.238E+01	-1.085E+00	-3.468E-02	1.920E+01
450.0	0.50	3.850E+00	6.300E+00	-2.450E+00	-6.364E-01	-8.237E+00
450.0	1.00	9.310E+00	1.114E+01	-1.825E+00	-1.961E-01	-2.777E+00
450.0	1.50	1.475E+01	1.480E+01	-4.904E-02	-3.325E-03	2.663E+00

State # 5

400.0	0.50	2.264E+01	2.184E+01	8.010E-01	3.538E-02	1.055E+01
400.0	1.00	1.350E+01	1.731E+01	-3.808E+00	-2.821E-01	1.413E+00
400.0	1.50	1.204E+01	1.575E+01	-3.707E+00	-3.079E-01	-4.750E-02
425.0	0.50	2.739E+01	3.024E+01	-2.845E+00	-1.039E-01	1.530E+01
425.0	1.00	1.789E+01	2.531E+01	-7.424E+00	-4.150E-01	5.803E+00
425.0	1.50	2.231E+01	2.218E+01	1.263E-01	5.663E-03	1.022E+01
450.0	0.50	2.870E+01	2.572E+01	2.977E+00	1.037E-01	1.661E+01
450.0	1.00	2.599E+01	2.776E+01	-1.768E+00	-6.801E-02	1.390E+01
450.0	1.50	2.493E+01	2.682E+01	-1.886E+00	-7.565E-02	1.284E+01

State # 6

400.0	0.50	5.700E+00	5.431E+00	2.690E-01	4.719E-02	-6.388E+00
400.0	1.00	5.100E+00	3.445E+00	1.655E+00	3.245E-01	-6.987E+00
400.0	1.50	2.170E+00	2.502E+00	-3.319E-01	-1.529E-01	-9.917E+00
425.0	0.50	9.870E+00	1.279E+01	-2.916E+00	-2.954E-01	-2.217E+00
425.0	1.00	1.006E+01	1.144E+01	-1.384E+00	-1.376E-01	-2.027E+00
425.0	1.50	5.400E+00	9.620E+00	-4.220E+00	-7.814E-01	-6.687E+00
450.0	0.50	2.297E+01	1.469E+01	8.279E+00	3.604E-01	1.088E+01
450.0	1.00	2.139E+01	1.815E+01	3.236E+00	1.512E-01	9.203E+00

450.0 1.50 1.314E+01 [illegible]

State # 7

400.0	0.50	2.550E+00	2.511E+00	3.939E-02	1.545E-02	-9.537E+00
400.0	1.00	1.000E-02	8.302E-01	-8.202E-01	-8.202E+01	-1.208E+01
400.0	1.50	1.280E+00	4.218E-01	8.582E-01	6.705E-01	-1.081E+01
425.0	0.50	9.760E+00	1.237E+01	-2.607E+00	-2.671E-01	-2.327E+00
425.0	1.00	5.440E+00	5.517E+00	-7.653E-02	-1.407E-02	-6.647E+00
425.0	1.50	4.120E+00	3.138E+00	9.817E-01	2.383E-01	-7.967E+00
450.0	0.50	2.009E+01	3.054E+01	-1.045E+01	-5.202E-01	8.003E+00
450.0	1.00	1.379E+01	1.886E+01	-5.072E+00	-3.678E-01	1.703E+00
450.0	1.50	1.249E+01	1.281E+01	-3.235E-01	-2.590E-02	4.025E-01

State # 8

400.0	0.50	1.540E+00	4.750E-01	1.065E+00	6.916E-01	-1.055E+01
400.0	1.00	1.000E-02	2.615E-01	-2.515E-01	-2.515E+01	-1.208E+01
400.0	1.50	5.500E-01	1.830E-01	3.670E-01	6.673E-01	-1.154E+01
425.0	0.50	3.640E+00	2.103E+00	1.537E+00	4.221E-01	-8.447E+00
425.0	1.00	2.100E+00	1.229E+00	8.709E-01	4.147E-01	-9.987E+00
425.0	1.50	1.560E+00	8.767E-01	6.833E-01	4.380E-01	-1.053E+01
450.0	0.50	9.550E+00	8.715E+00	8.348E-01	8.742E-02	-2.537E+00
450.0	1.00	5.350E+00	5.086E+00	2.643E-01	4.940E-02	-6.737E+00
450.0	1.50	5.110E+00	3.775E+00	1.335E+00	2.613E-01	-6.977E+00